MEDICAL UNIVERSITY OF VIENNA

Parallel genome-wide screens identify synthetic viable interactions between the BLM helicase complex and Fanconi anemia

Doctoral thesis at the Medical University of Vienna for obtaining the academic degree

Doctor of Philosophy

Submitted by

Martin Moder, MSc

Supervisor:

Joanna Loizou, PhD

CeMM Research Center for Molecular Medicine

of the Austrian Academy of Sciences

Lazarettgasse 14, AKH BT25.3

1090 Vienna, Austria

Vienna, 01/2018

Declaration

This thesis discusses the results of a CRISPR-based loss-of-function screen performed in parallel to a gene-trap insertional mutagenesis screen, that were published in Nature Communications. In this publication, the author of this thesis is shared first author, together with the postdoctoral scientist Georgia Velimezi.

The experimental work of this thesis was performed in the laboratory of Joanna Loizou at the CeMM Research Center for Molecular Medicine of the Austrian Academy of Sciences (CeMM). Sequencing of the genome-wide screening samples, both the insertional mutagenesis and genome-wide CRISPR knock-out library, was performed by the Biomedical Sequencing Facility (BSF) headed by Christoph Bock at CeMM. Georgia Velimezi performed the genome-wide insertional mutagenesis screen. Marc Wiedner generated the CRISPR-Cas9 knock-out clones and contributed to dose-response curves and immunoblots. Lydia Robinson-Garcia generated the shBRCA1 cells and the RT-qPCR data and together with Georgia Velimezi generated the NQO1 mutants using the double nickase Cas9 approach and performed survival assays. Michel Owusu contributed to dose-response curves and performed the γH2AX staining and analysis as well as the FACS for Annexin V. Fiorella Schischlik from the group of Robert Kralovics at CeMM analyzed the insertional mutagenesis data. Joana Ferreira da Silva assisted with data analysis, along with Jörg Menche from CeMM.

Table of contents

List of figures

Published figures:

Thesis figures:

List of tables

Published tables:

Thesis tables:

Abstract English

The continuous repair of DNA damage is a prerequisite for the maintenance of genome integrity. Therefore, cells have evolved a complex network of DNA damage repair mechanisms to deal with diverse forms of genomic lesions. Defects in those mechanisms frequently lead to diseases associated with cancer susceptibility, including Fanconi anemia (FA). Using a genome-wide CRISPR knock-out library as well as insertional mutagenesis, we identified synthetic viable (genetic suppressor) interactions in human haploid cells, deficient for FA complementation group C (FANCC). Here we show that the phenotype of Δ*FANCC* cells can be suppressed by additional loss of the BLM helicase complex. We demonstrate that this synthetic viable effect is not specific to Δ*FANCC* cells by confirming this interaction in cells deficient for FA complementation group I and D2 (FANCI and FANCD2) that function downstream of the FA core complex. This thesis demonstrates that systematic genome-wide screens can be used to identify genetic synthetic viable interactions for defects in the DNA damage response.

Zusammenfassung

Die kontinuierliche Reparatur von DNA Schäden ist die Voraussetzung für die Aufrechterhaltung der genomischen Integrität. Um mit den verschiedenen Arten von genetischen Läsionen umzugehen, entwickelten Zellen deshalb ein komplexes Netzwerk an DNA Reparatur Mechanismen. Defekte in diesen Mechanismen führen häufig zu Krankheiten die mit erhöhter Krebs-Anfälligkeit einhergehen, beispielsweise Fanconi Anämie (FA). Mithilfe einer Genom-weiten CRISPR funktionsverlust-Bibliothek, sowie Insertionsmutagenese, identifizierten wir synthetisch-lebensfähige Interaktionen in humanen haploiden Zellen, die einen Defekt in FA Komplementationsgruppe C (FANCC) tragen. Hier zeigen wir, dass der Phänotyp von Δ*FANCC* Zellen durch den zusätzlichen Verlust des BLM Helikasekomplexes supprimiert werden kann. Wir demonstrieren, dass dieser synthetisch-lebensfähige Effekt nicht spezifisch für Δ*FANCC* Zellen ist, indem wir diese Interaktion in Zellen bestätigen, die Defekte in FA Komplementationsgruppe I und D2 (FANCI und FANCD2) tragen. Diese Arbeit demonstriert, dass systematische Genom-weite Screens dazu geeignet sind, genetische synthetisch-lebensfähige Interaktionen für Defekte in der DNA Schadensreaktion zu identifizieren.

List of publications arising from this thesis

Moder, M., Velimezi, G., Owusu, M., Mazouzi, A., Wiedner, M., Silva, J.F. da, Robinson-Garcia, L., Schischlik, F., Slavkovsky, R., Kralovics, R., et al. Parallel genome-wide screens identify synthetic viable interactions between the BLM helicase complex and Fanconi anemia. *Nature Communications (2017), 8, 1238* (DOI: 10.1038/s41467-017-01439-x)

Abbreviations

6–4 PP	Pyrimidine pyrimidines (6–4) photoproduct
6-TG	6-thioguanosine
AGT	O6-alkylguanine-DNA alkyltransferase
alt-NHEJ	Alternative NHEJ
AML	Acute myeloid leukaemia
AP site	Apurinic/apyrimidinic site
APE1	AP-endonuclease 1
BER	Base excision repair
cDNA	Complementary DNA
CO	Crossover
CPD	Cyclobutane pyrimidine dimer
CRISPRa	CRISPR activation
CRISPRi	CRISPR interference
CSA	Cockayne syndrome protein A
CSB	Cockayne syndrome protein B
CTx-DTA	Cholera-diphtheria fusion toxin
dA	Deoxyadenosine
dCas9	Catalytically-dead Cas9
dCMP	Deoxycytidine monophosphate
DDR	DNA damage response
DEB	Diepoxybutane
dG	Deoxyguanosine
dHJ	Double Holiday Junction
DR	Direct repair
DSB	Double strand break
dsDNA	Double stranded DNA
dsRNA	Double stranded RNA
dT	Deoxythymidine
Exo1	Exonuclease 1
FA	Fanconi anemia
FACS	Fluorescence-activated cell sorting
GG-NER	Global genomic NER
gRNA	Guide RNA
HMGB1	High mobility group box 1
HMGN1	High mobility group nucleosome-binding domain-containing protein 1

HNPCC	Hereditary nonpolyposis colorectal cancer
HR	Homologous recombination
HU	Hydroxyurea
ICL	Interstrand crosslink
IDL	Insertion-deletion loop
IR	Ionizing radiation
KD	Knock-down
KO	Knock-out
KRAB	Krüppel associated box
LIG1	DNA ligase I
LIG3	DNA ligase III
MEF	Mouse embryonic fibroblasts
miRNA	MicroRNA
MMC	Mitomycin C
MMEJ	Microhomology-mediated end joining
MMR	Mismatch repair
MORR	Multiple orthologous RNAi reagents
mRNA	Messenger RNA
NCO	Non-crossover
NER	Nucleotide excision repair
NHEJ	Non-homologous end joining
nt	Nucleotide
PARP	Poly (ADP-ribose) polymerase
PARP1	Poly (ADPribose) polymerase 1
PCNA	Proliferating cell nuclear antigen
PCNA	Proliferating cell nuclear antigen
PNKP	Polynucleotide kinase-phosphatase
Pol β	DNA polymerase β
RFC	Replication factor C
RISC	RNA induced silencing complex
RNA Pol II	RNA polymerase II
RNAi	RNA interference
ROS	Reactive oxygen species
RPA	Replication protein A
SAM	Synergistic activation mediator
SCE	Sister chromatid exchange
shRNA	Short hairpin RNA

siRNA	Small interfering RNA
SSB	Single strand breaks
ssDNA	Single stranded DNA
TC-NER	Transcription coupled NER
TFIIH	Transcription initiation factor IIH
TLS	Translesion synthesis
TSS	Transcriptional start site
UV	Ultraviolet light
UV–DDB	Ultraviolet radiation–DNA damage-binding protein
UVSSA	UV-stimulated scaffold protein A
WRN	Werner syndrome RecQ like helicase
WRN	Werner syndrome ATP-dependent helicase
XAB21	XPA-binding protein 2
XPV	Xeroderma pigmentosum variant

Acknowledgments

I want to express my gratitude to CeMM for vastly expanding my scientific horizon and for providing me with an outstanding intellectual home for the past 3 years of my life.

Special thanks to my supervisor Joanna Loizou for giving me the opportunity to do my PhD in her laboratory, for her constant support, her outstanding guidance and her unbroken efforts to not only maintain scientific excellence but also an exemplary work environment.

I also want to thank all the members of the Loizou laboratory from which I have learned so much and whose personalities made it a constant pleasure for me to come to work.

I want to express my deepest gratitude to my parents for their unconditional support of all my endeavors, for being scientific, ethical and emotional role models and for empowering me to pursue what feels most meaningful to me. I also want to thank my sister for setting a high standard and affecting my decision to pursue a scientific career.

Special thanks to July for her patience, her constant support, her honesty and for sharing all aspects of my pursuits.

Finally, I want to thank Lorenz Hinterberger for the numerous inspiring conversations about chromosomal abnormalities.

CHAPTER ONE: INTRODUCTION

On average, each cell in the human body receives tens of thousands of DNA lesions per day (Lindahl and Barnes, 2000). These lesions are challenging the maintenance of the genomic integrity by blocking transcription and replication and potentially leading to mutations and chromosomal instability. They arise due to endogenous events such as mismatches during DNA replication, insufficient topoisomerase I and topoisomerase II activity, reactive oxygen species (ROS) generated by metabolic- or immune cell activity during inflammation, as well as the production of reactive metabolic byproducts such as aldehydes. DNA damage also occurs due to exogenous sources such as ionizing radiation (IR), ultraviolet light (UV) and tobacco smoke or pharmacological interventions like chemotherapeutic agents. The induced lesions include single- and double strand breaks, bulky adducts, interstrand crosslinks, abasic sites, DNA mismatches and alterations to the DNA sugar backbone. To allow the maintenance of genomic integrity, cells have evolved various mechanisms that facilitate the repair of those lesions, known as DNA damage response (DDR) pathways. The following introduction consists of three subchapters. The first subchapter (1.1) will give an overview over the major DDR pathways in human cells, whereby the Fanconi anemia pathway will be discussed in particular detail, since Fanconi anemia is the main focus of this thesis. The second subchapter (1.2) will introduce the concept of genetic synthetic interactions, describing the background and applications of synthetic lethal- and synthetic viable interactions. Subchapter three (1.3) will outline possible screening tools for the systematic identification of synthetic interactions in a genome-wide manner.

1.1 DNA repair pathways

This chapter provides an overview over the major DDR pathways, including translesion synthesis, direct repair, mismatch repair, nucleotide excision repair, base excision repair, non-homologous end joining, homologous recombination and the Fanconi anemia pathway.

1.1.1 Translesion synthesis (TLS)

During replication, damaged DNA bases or adducts may stall replications forks, leading to genomic instability (Prakash et al., 2005). Despite the multitude of DNA repair mechanisms, during each cell cycle, the replication machinery is likely to encounter DNA lesions that would arrest canonical DNA synthesis. To allow mitotic

progression in spite of those lesions, cells have evolved mechanisms to allow for DNA damage tolerance and the completion of the cell cycle. Specialized TLS DNA polymerases have unique features that enable them to synthesize DNA past damaged bases. In an initial step, the stalled replicative polymerase is replaced with a TLS polymerase, which inserts bases opposite to the lesion in an often error-prone manner. Extension of the incorporated base is either performed by the same- or a second TLS polymerase (Sale et al., 2012). After the replication fork has passed, the damaged bases can be excised. The most abundant class of TLS polymerases belongs to the Y-family, which, in mammalian cells, consists of four members encoded by *REV1* (encoding REV1), *POLH* (encoding Polη), *POLI* (encoding Polι) and *POLK* (encoding Polκ) (Ohmori et al., 2001).

REV1 acts as a scaffold that interacts with Polη, Polι and Polκ, as well as the B-family TLS polymerase Pol ζ (Nelson et al., 1996; Sale et al., 2012). It incorporates deoxycytidine monophosphate (dCMP) opposite deoxyguanosine (dG) and abasic sites, generating mutations at G-C base pairs. Polη accumulates in replication foci and allows the bypassing of T-T cyclobutane pyrimidine dimers (CPDs), generating mutations at A-T base pairs. Defects in Polη lead to Xeroderma pigmentosum variant (XPV) that is associated with increased incidence of UV-induced skin cancers due to defective replication of UV-damaged DNA (Masutani et al., 1999). Polι also accumulates in replication foci and has a high fidelity in replicating template deoxyadenosine (dA), but is error prone in replicating deoxythymidine (dT). Polκ can accurately bypass N^2-dG adducts, but is prone to making -1 frameshift mutations. TLS DNA polymerases allow cells to tolerate potentially lethal damage, which, due to their error-prone activity, is often accompanied by unwanted mutagenesis. The activity of Y-family polymerases is therefore strictly regulated in order to stay limited to damaged DNA sites.

1.1.2 Direct repair (DR)

Direct DNA repair allows cells to reverse covalently bound DNA adducts via single repair proteins, without the necessity of an incision in the DNA backbone. To date, three major mechanisms of direct DNA repair have been identified: photolyase-, alkyltransferase- and dioxygenase-mediated direct DNA repair (Eker et al., 2009). Photolyases can reverse DNA damage caused by UV-radiation that can result in two types of lesions: CPDs and the pyrimidine pyrimidones (6–4) photoproducts (6–4 PPs). Both can be repaired by photolyases that are specific to each of the two lesions. Photolyases require blue or near-UV light in order to repair UV-induced DNA damage. Alkyltransferases can directly reverse alkylation damage. Alkylating agents

are commonly used as chemotherapeutic drugs and can generate various base adducts including methyl groups and bulky alkyl additions (Drabløs et al., 2004; Fu et al., 2012; Shrivastav et al., 2010). The effects of alkylating agents can be reversed by two direct DNA repair pathways: O^6-alkylguanine-DNA alkyltransferases (AGTs) that reverse O^6-alkylated guanines and AlkB family dioxygenases that reverse N-alkylated lesions that block Watson-Crick DNA pairing. AlkB family dioxygenases can reverse alkylation damage via oxidation by using an iron(II) site to activate an O_2 molecule for oxidation of the alkyl group, resulting in an unmodified base and formaldehyde (Drabløs et al., 2004; Falnes et al., 2007; Koivisto et al., 2004; Yi et al., 2009). Only a small subset of DNA lesions can be repaired via direct repair mechanisms. However, their essentially error-free repair property makes them particularly valuable for the maintenance of genomic integrity.

1.1.3 Mismatch repair (MMR)

In the course of DNA replication, the newly synthesized strand commonly includes errors such as insertions, deletions and mis-incorporated bases, threatening the superhelical structure of the DNA. Evolutionary highly conserved MMR core proteins can be recruited to the erroneously replicated new DNA strand, recognize and remove mismatches, resynthesize the DNA and complete the repair by ligating the nick. Defects in MMR lead to spontaneous mutations and increased cancer susceptibility. Eukaryotic MMR is initiated by binding of MutSα (MSH2/MSH6 heterodimer) to single base-base mismatches, self-complementary insertion-deletion loops (IDLs), or 1-2 base insertions or deletions (Kunkel and Erie, 2015). Mismatches longer than 2 base pairs are recognized by MutSβ (MSH2/MSH3 heterodimer) (Drummond et al., 1995). In a next step, the MutLα (MLH1/PMS2 heterodimer) endonuclease is recruited to MutSα or MutSβ (Hombauer et al., 2011). The action of MutLα is directed via the proliferating cell nuclear antigen (PCNA) to one strand. PCNA permits loading of the replication factor C (RFC), allowing the interaction between PCNA and the MutLα endonuclease, which is excising the mismatch at the 3’ site of the DNA. The resulting nick is excised by the 5’-exonuclease 1 (Exo1). Replication protein A (RPA) is subsequently recruited to the single stranded DNA (ssDNA) and the DNA is resynthesized by DNA polymerase δ. Mutations in the MutS and MutL homologues are associated with hereditary nonpolyposis colorectal cancers (HNPCCs), which are therefore classified as tumor suppressors.

1.1.4 Nucleotide excision repair (NER)

NER removes helix-distorting and bulky DNA adducts such as those caused by tobacco or UV-radiation. Around 30 proteins are known to be involved in the NER pathway, which can be divided into two sub-pathways: global genomic NER (GG-NER) and transcription coupled NER (TC-NER). GG-NER prevents mutagenesis by repairing helix-distorting lesions whereby loss of GG-NER leads to cancer predisposition. TC-NER enables unperturbed gene expression by removing transcription-blocking lesions. Defects in TC-NER lead to UV-hypersensitivity and premature aging conditions such as Cockayne syndrome (Marteijn et al., 2014). Both sub-pathways differentially recognize DNA damage, but utilize the same basic main steps to repair damaged DNA: recognition of DNA damage, excision of the damaged DNA strand, DNA synthesis and ligation.

Global genome repair pathway (GG-NER)

In GG-NER, the genome is examined for helix distorting lesions by the damage sensor protein XPC (Sugasawa et al., 1998). XPC is able to bind nucleotide mismatches and DNA structures that can destabilize the helix structure and thereby initiate GG-NER. For lesions that do not severely alter the helical structure, such as UV-induced CPDs, the UV–DDB (ultraviolet radiation–DNA damage-binding protein) complex, comprising DDB1 and DDB2, binds to the lesion first and facilitates subsequent binding of XPC, which in turn provides a substrate for binding of the transcription initiation factor IIH (TFIIH) complex, which consist of ten protein subunits and acts as transcription initiation and repair factor (Riedl et al., 2003; Scrima et al., 2008; Volker et al., 2001; Wakasugi et al., 2002). Upon loading onto DNA by XPC, the TFIIH complex scans the DNA in 5'-3' direction. Two of its components, the DNA helicases XPB and XPD, open the DNA surrounding helix-distorting lesions (Compe and Egly, 2012; Tapias et al., 2004). It is suggested that XPD contains an internal channel, through which only undamaged ssDNA, but not damaged DNA can pass (Fan et al., 2008; Liu et al., 2008; Mathieu et al., 2013; Pugh et al., 2012; Wolski et al., 2008). The XPA protein, which is a part of the TFIIH complex and due to its diverse functions plays a central role in coordinating NER, detects nucleotides with altered structures in ssDNA (Camenisch et al., 2006; Sugasawa et al., 2009). After detections, 5' and 3' lesion excision is catalyzed by the XPF-ERCC1 and XPG endonucleases in proximity to the lesion site, leaving behind a 22-30 nucleotide (nt) single-strand gap that is protected from endonucleases by binding of RPA and elicits further DNA damage signaling (Fagbemi et al., 2011). The 5' incision elicits gap-filling DNA synthesis, which, together with ligation of the

synthesized DNA fragment, is executed by PCNA, RFC, DNAPolε or DNAPolκ, DNAPolδ, DNA ligase 1 or XRCC1–DNA ligase 3 depending on the cell cycle stage (Marteijn et al., 2014; Moser et al., 2007; Ogi et al., 2010; Staresincic et al., 2009).

Transcription coupled repair pathway (TC-NER)

TC-NER is activated when RNA polymerase II (RNA Pol II) is stalled during transcription due to lesions in the template strand, leading to the recruitment of Cockayne syndrome protein A (CSA) and Cockayne syndrome protein B (CSB), which are required for the assembly of the TC-NER machinery, including UV-stimulated scaffold protein A (UVSSA), XPA-binding protein 2 (XAB21), the high mobility group nucleosome-binding domain-containing protein 1 (HMGN1) and additional core NER factors (Fousteri et al., 2006; Vermeulen and Fousteri, 2013). CSB is protected from CSA-dependent degradation by the ubiquitin-specific-processing protease USP7 (Schwertman et al., 2012). An essential step in TC-NER is the removal of the stalled RNA Pol II to allow the NER incision machinery access to the lesion. In the case of CPDs, RNA Pol II covers about 35 nucleotides on the transcribed strand (Tornaletti et al., 1999). Several RNA Pol II-removal mechanisms have been proposed, such as dissociation from the DNA strand, degradation as well as backtracking. Backtracking, a process commonly associated with transcriptional proofreading, is currently thought to be the most probable mechanism of RNA Pol II removal. CSB is thought to play a role in backtracking due to the observed translocation activity of CSB in DNA–protein complexes (Beerens et al., 2005; Citterio et al., 2000).

1.1.5 Base excision repair (BER)

The BER pathway corrects small, non-helix-distorting DNA lesions throughout the cell cycle by excising damaged bases and abasic sugars and protects against cancer, aging and neurodegeneration (Jeppesen et al., 2011; Krokan and Bjørås, 2013; Wallace et al., 2012). Lesions targeted by BER often result from spontaneous deamination, oxidation or alkylation due to spontaneous DNA decay or environmental factors such as radiation or cytostatic drug treatment (Lindahl, 1993). BER steps include excision of the base, incision, end processing, repair synthesis and ligation. Initially, lesion-specific DNA glycosylases bind to the minor DNA groove, kink the DNA and flip the damaged base out of the major groove to enable its removal and to generate an apurinic/apyrimidinic site (AP site, also called abasic site) (Huffman et al., 2005; Krokan and Bjørås, 2013). In mammalian cells, there are at least 11 different DNA glycosylases that can initiate BER. Each one of them

recognizes a small number of base lesions with varying degrees of selectivity. Glycosylases are subdivided into mono- and bifunctional glycosylases. Monofunctional glycosylases have glycosylase activity only and require AP endonucleases to cleave an AP site. Bifunctional glycosylases additionally have AP lyase activity themselves and can convert lesions into single-strand breaks without requiring AP endonucleases (Fromme et al., 2004). Ligation can only occur, when the DNA strand break has a hydroxyl group at its 3' end and a phosphate at its 5' end. In human cells, this is ensured by the polynucleotide kinase-phosphatase (PNKP) that promotes the formation of these ends during BER by phosphorylating 5' hydroxyl ends and removing phosphates from 3' ends. Lesions can be further processed either by 'short patch' BER or 'long patch' BER. In short patch BER, a single nucleotide gap is generated and subsequently filled and ligated. It is equally efficient in proliferating and non-proliferating cells and requires proteins such as DNA polymerase β (Pol β), DNA ligase I or III (LIG1, LIG3), poly (ADPribose) polymerase 1 (PARP1) and XRCC1. Long patch BER repair primarily happens in proliferating cells, whereby a 2-10 nucleotide gap is generated and filled (Almeida and Sobol, 2007; Fortini and Dogliotti, 2007; Lindahl, 2001; Robertson et al., 2009; Svilar et al., 2011; Wallace et al., 2012). Key long patch repair factors include DNA polymerase δ/ε, PCNA, the flap endonuclease FEN1, and LIG1. The choice between short- and long patch BER is depending on the specificity of the initiating glycosylase, the cell type and the cellular availability of BER factors (Bauer et al., 2011; Fortini et al., 1999; Narciso et al., 2007; Tichy et al., 2011). The choice of long patch repair is also directed by the chromatin protein high mobility group box 1 (HMGB1) that interacts with APE1 and FEN1 (Liu et al., 2010b; Prasad et al., 2007). Some BER proteins were shown to play a role in adaptive immunity and epigenetics.

1.1.6 Non-homologous end joining (NHEJ)

DNA double strand breaks (DSBs) are common events in eukaryotic cells and among the most deleterious forms of DNA damage, potentially leading to chromosomal aberrations, cellular senescence or apoptosis. Two major pathways can repair DSBs: homologous recombination (HR) and non-homologous end joining (NHEJ) (Davis and Chen, 2013; Lieber, 2010). NHEJ is active throughout the cell cycle and is likely to play the major role in DSB repair in human cells (Burma et al., 2006). It is also essential for V(D)J recombination and class switch recombination during lymphocyte development (Malu et al., 2012). NHEJ can ligate any type of DNA break ends without the need of a homologous DNA template, hence the name non-homologous end joining. NHEJ can be divided into sequential steps: 1) DNA end

recognition and complex assembly, 2) bridging of DNA ends, 3) DNA end processing 4) ligation and complex dissolution. In the first step, the Ku heterodimer, consisting of Ku70 and Ku80, is binding to the DSB (Mari et al., 2006; Uematsu et al., 2007). The Ku proteins have high affinity to DNA ends and are highly abundant in cells, which allows their rapid recruitment to DSBs (Blier et al., 1993; Downs and Jackson, 2004; Mimori et al., 1986; Walker et al., 2001). The Ku heterodimer acts as a scaffold and promotes the recruitment of the NHEJ core factors DNA-dependent protein kinase catalytic subunit (DNA-PKcs) (Uematsu et al., 2007), X- ray cross complementing protein 4 (XRCC4) (Costantini et al., 2007; Mari et al., 2006; Nick McElhinny et al., 2000), DNA Ligase IV (LIG4) (Costantini et al., 2007), XRCC4-like factor (XLF) (Yano et al., 2008) and Aprataxin-and-PNK-like factor (APLF) (Grundy et al., 2013; Kanno et al., 2007; Macrae et al., 2008). These factors interact with each other and form a stable complex at the DSB site. Upon binding of DNA-PKcs to the Ku-DNA complex, the Ku heterodimer translocates inwards on the dsDNA and the kinase activity of DNA-PKcs gets activated (Falck et al., 2005; Gell and Jackson, 1999; Singleton et al., 1999). Autophosphorylation of DNA-PKcs is thought to induce a conformational change that allows the binding of end processing enzymes to the DSB. XRCC4 directly interacts with the Ku70 subunit of the Ku heterodimer, does not possess enzymatic activity and acts as a second scaffold, allowing the recruitment of additional NHEJ factors to the DSB. It can form homodimers and tetramers, interacts with LIG4 and allows the recruitment of polymerase μ and the Werner syndrome RecQ like helicase (WRN), highlighting the importance of XRCC4 for the recruitment of processing enzymes (Cooper et al., 2000; Karmakar et al., 2002; Kusumoto et al., 2008). APLF is thought to promote the assembly of the NHEJ complex and is required for the retention of XRCC4, LIG4, and XLF at the DSB (Grundy et al., 2013; Rulten et al., 2011). In the second step, DNA ends are bridged and end stability is promoted. Upon binding of Ku70/Ku80, the heterodimer protects the DNA ends from non-specific processing, which could otherwise lead to genomic instability and holds the DNA break sites in close proximity to one another (Pang et al., 1997; Soutoglou et al., 2007), together with DNA-PKcs, which is recruited to the DSB site by the Ku heterodimer and likely promotes the formation of an end-stabilizing synaptic complex (Cary et al., 1997; Weterings and van Gent, 2004). Additional bridging of the DNA ends is achieved through the formation of super helical filaments by the XRCC4-XLF complex that also recruits further end processing enzymes. In the third step, DNA ends are processed into a ligatable form by different end processing enzymes, depending on the nature of the break (Andres et al., 2012; Hammel et al., 2010, 2011; Malivert et al., 2010). Resection enzymes include Artemis, WRN and APLF.

The processed DNA gaps are subsequently filled by the template-dependent polymerase μ and the template-independent polymerase λ (Moon et al., 2007; Nick McElhinny et al., 2005; Ramadan et al., 2004). In the fourth and final step, the broken ends are ligated by LIG4, which can ligate across gaps and ligate incompatible DNA ends (Gu et al., 2007). XRCC4 stabilizes LIG4 and stimulates its ligation activity (Grawunder et al., 1997).

When the NHEJ pathway is inactivated, DSBs can be repaired by 'alternative NHEJ' (alt-NHEJ), also known as 'microhomology-mediated end joining' (MMEJ), which functions independent of Ku proteins, LIG4 and DNA-PKcs (Wang and Xu, 2017). Several reports found alt-NHEJ to be dependent on PARP1 that binds to single strand breaks (SSBs) and DSBs and acts as a DNA damage sensor in an early step of alt-NHEJ (De Vos et al., 2012; Hassa et al., 2006). The pathway relies on exposed microhomologous sequences flanking the broken DNA ends and is associated with DNA deletions surrounding the original DSB site and chromosomal translocations. In a first step, 5'-3' end resection exposes microhomologous regions on both ends of the broken DNA. The microhomologous sequences are then annealed, forming an intermediate structure with 3'-flap and gaps on both break sides, which are subsequently removed by endonucleases such as XPF/ERCC1. Polymerases fill in the gaps and in a final step, DNA ligase III/I (LIG3/LIG1) mediate end ligation. Since MMEJ removes a substantial part of the DNA surrounding the break site, it is a highly mutagenic repair pathway.

1.1.7 Homologous recombination (HR)

Homologous recombination is the most error-free mechanism that allows cells to repair DSBs. During HR, DSBs are repaired using sister- daughter- or homologous chromosomes as a template. This ensures a higher probability of joining the correct ends compared to NHEJ, but limits HR to the S- and G2 phase of the cell cycle. Although HR is a highly complex mechanism with several sub-pathway choices, it can be divided into four basic steps: Initiation (DNA resection); homologous DNA pairing and strand exchange; branch migration and dissolution and resolution of Holiday junctions (Kowalczykowski, 2015). To initiate HR, broken DNA ends are processed to produce ssDNA that allows the formation of RecA/RAD51 filaments. This is achieved via recombination-specific helicases and nucleases (Symington, 2014). The CtIP-regulated MRN complex consists of Mre11, Rad50 and Nbs1 and initiates HR by binding to dsDNA breaks and resecting from 3' to 5' (Paull and Gellert, 1999). After this initial processing, further resection generates larger regions of ssDNA that are required for further progression of HR (Lamarche et al., 2010).

This resection requires the helicase activity of the RecQ helicase BLM, as well as the nuclease activity of DNA2 and generates kilobase-sized 3' ssDNA overhangs (Mimitou and Symington, 2008; Zhu et al., 2008). The helicase activity of BLM is stimulated by TOPOIIIα, RMI1 and RMI2, which together form the 'BLM complex' (sometimes referred to as 'BTR complex'), as well as by DNA2 (Daley et al., 2014). Besides BLM, another RecQ helicase called WRN also interacts with DNA2 and contributes to long-range resection of DSBs (Sturzenegger et al., 2014). Alternatively, long-range resection can be carried out by the exonuclease EXO1, whereby its affinity to DNA ends is increased by BLM and its processivity is increased by EXO1 (Tomimatsu et al., 2012). The resection product is protected from BLM-dependent disruption by RAD51 (Nimonkar et al., 2008). After resection, RAD51 binds to the ssDNA and assembles into filaments that allow pairing of homologous DNA and strand exchange in an ATP-dependent manner that is stimulated by RPA. The RAD51 filaments on ssDNA are termed 'presynaptic complex', due to their formation before the 'synaptic' DNA pairing step. The presynaptic complex searches for DNA sequence homology and mediates the pairing and exchange of DNA strands. The assembly of RAD51 onto RPA-bound ssDNA is mediated by BRCA2, which delivers RAD51 molecules to the ssDNA (Jensen et al., 2010; Liu et al., 2010a). The annealing to the homologous sequence is mediated by RAD52 (Jensen et al., 2010). RAD51 interacts with the tumor suppressor PALB2, which stimulates joint DNA molecule formation (Buisson et al., 2010; Dray et al., 2010). Helicases such as BLM or FANCM bind to the resulting structure with high affinity and promote branch migration (Gari et al., 2008; Karow et al., 2000). The joint duplexes form an intermediate structure called double Holiday Junction (dHJ) (Holliday, 2007; Matos and West, 2014). The separation of the joint molecules can happen in two distinct ways: either 'dissolution', resulting in non-crossover (NCO) recombinants or 'resolution', resulting either in crossover (CO) or NCO recombinants. Dissolution is mediated by the BLM complex, consisting of the BLM helicase (BLM), the topoisomerase IIIα (TOP3A), RMI1 and RMI2, which were shown to migrate and decatenate dHJs (Cejka et al., 2010; Ellis et al., 1995; Wu and Hickson, 2003). This complex can separate and unlink the DNA molecules topologically (Wu and Hickson, 2003). Cells that lose the ability of dissolution due to BLM loss-of-function show an increased frequency of COs, resulting in excessive sister chromatid exchanges (SCEs) (Ray and German, 1984). The associated disease is called Bloom syndrome, which is an autosomal recessive disorder, characterized by short stature, cancer predisposition and genomic instability (Karow et al., 2000; Straughen et al., 1998). In these cells, the formation of COs is largely

depending on MUS81-EME1, SLX1-SLX4 and GEN1, which mediate the resolution of dHJs (Wechsler et al., 2011; Wyatt et al., 2013). The MUS81-EME1 complex forms a structure-selective nuclease that cleaves HJs (Amangyeld et al., 2014; Pepe and West, 2014). SLX1-SLX4, which can also cleave HJs, binds to MUS81-EME1 to form a hetero-tetrameric complex that cleaves dHJs more effective than both complexes alone (Fekairi et al., 2009; Svendsen et al., 2009; Wyatt et al., 2013). GEN1 acts as a debranching enzyme that removes unprocessed HJs and Y-forks that remain after unfinished recombination and replications. HR is a universal biological mechanism that is conserved across all three domains of life as well as viruses. The proteins involved in HR are topics of intensive research, due to their association with various forms of cancer.

1.1.8 Fanconi anemia (FA)

The Fanconi anemia pathway protects genomic integrity by repairing DNA interstrand crosslinks (ICLs), which are covalently binding the Watson and Crick strands of DNA and thereby impede transcription and replication (Kottemann and Smogorzewska, 2013). Proteins within the FA pathway are called FA complementation groups, whose gene symbols carry the root FANC, followed by a letter that is assigned in alphabetical order, according to the discovery of their role in FA. In humans, defects in the FA signaling pathway lead to a rare disease ‘Fanconi anemia’ that affects about 1 in every 100.000 births and is associated with severe conditions such as bone-marrow failure, susceptibility to solid tumors and acute myeloid leukaemia (AML), infertility and congenital abnormalities (Auerbach, 2009; Rosenberg et al., 2011). FA is inherited in an autosomal recessive manner, except for FANCB, which is located on the X-chromosome. So far, 22 genes are considered FA complementation groups (**Table 1**) (Fanconi anemia complementation groups | HUGO Gene Nomenclature Committee). The FA complementation group most frequently mutated in FA patients is *FANCA* with a patient frequency of 64%, followed by *FANCC* with 12% and *FANCG* with 8% (Wang and Smogorzewska, 2015).

FANC gene	Synonyms
FANCA	FACA, FANCH, FAA, FA-H, FAH
FANCB	FAB, FLJ34064, FAAP95
FANCC	FACC, FAC, FA3
FANCD1	BRCA2, FACD, FAD, FAD1, BRCC2, XRCC11
FANCD2	FACD, FAD, FA-D2
FANCE	FACE, FAE
FANCF	FAF
FANCG	XRCC9, FAG
FANCI	KIAA1794, FLJ10719
FANCJ	BRIP1, OF, BACH1
FANCL	PHF9, FLJ10335, FAAP43, Pog
FANCM	KIAA1596, FAAP250
FANCN	PALB2, FLJ21816
FANCO	RAD51C, RAD51L2
FANCP	SLX4, BTBD12, KIAA1784, KIAA1987
FANCQ	ERCC4, XPF, RAD1
FANCR	RAD51, RAD51A, RECA, HsRad51, HsT16930, BRCC5
FANCS	BRCA1, RNF53, BRCC1, PPP1R53
FANCT	UBE2T, HSPC150
FANCU	XRCC2
FANCV	MAD2L2, MAD2B, REV7, POLZ2
FANCW	RFWD3, FLJ10520, RNF201

Table 1: Overview of all characterized FA complementation groups in alphabetical order. *FANCK* has not been used for nomenclature to avoid verbal confusion with *FANCA*. *FANCH* was later merged into *FANCA*, since the sole identified *FANCH* patient in retrospect turned out to be a *FANCA* patient (Joenje et al., 2000).

Cells derived from FA patients show increased sensitivity to DNA interstrand crosslinking agents such as mitomycin C (MMC) or diepoxybutane (DEB), which is why those agents are commonly used for the diagnosis of FA (Auerbach, 2009). These compounds constitute potential exogenous sources of ICLs, together with chemotherapeutic agents such as Cisplatin (Clauson et al., 2013). However, most people, including FA patients, never come into contact with those crosslinking agents throughout their lives, indicating a role of endogenous crosslinking sources in FA. Oxidative stress can form the nucleophilic crosslinking agents malondialdehyde and acrolein from lipid peroxidation. The most intensively studied endogenous source of ICLs in FA however are reactive aldehydes that are by-products of alcohol detoxification and histone demethylation.

The FA pathway is involved in numerous cellular functions, resulting in a multitude of biological effects upon disruption. One is the dysfunction of haematopoietic (and other) stem- and progenitor cells, resulting from elevated p53 signaling in stem cells that impairs cellular differentiation, resulting in a reduced stem cell pool at birth. This is thought to be responsible for the developmental abnormalities and infertility of FA patients. The FA pathway also functions as a barrier to more mutagenic repair pathways such as NHEJ, thereby suppressing the accumulation of genomic mutations and preventing tumorigenesis. Finally, the FA pathway was shown to preserve replication-fork stability during S-phase. This interaction with various genome maintenance pathways makes FA signaling an excellent research topic to investigate the interplay of cellular networks, which will subsequently be discussed in further detail.

Fanconi anemia and ICL repair: The FA proteins work together to enable ICL repair by coordinating nucleases for cutting out the ICL and further nucleolytic processing needed for TLS and HR. Unrepaired ICLs lead to an accumulation of stalled replication forks in S phase, which leads to the activation of the FA pathway by ATR mediated phosphorylation of the FA core complex, which consists of FANCA, B, C, E, F, G, L, and M, as well as accessory proteins such as FAAP20 and FAAP24. Upon recruitment of the core complex to the stalled replication fork, the catalytic E3 ligase FANCL together with the E2 ligase UBE2T, ubiquitinate the downstream I-D2 complex, consisting of FANCI and FANCD2 (Alpi et al., 2008; Machida et al., 2006; Meetei et al., 2003). This is considered to be the main activation step in FA signaling, whereby FANCD2 is monoubiquitinated at Lys561 and FANCI to a lesser extent at Lys523 (Smogorzewska et al., 2007; Taniguchi et al., 2002). This ubiquitination is stimulated by the presence of DNA, suggesting its occurrence on chromatin (Sato et al., 2012). The components of the FA core complex as well as the I-D2 complex were shown to bind to ICLs in a replication independent manner (Shen et al., 2009). The phosphorylated I-D2 complex orchestrates the actions of further repair factors such as SLX4/FANCP, which acts as a scaffold for the nucleases XPF/FANCQ-ERCC1, MUS81-EME1 and SLX1 (Andersen et al., 2009; Fekairi et al., 2009; Muñoz et al., 2009; Svendsen et al., 2009). At the site of DNA damage, these nucleases make incisions on both sides of the cross-linked nucleotides, ‘unhooking’ the ICL. In this process, XPF-ERCC1 is the most important nuclease for ICL resistance, while MUS81-EME1 and SLX1 play less prominent roles (Bhagwat et al., 2009; Kim et al., 2013). Other, non-SLX4-bound nucleases such as FAN1 and SNM1A are involved in this incision step as well. The SNM1A exonuclease prepares the DNA substrate to

be further processed by TLS polymerases, which facilitate the repair of one DNA duplex that then acts as a template for the repair of the other strand using HR (Wang et al., 2011). After activation, the I-D2 complex needs to be de-ubiquitinated by USP1.

Tumorigenesis upon loss of FA components: The most common tumor susceptibility in FA patients is a predisposition for AML, which may derive from the same stem cell instability that triggers the anemia phenotype, followed by squamous head and neck cell carcinomas. These disease phenotypes are characteristic for patients with homozygotes mutations in *FANC* genes, however downstream effectors of FA signaling that are directly involved in HR can increase the tumor susceptibility even when mutated in only one copy (Deans and West, 2011; Meindl et al., 2010; Rafnar et al., 2011; Rahman et al., 2007; Seal et al., 2006; Tischkowitz et al., 2007; Walsh et al., 2011). Those factors include FANCD1/BRCA2, FANCN/PALB2, FANCJ/BRIP1 and FANCO/RAD51C. Their stronger correlation with cancer stems from their general involvement in DNA repair that is not confined to the FA pathway, as it is the case with members of the FA core- or I-D2 complex.

Sensitivity to replication stress: Besides its role in ICL repair, the FA pathway is required for the protection of replication-forks under stress conditions. Even in cells not treated with ICL-inducing agents, the I-D2 complex gets monoubiquitinated during S-phase (Howlett et al., 2002). Also non-ICL inducing agents such as hydroxyurea (HU) induce FA signaling by depleting nucleotide pools, exposing the cells to replication stress (Howlett et al., 2005).

Interaction with other repair pathways: The FA pathway intersects with numerous other DNA repair pathways. Especially interactions of FA with the BLM helicase, which was discussed in detail in the section ‘1.1.7 Homologous recombination’, were shown to occur at a clinical and a molecular level. Loss of BLM leads to the autosomal recessive disease called Bloom syndrome. Some individuals with BLM mutations were diagnosed with FA, due to their symptomatic overlaps, which include pigmentation lesions, immunological defects, reduced fertility, short stature, genomic instability and cancer predisposition (Ellis and Offit, 2012). BLM participates in the dissolution of dHJs, which are an intermediate structure in HR (Wu and Hickson, 2003). On a molecular level, the FA core complex physically interacts with the BLM complex via FANCM, forming a super-complex at sites of replication forks that are impeded by ICLs (Deans and West, 2009). Also molecular interactions between BLM

and FANCJ at stalled replication forks have been described (Suhasini et al., 2011). Both the FA I-D2 complex and BLM were shown to localize to ultrafine anaphase bridges, which are narrow DNA structures that from between condensed DNA during anaphase as a result of unresolved recombination intermediates (Chan et al., 2009). Additionally, SLX4/FANCP was shown to collaborate with BLM during the resolution of dHJs (Wechsler et al., 2011). Another repair pathway that is closely linked to the FA pathway is NHEJ. The FA pathway is thought to play a role in pathway choice, whereby it funnels the repair of ICL induced DSBs towards HR, instead of the more mutagenic NHEJ pathway. This is thought to contribute to the chromosomal abnormalities, observed in the absence of FA signaling upon induction of ICLs. Previous studies in different cellular and genetic backgrounds have demonstrated, that the sensitivity of FANC deficient cells to ICL-inducing agents can be alleviated by additional loss of NHEJ components. This was shown in *C. elegans*, where loss of LIG4 reduced crosslink sensitivity in a fcd-2 (FANCD2) deficient background (Adamo et al., 2010). In chicken DT40 cells, loss of Ku70 partially rescued crosslink sensitivity in a FANCC deficient background (Pace et al., 2010). In mouse embryonic fibroblasts (MEFs), inhibition of DNA-PKcs by NU7026 lead to a partial rescue of crosslink sensitivity in Fanca and Fancc deficient cells (Adamo et al., 2010). In human, cells depleted for FANCD2 by small interfering RNA (siRNA) showed decreased sensitivity to ICLs in a DNA-PKcs deficient background. Likewise, inhibition of DNA-PKcs lead to partial rescue of sensitivity to ICLs in HeLa cells depleted for FANCA as well as FANCD2. Finally, depletion of KU80 via siRNA resulted in partial rescue of crosslink sensitivity in FANCD2- as well as FANCC deficient patient cells (Adamo et al., 2010).

Taken together, these findings demonstrate that deficiencies in one pathway can, at least partially, be compensated by inhibiting a competing pathway that might otherwise lead to a more unfavorable outcome. Those compensating interactions are commonly referred to as synthetic viability, synthetic rescue or synthetic suppression and will be discussed in detail in the following subchapter.

1.2 Synthetic interactions

To date, more than 6,000 Mendelian disorders have been described (McKusick, 2007). Despite the rapid development of novel therapeutic interventions, a majority of those disorders can only be treated symptomatically with no curative treatment in sight (Dietz, 2010). One reason for this sobering rate of success is that the use of small-molecule inhibitors can hardly restore protein activity in loss-of-function (LOF) mutations, which underlie many of the Mendelian disorders. Although gene therapy

could one day help overcoming this limitation in certain cases, the current inability to precisely and reliably deliver genetic constructs to various parts of the body is hindering the application of this approach. However, it is possible to inhibit certain gene-products using small molecule inhibitors. In the context of cancer therapy, small molecule inhibitors are thoroughly researched to develop drugs that induce synthetic lethality in cancer cells. Likewise, genetic defects that cannot be corrected directly might be compensable by exploiting synthetic viable interactions.

1.2.1 Synthetic lethality

Synthetic lethality occurs when a combination of deficiencies in two or more genes leads to cell death, whereas a deficiency in only one of them is viable (**Fig. 1a**) (Nijman, 2011). Synthetic lethality was first observed by the American geneticist Calvin Bridges in 1922 to describe combinations of mutations in *D. melanogaster* that in combination confer lethality (Bridges, 1922). However, the term synthetic lethality was not introduced before 1946, when Theodore Dobzhansky observed a similar phenomenon in *D. pseudoobscura* (Dobzhansky, 1946). In this context, the term 'synthetic' is used in its ancient Greek sense, meaning that the combination of two entities can yield something new that is different from a mere combination of the initial attributes. Synthetic lethality can also occur between genes and small molecules. In this context, the lethal interactions are typically used to develop cancer therapies that exploit the mutational background of cancer cells to specifically kill the malignant cells. The first approved molecular targeted therapy exploiting synthetic lethality for cancer treatment was the inhibition of PARP to target BRCA1 and BRCA2 deficient tumor cells (Bryant et al., 2005; Farmer et al., 2005; Fong et al., 2009). This treatment receiving FDA approval in 2016 and has remarkably mild side effects. This success inspired the systematic search for synthetic viable interactions throughout the whole genome. Historically, many of the first screens for synthetic lethality were performed in *S. cerevisiae*. Its small genome, the fast doubling time, its ability to exist in a haploid- as well as a diploid state and the fact that knock-out (KO) collections for all annotated yeast genes are publicly available, made it the model organism of choice for this endeavor (Winzeler et al., 1999). In recent years, the development of novel technologies such as haploid genetic screens in human cells (Carette et al., 2009, 2011; Forment et al., 2017), whole genome CRISPR knock-out libraries (Shalem et al., 2014) and affordable high-throughput sequencing enabled the genome-wide search for synthetic interactions in human cells. Though these approaches are commonly used to identify synthetic lethal interactions for cancer therapy, they also allow the search for synthetic viable interactions (**Fig. 1b**).

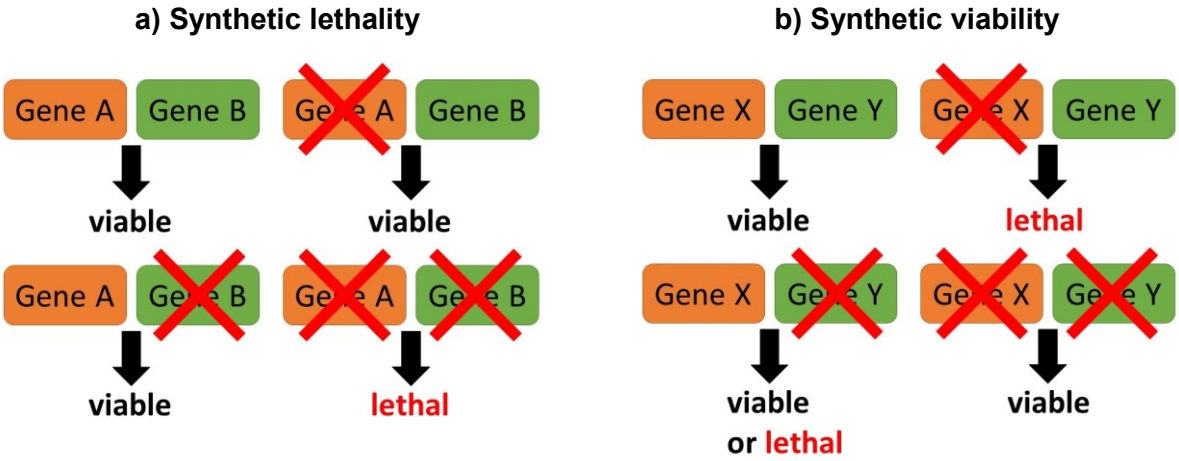

Thesis Figure 1: Schematic of synthetic lethality and synthetic viability. (a) Synthetic lethality occurs, when simultaneous mutations in a gene pair are lethal, whereas mutation of each gene alone is viable. (b) Synthetic viability occurs, when loss of one gene leads to cell death, while additional loss of a second gene compensates the initial defect and confers cell viability.

1.2.2 Synthetic viability

Synthetic viability allows the suppression of a disease phenotype by mutation of another gene or inhibition of the corresponding gene product respectively. Synthetic viability is a promising concept for the treatment of Mendelian LOF mutations, since it aims at restoring a healthy phenotype, without the necessity of re-introducing a functional version of the initially mutated gene. Instead, the defect is compensated by loss or functional inhibition of a second gene or gene product, which is clinically more practical than the re-introduction of genes. Therefore, exploiting synthetic viable interactions to alleviate disease phenotypes is a promising avenue to compensate for LOF mutations in Mendelian disease. The identification of disease-compensating mutations has proven successful in several model organisms. For example, mutations in globulin genes were shown to partially compensate primary mutations in β-globin genes and thereby diminish the severity of sickle cell anemia (Galarneau et al., 2010). In some cases, the introduction of a mutation reduces a disease phenotype that is not caused by an initial mutation. Mutations in the *CCR5* gene were shown to confer resistance against HIV infections (Philpott et al., 1999). Nevertheless, these interactions are also commonly described as synthetic viable, since a disease phenotype is suppressed by the presence of a specific mutation. Likewise, a LOF mutation in *PCSK9* was shown to protect carriers from high lipid levels and associated heart disease (Cohen et al., 2005) and LOF mutations in the zinc transporter *SLC30A8* were found to protect from type 2 diabetes (Flannick et al.,

2014). Recently, a dog was identified, carrying a mutation in the gene *Jagged1* that compensated for Duchenne muscular dystrophy (Vieira et al., 2015). This illustrates *Jagged1* as a promising target for an analogous treatment in human. The potential for synthetic viable interactions to alleviate human disease was recently demonstrated by a study analyzing sequence- and genotype data from 589,306 people to identify healthy individuals carrying penetrant Mendelian disease-causing mutations, without expressing any identifiable disease phenotype (Chen et al., 2016). The study identified 13 healthy individuals, carrying mutations for 8 different diseases which are Cystic fibrosis, Smith-Lemli-Opitz syndrome, Familial dysautonomia, Epidermolysis Bullosa simplex, Pfeiffer syndrome, Autoimmune polyendocrinopathy-candidiasis-ectodermal dystrophy syndrome, Acampomelic campomelic dysplasia and Atelosteogenesis. Whether those disease-causing mutations were compensated by mutations in other genes, second-site mutations or environmental factors was not determined. The results nevertheless impressively demonstrate that several mutations that are strongly associated with severe human diseases can in principal be compensated. This population-driven approach of identifying synthetic viable interactions is limited by the availability of genomic datasets from healthy individuals and restricted to early-onset diseases that have an exceptionally strong genotype-phenotype correlation. Systematic cell culture-based screens for synthetic viable interactions would offer a more unbiased approach for discovery, however the lack of suitable functional readouts exacerbates this endeavor. Extragenic synthetic viable mutations can be subdivided into two classes. Informational suppressor mutations change either the protein translational or mRNA transcriptional machinery, thereby reinterpreting the primary mutation. Functional suppressor mutations occur in a second gene and functionally compensate for the initial defect (Dronamraju, 2017). A recent publication examined literature-curated and unbiased experimental data to generate a network of functional synthetic viable interactions throughout the yeast genome, using growth rate as a proxy for cellular fitness (van Leeuwen et al., 2016). The results showed that many synthetic viable interactions in the context of DNA replication and repair emerge due to the activation of alternative DNA repair pathways. Many synthetic viable interactions occurred between functionally related genes that are involved in the same biological process (Costanzo et al., 2010; Huttlin et al., 2015; Magtanong et al., 2011). Genes interacting in a synthetic viable manner showed the tendency of being co-expressed and encoding proteins that function in the same cellular compartment or belong to the same pathway or protein complex. This finding reinforces the results of our study, which will be discussed in chapter

two, since the synthetic viable interactions described in our study also occur within the same pathway.

1.3 Genome wide screening tools

Throughout most of the twentieth century, large-scale genetic studies were hampered by the limitations of human population studies, laborious animal models and the inability to efficiently perturb cell culture models in a targeted manner. The discovery of genome-wide perturbation tools such as random mutagenesis, RNA interference (RNAi) and CRISPR-Cas9 allowed the systematic study of gene function in human cells (Fire et al., 1998; High Throughput Screening Methods, 2016; Jinek et al., 2012). These tools enable the efficient screening for genetic interactions, including synthetic lethal and viable interactions, in a genome-wide manner using forward genetics that perturbs gene function and selects for a desired phenotype. Throughout the past decade, pooled screens in mammalian cells became increasingly popular due to their simple implementability in almost any laboratory performing cell culture (Koike-Yusa et al., 2014; Shalem et al., 2014; Wang et al., 2014). This subchapter will discuss the background as well as the advantages and disadvantages of the most common high-throughput screening methods to vindicate the choice of genome-wide screening tools utilized in our study.

1.3.1 Random mutagenesis

The oldest method for introducing genetic perturbations in a genome-wide manner is random mutagenesis using mutagenic chemicals or ionizing radiation. The disadvantage of this method however is the challenging identification of the genetic alterations that are responsible for a certain phenotype, limiting this approach to low or medium throughput screens. Historically, the identification of underlying mutations was achieved by effortful cloning of genomic libraries. With the emergence of affordable high-throughput sequencing technologies, this effort got obsolete due to the ability of multiplexing genomic samples. Random mutagenesis has therefore been successfully applied for compound target identification in mammalian cells (Junne et al., 2015; Wacker et al., 2012). Compared to more targeted approaches however, random mutagenesis is still far from high-throughput due to its effortful and costly analysis. Furthermore, a major disadvantage is the difficulty to distinguish between phenotype-causing- and bystander mutations.

1.3.2 RNA interference

RNAi is a mechanism by which double stranded RNA (dsRNA) is suppressing the expression of genes through targeted degradation of complementary messenger RNA (mRNA) (Fire et al., 1998). Originally the RNAi system was described in *C. elegans*, however it is conserved in eukaryotic cells and was used extensively to systematically knock-down (KD) gene expression in pooled and arrayed screens. For the first time, this technology enabled targeted genetic screens in higher eukaryotic cells by allowing the design of genome-wide KD libraries (Boutros and Ahringer, 2008). RNAi screens can be carried out using transient transfection of siRNA or long double stranded siRNA precursors. This approach is typically chosen for arrayed screening processes in which each siRNA clone is positioned in an individual well. This allows automated high-throughput well-by-well screens that have been utilized to examine a broad range of biological processes (Boutros et al., 2004; Lipinski et al., 2010; MacKeigan et al., 2005; Yin et al., 2013). However, early siRNA screens revealed potential sources of error: A high false positive rate due to off target effects as well as a high false negative rate due to lack of efficacy for many siRNAs. The results of HIV host factor screens published by four independent groups revealed a hit-overlap of less than 7%, raising the question regarding the reliability of siRNA screens (Brass et al., 2008; Goff, 2008; König et al., 2008; Yeung et al., 2009; Zhou et al., 2008). These limitations can be partially constrained by the use of multiple independent siRNA libraries (Zhu et al., 2014). This redundancy approach is commonly referred to as MORR (multiple orthologous RNAi reagents).

In contrast to arrayed transient siRNA screens, pooled RNAi screens are commonly performed using stable expression of RNAi constructs via lentiviral delivery of short hairpin RNAs (shRNAs) (Berns et al., 2004; Moffat et al., 2006; Paddison et al., 2004). Pooled shRNA screens are using molecular barcodes for the retrospective assignment of an observed phenotype to the responsible shRNA. This process is called back-end deconvolution and requires deep sequencing. Compared to arrayed screens, this method comes at lower experimental costs and enables screening for phenotypes at alter time points that could not be observed with transiently transfected siRNAs (Paddison et al., 2004; Silva et al., 2005). The scalability of pooled screening approaches and the efficiency of lentiviral transfection of numerous cell types made pooled shRNA screens a valuable tool for identifying synthetic lethal interactions in cancer cells (Barretina et al., 2012; Cowley et al., 2014; Marcotte et al., 2012; Silva et al., 2008), as well as studying the mechanisms of action for chemical compounds and toxins (Bassik et al., 2013). The RNAi pathway enables gene silencing via two convergent mechanisms (Sigoillot and King, 2011; Wilson and

Doudna, 2013). In the canonical pathway, the siRNA guide strand incorporates into the RNA induced silencing complex (RISC) and binds with perfect complementary to a target RNA molecule, thereby initiating its degradation. In the related microRNA (miRNA) pathway, mRNA translation is comparably repressed by miRNA that is loaded onto the RISC. However, miRNA can inhibit the translation of different mRNAs because its pairing via a six nucleotide seed region is imperfect. Large scale screens try to compensate this vulnerability by using ultra-complex pooled libraries that target each gene with up to 25 unique RNAi constructs (Hoffman et al., 2014; Kampmann et al., 2013, 2014). This comes at the expense of additional experimental and sequencing costs. Furthermore, algorithms have been developed that allow the prediction of potential off target effects and the according removal of false positive hits from screening data (Buehler et al., 2012; Sigoillot et al., 2012). Another major disadvantage of RNAi screens is the likelihood of low KD efficiency. Especially transcripts with a high turnover rate tend to be difficult so silence whereby a high percentage of functional protein can retain within the cell. At the same time, this partial KD can be an advantage, since it allows the investigation of essential or lethal genes. Another shortcoming of RNAi screens is that in order for mRNAs to be degraded, they must be exported to the cytoplasm. This hinders the functional analysis of noncoding genes that express regulatory RNAs. Those RNAs often control translation and transcription within the nucleus, where they are not accessible to the RNAi machinery. Taking these obstacles into account, the latest generations of optimized RNAi libraries together with advanced quality control algorithms provide considerably more robustness than earlier KD approaches. In a recent publication, an ultra-complex pooled shRNA library performed in a comparable way to a CRISPR-based screen (Kampmann et al., 2015). Using a sub-library targeting a total of 2,933 genes associated with proteostasis in K562 cells, the investigators were screening for genes controlling the sensitivity to a cholera-diphtheria fusion toxin (CTx-DTA) using both an RNAi, as well as a CRISPR-based screening approach. In total, the data showed 48 robust hits unique to RNAi, 40 hits unique to CRISPR and an overlap of 21 hits. These data suggest that although RNAi screens have considerable limitations, they can be utilized to complement more recent KO screening approaches.

1.3.3 Insertional mutagenesis

Before the development of CRISPR, targeted gene KO was laborious and time consuming and therefore not applicable to large-scale screening applications. Instead, LOF screens were performed by insertional mutagenesis either via the use

of transposons or retroviruses. Upon development, transposon screens were mostly carried out in *D. melanogaster* and *C. elegans*, requiring extensive back-crossing to generate homozygous mutants (Boulin and Bessereau, 2007). In mammalian cells, transposon-dependent insertional mutagenesis was hampered by a lack of active transposons until the development of a synthetic transposon termed 'Sleeping Beauty' in 1997 (Ivics et al., 1997), followed by the development of numerous transposable elements suitable for random genetic disruption in human cells (Skipper et al., 2013). In parallel, the technology for random genetic disruption via the integration of retroviral elements was developed (Uren et al., 2005). Random insertional mutagenesis approaches are aggravated by the fact, that protein coding genes account for less than 2% of the human genome, leaving the majority of insertions without observable phenotype. The selection for integration events within coding regions was enabled by the development of gene trapping cassettes, consisting of a promoterless reporter gene that is flanked by an upstream 3' splice site and a downstream transcription termination sequence (Friedrich and Soriano, 1991). When inserted into an intron of an expressed gene, the endogenous promoter transcribes the gene trap cassette as a fusion transcript, whereby the exon upstream of the insert is spliced in frame to the reporter. At the integrated termination sequence, transcription is terminated prematurely, generating a nonfunctional truncated transcript. Gene trap cassettes therefore both inactivate and report the expression of the gene at the insertion site and simultaneously provide a DNA tag that allows the identification of the disrupted gene by sequencing. When generating random loss-of-function mutations in diploid cells, the effects of a genetic disruption are likely to be masked by the second, functional copy of the gene. A milestone in random disruption screens was therefore the development of haploid human and mouse cell lines, enabling the reliable manifestation of associated phenotypes (Carette et al., 2009; Elling et al., 2011; Essletzbichler et al., 2014; Leeb and Wutz, 2011). This prompted the systematic investigation of gene essentiality and synthetic lethal interactions and also enabled the robust identification of synthetic viable interactions using gene trap vectors in haploid backgrounds (Blomen et al., 2015). Given sufficient cell numbers, gene trap screens can yield genome-wide coverage of the inserted cassette.

1.3.4 CRISPR library screens

The latest tool for genetic studies on a genome-wide level, are CRISPR-based library screens, enabling targeted genetic perturbations in numerous cellular backgrounds. The CRISPR system was first identified as an adaptive immune system within

bacteria that functions via an RNA-guided endonuclease that degrades the DNA of invading phages (Sternberg and Doudna, 2015; Wright et al., 2016). The adaptability of this system to introduce targeted DSBs in mammalian cells made CRISPR one of the most remarkable genetic developments of the recent past, enabling targeted genome-wide LOF screens in human cells for the first time (Cho et al., 2013; Cong et al., 2013; Jinek et al., 2013; Mali et al., 2013a; Shalem et al., 2015; Xue et al., 2016). The most widely adopted CRISPR tool is the CRISPR-Cas9 system derived from *S. pyogenes* (Gasiunas et al., 2012), in which the Cas9 endonuclease is directed to a genomic DNA locus via a guide RNA (gRNA), containing a 20 nucleotide sequence that base pairs with a genomic target sequence (Jinek et al., 2012). This binding requires the presence of a protospacer adjacent motif (PAM) at the target site (Mojica et al., 2009). The PAM sequence is 'NGG'. This low PAM sequence complexity allows the targeting of even small genes at multiple sites. Upon recruitment to a target site, Cas9 introduces blunt ended DSBs. Repair of those lesions via NHEJ can lead to insertions or deletions that frequently result in gene-inactivating frame-shift mutations (Hou et al., 2015; Mandal et al., 2014). Stochastically, the genomic three-letter code would suggests, that roughly two thirds of all insertion/deletion mutants result in a gene distorting frame-shift mutation (Dolan et al., 2015; Li et al., 2012). Empirically however, it was shown that the sequence of a gRNA influences the probability of producing frame-shift mutations according to rules, that are not yet fully understood (Bae et al., 2014a). Furthermore, targeting of conserved domains shows increased gRNA efficacy, presumably because in-frame mutations are less well tolerated in those regions (Munoz et al., 2016; Shi et al., 2015). The availability of a broad range of targeted CRISPR libraries, as well as the simple producibility of custom made libraries make this technology easy to adopt in most cell culture based laboratories (Doench et al., 2016; Horlbeck et al., 2016; Read et al., 2017; Wang et al., 2014). A multitude of websites can assist the design of desired gRNAs (Bae et al., 2014b; Doench et al., 2014; Graham and Root, 2015; Haeussler et al., 2016; Heigwer et al., 2014; Meier et al., 2017). Most commonly, CRISPR screens are performed in a pooled manner by introducing a lentiviral library into a desired cell line to KO a defined set of genes-of-interest. The virus acts a vector to stably integrate the genetic sequence of Cas9 and the gRNA into the cellular genome. This can be achieved by using a single lentiviral vector that is transfecting Cas9 as well as the gRNA sequence simultaneously, or by using a two-vector system, in which only the gRNAs are transfected into a cell line, that was previously infected with Cas9 to create a cell line that stably expresses the endonuclease. The two-vector system offers higher virus titers due to the

considerable size of the Cas9 sequence that aggravates simultaneous packaging of Cas9 and a gRNA sequence into one viral capsid (Sanjana et al., 2014). However, the generation of stable Cas9 expressing cell lines can be challenging in primary cells. Besides defining the genomic target site, the integrated gRNA sequences act as molecular barcodes that allow the quantification of edited cells using next generation sequencing of isolated genomic DNA (Shalem et al., 2014; Wang et al., 2014). The choice or design of the gRNA library is a key determinant for the success of a CRISPR library screen. To increase the statistical reliability of hits, most primary screens target each gene with multiple different gRNAs. Compared to the first generation of CRISPR library screens, optimizations in gRNA design, taking into account the GC content and additional factors, have led to more effective second generation libraries (Doench et al., 2016). Pooled CRISPR screens require an assay that separates cells displaying a desired phenotype from those that do not. This can be achieved using a viability readout and a positive or negative selection of cells. Positive selection screens generally show a large signal window due to the prominent expansion of desired clones, while most cells in the population are killed. Among the first published CRISPR screens were drug resistance screens using positive selection in the presence of 6-thioguanosine (6-TG), etoposide or vemurafenib (Koike-Yusa et al., 2014; Shalem et al., 2014; Wang et al., 2014). Since the majority of cells is eliminated, positive selection screens often yield a small number of highly enriched hits, simplifying the choice of follow-up experiments. In contrast, negative selection screens, also referred to as dropout screens, require a higher total gRNA representation, therefore cell numbers, to avoid bottlenecks and more sequencing depth compared to positive selection screens. Negative selection screens are often used to identify tumor cell specific dependencies (Anderson et al., 2008; Cheung et al., 2011; Hart et al., 2015; Kryukov et al., 2016; McDonald et al., 2017; Tsherniak et al., 2017; Tzelepis et al., 2016; Wang et al., 2017). Recently, two studies aimed at cataloging all essential human genes using CRISPR library negative selection screens (Hart et al., 2015; Wang et al., 2015). Both CRISPR screens recovered 4-5 times more essential genes per cell line compared to shRNA screens. A gene trap screen that was performed in parallel pointed to the superior performance of CRISPR based screens for the identification of essential genes (Wang et al., 2015). Analogous to RNAi screens, CRISPR screens can have unwanted off-target effects, since Cas9 tolerates some degree of mismatch between the gRNA and the genomic target sequence. However, using optimized gRNA design and multiple gRNAs targeting the same genes helps to compensate this risk. Meanwhile, high-fidelity Cas9 variants with reduced off-target susceptibility were

developed and methods for the genome-wide detection of DSBs show that the risk for off-target effects using CRISPR is particularly low (Frock et al., 2015; Kleinstiver et al., 2016; Smith et al., 2014; Tsai et al., 2015; Veres et al., 2014). However, early CRISPR screens showed that gRNAs targeting amplified genomic regions tend to drop out of the cell pool. This was shown to depend on the induction of cell death due to the concurrent generation of multiple DSBs (Hart et al., 2015). CRISPR screens can be used to target non-coding regions and can therefore be used to identify regulatory RNAs or transcription factor binding sites (Doudna and Charpentier, 2014; Maeder and Gersbach, 2016). Recently, CRISPR libraries became available in an arrayed format, enabling screening in 96- or 384-well plates that outperformed corresponding siRNA screens (Schmidt et al., 2015; Tan and Martin, 2016). In contrast to pooled screening approaches, arrayed CRISPR screens simplify the application of readouts that are not solely depending on the dropout or enrichment of gRNAs, but enable the application of more analytical measures such as high-content imaging. Arrayed screens also help to overcome the bias of paracrine signaling, that is inherent in pooled approaches. In pooled CRISPR screens, KO of an essential growth factor might not result in cell death due to the external availability of the growth factor from cells that lost other genes. A pooled genome-wide screen might therefore not identify all genes that are relevant to a specific phenotype. In arrayed screens however, KO clones are not affected by surrounding cells with different genotypes and loss of essential growth factors will result in cell death. Arrayed CRISPR screens can be performed by transiently transfecting gRNA oligos into cell lines stably expressing Cas9 (Cho et al., 2013; González et al., 2014). Alternatively, DNA constructs expressing the gRNA from a RNA polymerase III promoter can be used. The latter method has the advantage of higher genetic stability compared to the direct usage of RNA sequences (Liang et al., 2015; Mali et al., 2013b). Recently, the CRISPR technology was modified to allow the targeted silencing or activation of gene expression. To this end, catalytically-dead Cas9 (dCas9) mutants were generated that do not possess endonuclease activity, yet retain DNA binding activity. This allows gRNA dependent recruitment of dCas9 to desired transcriptional start sites (TSSs), whereby attached transcriptional activators or repressors can locally affect gene expression (Dominguez et al., 2016; Gilbert et al., 2013; Larson et al., 2013; Qi et al., 2013; Sander and Joung, 2014). Transcriptional repression using CRISPR is called CRISPR interference (CRISPRi) and can be achieved by fusing dCas9 to the Krüppel associated box (KRAB) domain (Gilbert et al., 2013). A comparison of CRISPRi and shRNA mediated KD monitoring ricin resistance showed stronger phenotypes using CRISPRi, indicating the

superiority of this approach compared to shRNA (Gilbert et al., 2014). Transcriptional activation using CRISPR (CRISPRa) is achieved by fusing dCas9 to transcriptional activator domains (Maeder et al., 2013; Perez-Pinera et al., 2013). Several CRISPRa systems have been developed, whereby the synergistic activation mediator (SAM) system has shown the most potent gene activation (Chavez et al., 2015, 2016; Konermann et al., 2015; Tanenbaum et al., 2014). Using a CRISPRa screen for BRAF inhibitor sensitivity revealed the involvement of the ERK pathway in the resistance to BRAF inhibition (Konermann et al., 2015). However, CRISPR based transcriptional modulators have present unique challenges. A recent study has shown that the activity of CRISPRi is blocked by nucleosomes, indicating particular difficulties in the design of effective CRISPRi libraries (Horlbeck et al., 2016). Another challenge is that the human genome consists of more than 70,000 TSSs with multiple TSSs per gene, that are not used homogeneously throughout various cell types, indicating the need for larger, cell type and tissue specific libraries (FANTOM Consortium and the RIKEN PMI and CLST (DGT) et al., 2014).

The choice of the screening technique depends on the research question. To investigate the phenotype of essential genes, the incomplete KD of RNAi can be advantageous. Random insertional mutagenesis screens result in genetic LOF and show stronger phenotypes, yet they are limited to haploid cell lines, biased towards knocking-out highly transcribed genes and rely on expensive deep-sequencing. CRISPR screens allow screening in diploid cells and cost-effective multiplexed sequencing, but can be biased as a consequence of imperfect library design. For the robust identification of synthetic viable interactions in the context of defects in the Fanconi anemia pathway, we utilized two different genome-wide screening approaches. A CRISPR library screen (Shalem et al., 2014), targeting 18,080 human genes with 64,751 unique gRNAs was performed in parallel to a gene-trap insertional mutagenesis screen (Blomen et al., 2015). Our results illustrate the potential of this approach to identify synthetic viable interactions in human cells with defects in the DDR.

1.4 Aims of this thesis

The maintenance of genomic integrity is a prerequisite for the preservation of cellular function and the prevention of numerous diseases. This is ensured by a complex network of DNA repair mechanisms that work together to safeguard the genome. Defects in those repair mechanisms are frequently associated with hereditable diseases that increase the likelihood of developing cancer and other severe abnormalities. To date, the majority of these diseases can only be treated symptomatically due to the inability of re-introducing functional genes in a clinical setting. Synthetic viable interactions could offer a way of compensating defects in the DNA damage response by resorting a healthier phenotype via loss of a second gene or inhibition of the corresponding protein. This thesis explores the possibility of exploiting synthetic viable interactions to compensate defects in the DNA damage response and aims at:

1) Exploring the feasibility of using systematic genome-wide loss-of-function screens to identify synthetic viable interactions in human cells harboring defects in the DNA damage response. To that end, cells defective in the Fanconi anemia pathway are chosen as a model system.

2) Follow up on a prominent hit to monitor the effects of the synthetic viable interaction on DNA damage.

3) Compare a gene-trap mutagenesis screen to an analogous CRISPR screen to contrast their suitability for the identification of synthetic viable interactions.

CHAPTER TWO: RESULTS

2.1 Prologue

Here we use two independent screening approaches to identify synthetic viable interactions in Fanconi anemia deficient HAP1 cells: A genome-wide CRISPR knock-out screen and a gene-trap insertional mutagenesis screen. Both approaches revealed that loss of the BLM helicase complex decreases the sensitivity of FANCC deficient cells to the DNA interstrand crosslink agent mitomycin C. We confirm the synthetic viable interaction between the BLM helicase complex and the Fanconi anemia pathway in additional FANC deficient backgrounds and with other interstrand crosslink inducing agents. We monitor the effects of this interaction on the development of induced DNA damage and apoptosis and demonstrate that the reduced sensitivity is partially depending on alternative non-homologous end joining.

The author of this thesis performed and analyzed the genome-wide CRISPR knockout screen, performed the majority of dose-response curves, measured cellular sensitivity to different crosslink-inducing agents, knocked-down MUS81 and analyzed the sensitivity of the resulting cells, monitored apoptotic behavior using Annexin V staining with the help of Michel Owusu who also performed the γH2AX staining and analysis. Georgia Velimezi performed the gene-trap mutagenesis screen, several dose-response curves and immunoblots and knocked out *NQO1* together with Lydia Robinson-Garcia, who also knocked down BRCA1. Marc Wiedner generated the HAP1 single knock-out clones and performed several immunoblots. Joana Ferreira da Silva assisted with data analysis and visualization. Joanna Loizou wrote the manuscript with input from all the authors.

nature COMMUNICATIONS

ARTICLE

DOI: 10.1038/s41467-017-01439-x OPEN

Parallel genome-wide screens identify synthetic viable interactions between the BLM helicase complex and Fanconi anemia

Martin Moder[1], Georgia Velimezi[1], Michel Owusu[1], Abdelghani Mazouzi[1], Marc Wiedner[1], Joana Ferreira da Silva[1], Lydia Robinson-Garcia[1], Fiorella Schischlik[1], Rastislav Slavkovsky[1,8], Robert Kralovics[1], Michael Schuster[1], Christoph Bock[1], Trey Ideker[2,3,4,5], Stephen P. Jackson[6,7], Jörg Menche[1] & Joanna I. Loizou[1]

Maintenance of genome integrity via repair of DNA damage is a key biological process required to suppress diseases, including Fanconi anemia (FA). We generated loss-of-function human haploid cells for FA complementation group C (FANCC), a gene encoding a component of the FA core complex, and used genome-wide CRISPR libraries as well as insertional mutagenesis to identify synthetic viable (genetic suppressor) interactions for FA. Here we show that loss of the BLM helicase complex suppresses FANCC phenotypes and we confirm this interaction in cells deficient for FA complementation group I and D2 (FANCI and FANCD2) that function as part of the FA I-D2 complex, indicating that this interaction is not limited to the FA core complex, hence demonstrating that systematic genome-wide screening approaches can be used to reveal genetic viable interactions for DNA repair defects.

[1] CeMM Research Center for Molecular Medicine of the Austrian Academy of Sciences, Lazarettgasse 14, AKH BT 25.3, 1090 Vienna, Austria. [2] Department of Medicine, Division of Genetics, University of California San Diego, La Jolla, CA 92093, USA. [3] Department of Bioengineering, University of California San Diego, La Jolla, CA 92093, USA. [4] Moores Cancer Center, University of California San Diego, La Jolla, CA 92093, USA. [5] The Cancer Cell Map Initiative, La Jolla, CA 92093, USA. [6] The Wellcome Trust and Cancer Research UK Gurdon Institute, and Department of Biochemistry, University of Cambridge, Cambridge, CB2 1QN, UK. [7] The Wellcome Trust Sanger Institute, Hinxton, Cambridge, CB10 1SA, UK. [8] Present address: Institute of Molecular and Translational Medicine, Faculty of Medicine and Dentistry, Palacky University Olomouc, Olomouc, Czech Republic. Martin Moder and Georgia Velimezi contributed equally to this work. Correspondence and requests for materials should be addressed to J.I.L. (email: jloizou@cemm.oeaw.ac.at)

Maintaining genome integrity via repair of DNA damage is a key biological process required to suppress diseases including cancer, ageing-related pathologies and diseases associated with developmental defects and neurological disorders[1,2]. Defects in DNA repair genes cause various rare heritable diseases. One such disease is Fanconi anemia (FA) that is caused by defects in FA genes and is characterized by bone marrow failure, congenital defects, cancer predisposition and chromosome fragility[3]. FA is believed to result from impaired repair of DNA interstrand crosslink (ICL) damage, leading to accumulation of DNA damage and genome instability. Furthermore, FA patients that develop cancer cannot be treated with standard chemotherapy, including crosslinking agents, as they are hypersensitive to such compounds.

Synthetic viability is the suppression of a genetic defect or phenotype by mutation or abrogation of another gene or pathway. Recently, haploid genetic screens have emerged as a powerful method to perform suppression screens in human cells[4–6]. Using near-haploid cell lines, such as HAP1, in combination with a CRISPR-Cas9 inactivating library and insertional mutagenesis, knock-outs for nearly all non-essential human genes can be generated[7,8].

Here, we introduce an approach for the systematic identification of synthetic viable interactions in human cells, illustrated with FA defective cells. We identified synthetic viable interactions for FA by performing genome-wide screens on isogenic human haploid cells lacking the FA complementation group C (FANCC) protein, following exposure to the DNA ICL-inducing agent mitomycin C (MMC). We identify the BLM helicase complex as a suppressor of Fanconi anemia phenotypes in human cells, demonstrating that systematic screening approaches can be used to reveal genetic viable interactions for DNA repair defects.

Results

Genome-wide screens identify synthetic viable interactions. To validate the use of HAP1 as a cellular model system in which to identify genetic synthetic viable interactions for genes associated with DNA repair, we reproduced a reported synthetic viable interaction that occurs between lamin A (mutated in the premature-ageing disease Hutchinson-Gilford progeria syndrome) and the acetyl-transferase protein NAT10[9]. Hence, we utilized CRISPR-Cas9 lamin A mutant HAP1 cells (Δ*LMNA*) (Supplementary Fig. 1a) which displayed a misshaped nuclear morphology that could be corrected upon the addition of a NAT10 inhibitor (Remodelin) (Supplementary Fig. 1b). Next, we targeted *FANCC* in HAP1 cells using CRISPR-Cas9, generating a frame-shift mutation (Supplementary Fig. 1c) and subsequently the loss of FANCC protein expression (Supplementary Fig. 1d). Resulting *FANCC* mutant cells (Δ*FANCC*) were hypersensitive to MMC, both in a short-term dose-response assay (Supplementary Fig. 1e) and in a long-term colony formation assay (Supplementary Fig. 1f, g).

To identify synthetic viable interactions for FANCC, we set up two genome-wide approaches to screen for mutations that alleviate the hypersensitivity of Δ*FANCC* cells to MMC-induced DNA damage (Fig. 1a). To this end, we exposed these cells to the Genome-Scale CRISPR Knock-Out (GeCKO) library[10] or insertional mutagenesis[8], the latter disrupting genes by random insertion of a gene-trap cassette into the genome. Cells were subsequently grown under MMC selection, leaving 5–10% of Δ*FANCC* cells viable. Cells resistant to MMC were recovered and subjected to next generation sequencing, to identify either the enriched guide RNAs (gRNAs) or positions of insertional gene-trap mutagenesis. Sequencing of the CRISPR library revealed a sufficient number of reads, covering each gRNA around 300 times (Supplementary Fig. 2a, b). More than 99% of all gRNAs present in the CRISPR library were detected (Supplementary Fig. 2c). Use of insertional mutagenesis resulted in the targeting of >7000 genes with a total number of 22,772 unique insertions (Supplementary Table 1). For both genome-wide screens, the CRISPR-Cas9 mediated editing and insertional mutagenesis screen, we used human haploid HAP1 cells since the likelihood to receive loss-of-function mutations is increased by the fact that only one genetic allele needs to be altered to yield a null phenotype[4,5,8,11]. All experiments confirming the results of the genome-wide screens were performed using diploid HAP1 clones.

Encouragingly, both approaches led to the identification of NAD(P)H:quinone oxidoreductase1 (NQO1) as highly enriched in Δ*FANCC* cells treated with MMC, compared to untreated wild-type (WT) cells (Fig. 1b, c). NQO1 functions as a positive control, since it is known that loss of NQO1 renders cells less sensitive to MMC due to its functions as one of several bioreductases, converting MMC from a pro-drug to an active form that can lead to ICLs[12]. Moreover, *NQO1* is found to carry loss-of-function mutations in cancers that are MMC resistant[13]. Using the CRISPR library, as well as insertional mutagenesis, we identified the enrichment of several NQO1 gRNAs and multiple *NQO1* inactivating insertions, respectively (Supplementary Fig. 3a, b). To validate this genetic interaction, we designed gRNAs to target NQO1 with Cas9 nickase[14] (Supplementary Fig. 3c) and confirmed that editing resulted in a pool of frame-shift mutations by immunoblotting (Supplementary Fig. 3d). Both WT and Δ*FANCC* cells targeted for NQO1 ('WT + *NQO1* gRNA' and 'Δ*FANCC* + *NQO1* gRNA', respectively) displayed reduced MMC toxicity in both a short-term dose-response assay (Supplementary Fig. 3e) and a long-term colony formation assay (Supplementary Fig. 3f, g).

Loss of BLM complex rescues sensitivity of FA cells to ICLs. We identified several members of the BLM complex, using both genome-wide CRISPR libraries (where we identified all four complex members: BLM, RMI1, RMI2 and TOP3A) and insertional mutagenesis (where we identified BLM and RMI1) (Fig. 1b, c), and followed up on this finding. The BLM complex forms part of a multienzyme DNA helicase and includes DNA Topoisomerase III Alpha (TOP3A), RMI1, RMI2, and the BLM helicase. The BLM complex is bridged to the FA complex via FANCM[15], and indeed gRNAs targeting *FANCM* were also enriched using the CRISPR library (Fig. 1b and Supplementary Fig. 4a). The BLM complex functions in the resolution of DNA structures that arise during the process of homologous recombination (HR) repair[16]. By comparing enriched genes in the CRISPR screen performed on MMC-treated Δ*FANCC* cells to enriched genes identified by an additional CRISPR screen performed on MMC-treated WT cells, we found that loss of the BLM complex specifically rescued Δ*FANCC* but had little or no effect in WT cells (Supplementary Fig. 4a). This indicates that the observed phenotype of increased resistance upon loss of BLM is specific to FANCC deficient cells and most likely does not result from general pro-survival effects due to diminished MMC uptake, impaired apoptotic signaling or perturbed MMC activation. All six gRNAs for *BLM* and *RMI1* were enriched in the CRISPR screen (Supplementary Fig. 4b). In addition, inactivating insertion sites within *BLM* and *RMI1* in the gene-trap screen were identified (Supplementary Fig. 4c).

To validate the above findings, we generated BLM, RMI1 or FANCM deficient cells both in a WT background and in a Δ*FANCC* background. Single and double knock-out clones were confirmed by Sanger sequencing (Supplementary Fig. 4d) and immunoblotting (Supplementary Fig. 4e). Thus we confirmed that while loss of RMI1, BLM or FANCM in a WT background

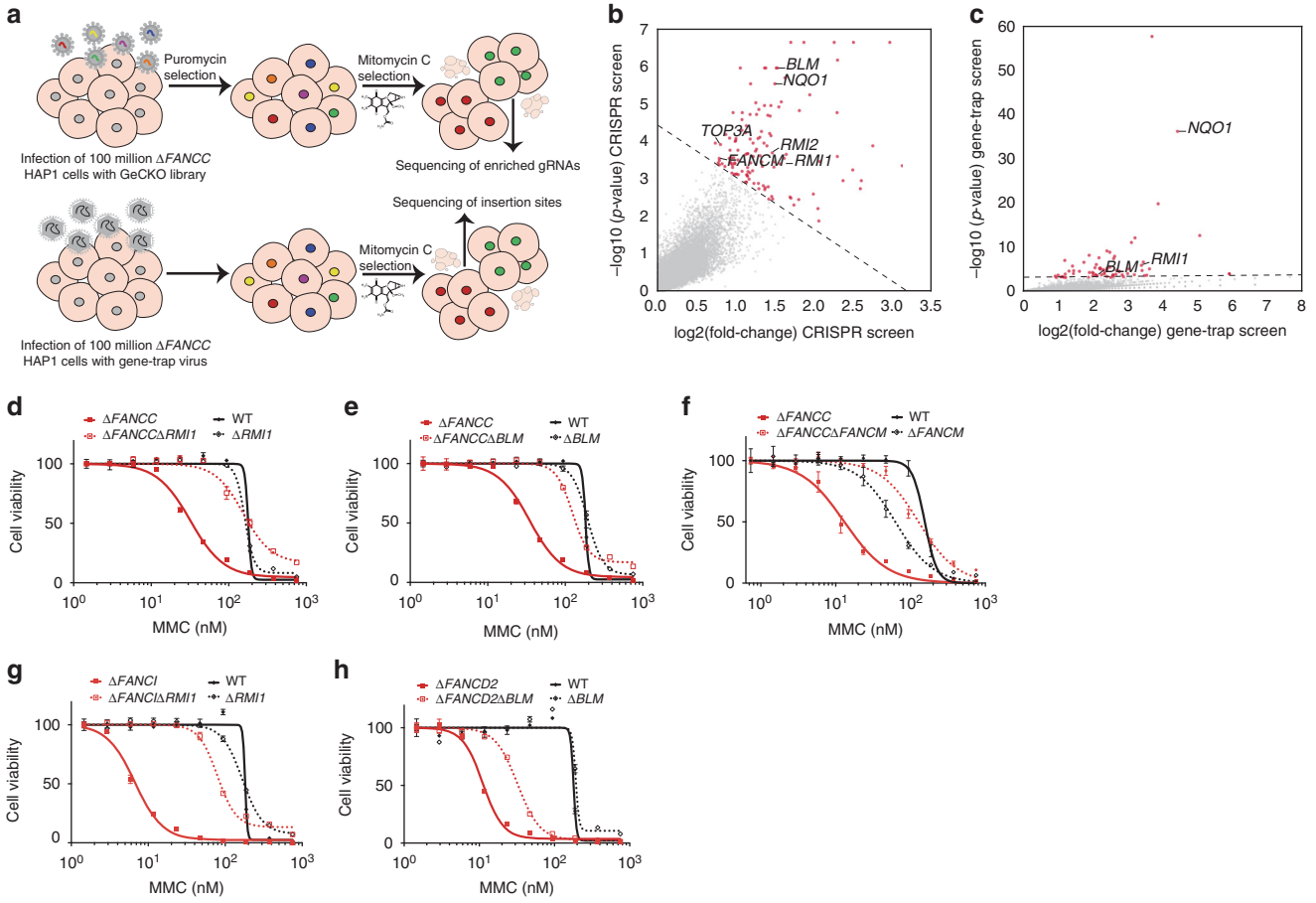

Fig. 1 Genome-wide CRISPR-Cas9 and insertional mutagenesis screens identify the BLM complex as a synthetic viable interaction for FANCC. **a** Workflow for the identification of genetic synthetic viable interactions for Δ*FANCC* cells following MMC exposure by two parallel genome-wide approaches: CRISPR-Cas9 and insertional mutagenesis. **b** Viability-inducing genes identified using a genome scale CRISPR knock-out (GeCKO) library in Δ*FANCC* cells treated with MMC, compared to untreated WT cells are shown in red, and include members of the BLM complex, *FANCM* and *NQO1*. Each dot represents the average score of the six guide RNAs (gRNAs) per gene. **c** Viability-inducing genes identified using gene-trap insertional mutagenesis in Δ*FANCC* cells treated with MMC, compared to untreated WT cells. Members of the BLM complex and *NQO1* are labeled. For robust identification of enriched genes in **b**, **c**, hit selection was performed in two steps. First, each data set was partitioned into two groups, defining the hit-group as data points with $p < 0.001$ and fold-change $>2^{1.5}$. In a second step, hit selection was optimized using linear discriminant function analysis. **d**–**h** Indicated cell lines were exposed to MMC for 4 days and cellular survival was assessed by CellTiter-Glo. Means and S.E.M. of biological triplicates are plotted

(Δ*RMI1*, Δ*BLM*, and Δ*FANCM*, respectively) had little effect on MMC sensitivity, loss of one of these three factors in a FANCC-deficient background (Δ*FANCC*Δ*BLM*, Δ*FANCC*Δ*RMI1*, and Δ*FANCC*Δ*FANCM*) resulted in enhanced MMC resistance (Fig. 1d–f). In support of our findings, it has been reported that disruption of *FANCM* (Protein Hef ortholog) in a FANCC-deficient background in chicken DT40 cells suppresses cellular sensitivity to cisplatin[17]. In addition, it has been shown that mouse embryonic fibroblasts lacking both FANCB (another member of the FA core complex) and BLM are less sensitive to MMC than FANCB single mutants[18]. However, intriguingly chicken DT40 cells lacking both FANCC and BLM are not noticeably less sensitive than FANCC single mutants[19] and this discrepancy may be due to species variation.

Since FANCC is part of the FA core complex, we next investigated whether loss of BLM or RMI1 could rescue cells lacking FANCI and FANCD2, that make up the FA I-D2 complex and function downstream of the FA core complex. To this end, we generated FANCI and FANCD2 mutant HAP1 cells (Δ*FANCI and* Δ*FANCD2*), as well as Δ*FANCI*Δ*RMI1* and Δ*FANCD2*Δ*BLM* double-deficient cells (Supplementary Fig. 4f, g). We observed that loss of RMI1 or BLM could rescue the MMC hypersensitivity of FANCI and FANCD2 deficient cells, but did not enhance MMC resistance in WT cells (Fig. 1g, h), indicating that this synthetic viable (genetic suppression) interaction is not limited to FA core complex components.

To investigate whether the observed genetic interaction between FA and the BLM complex was specific to MMC, we treated cells with two additional crosslinking agents, cisplatin and 1,2,3,4-diepoxybutane (DEB) (Fig. 2a, b). In addition, we treated cells with acetaldehyde, which is considered to be an endogenous source of crosslinking damage in FA cells[20–22] (Fig. 2c). We noted that loss of BLM alleviated the cellular hypersensitivity of Δ*FANCC* cells to all of these crosslinking agents.

p53 is partially functional in HAP1 cells. Because DNA-damage induced cell death of FA cells has been shown to occur in a p53 dependent manner[23], and since we did not retrieve *TP53* or its effectors in either of the genome-wide loss-of-function screens, we next investigated the functionality of p53 in HAP1 cells. Sequencing of *TP53* confirmed a previously reported point mutation[24,25] (Supplementary Fig. 5a). To test whether this mutation impacted on cell survival of FA cells following exposure

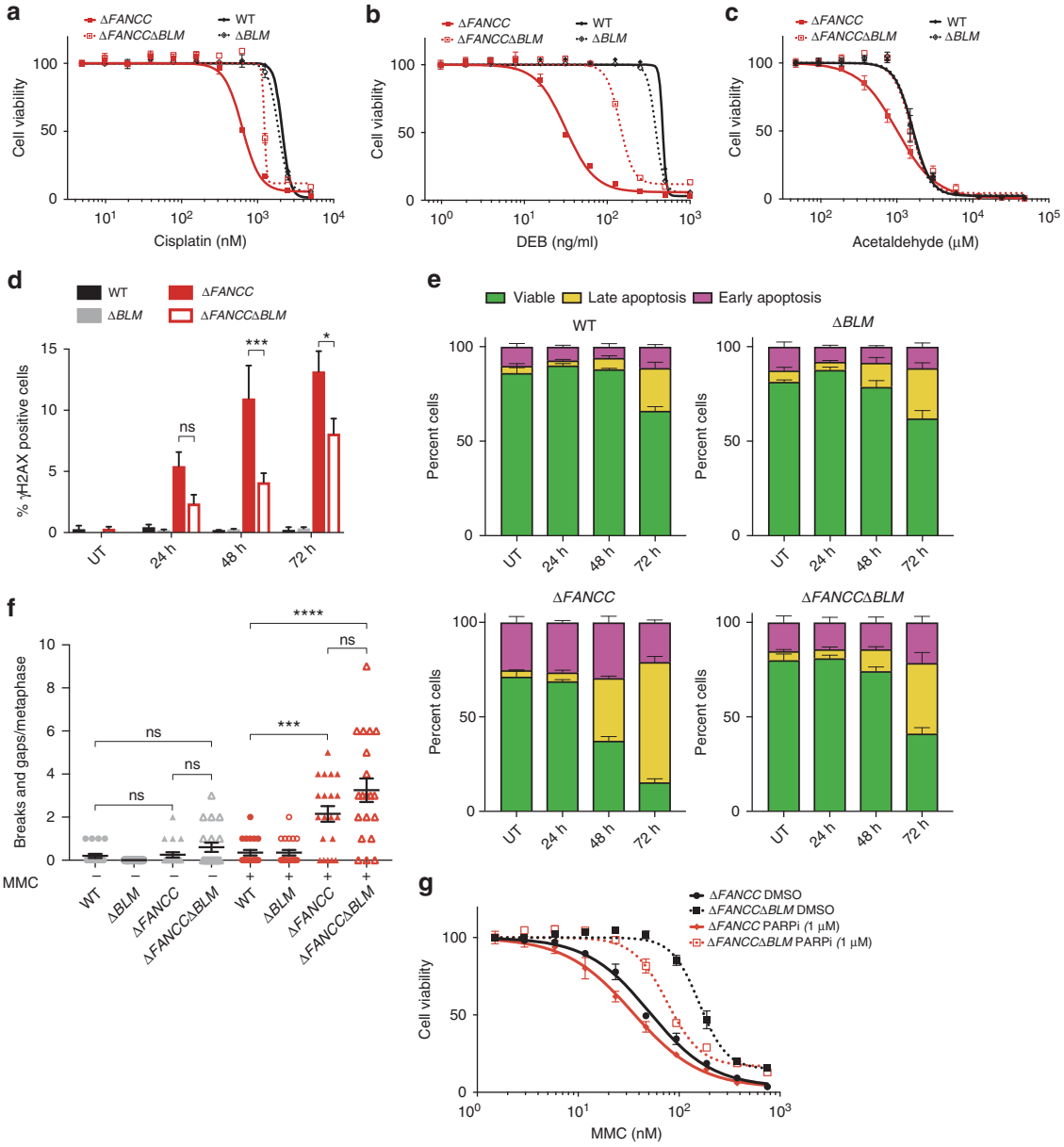

Fig. 2 Loss of the BLM complex in FANCC deficient cells alleviates DNA damage and apoptosis induced by ICLs. **a**–**c** Treatment of indicated cell lines with cisplatin, diepoxybutane (DEB) and acetaldehyde for 4 days. Survival assessed by CellTiter-Glo. **d** Indicated cells were left untreated (UT) or treated with MMC for 24, 48, or 72 h, stained for γH2AX and analyzed by High Content Imaging. *p*-values determined by two-way ANOVA. **e** Cells were either left untreated or treated with MMC for 24, 48, and 72 h, then apoptosis was measurement using propidium iodide (PE) Annexin V staining, followed by flow cytometry analysis. **f** Quantification of chromosome breaks and gaps of 40 cells per cell line treated with MMC for 24 h followed by analysis of metaphase spreads. *p*-value determined by Mann–Whitney U test. **g** Survival of indicated cells treated with either the PARP inhibitor olaparib (PARPi) or DMSO for 4 h, followed by MMC exposure for 4 days. Survival assessed by CellTiter-Glo. For all panels, means and S.E.M. of biological triplicates are plotted. ns = $p > 0.05$; $^{*}p < 0.05$; $^{**}p < 0.01$; $^{***}p < 0.001$; $^{****}p < 0.0001$

to MMC, we generated HAP1 cells lacking p53 (Δ*TP53)* as well as cells lacking both FANCC and p53 *(*Δ*FANCC*Δ*TP53)* (Supplementary Fig. 5b, c). Next, we treated these cells with MMC in both short-term and long-term dose-response assays (Supplementary Fig. 5d–f). We noted that loss of p53 only slightly increased the resistance of Δ*FANCC* cells to MMC (Supplementary Fig. 5d–f). This led us to address p53 functionality in HAP1 cells. Thus, we treated human A549 cells (a *TP53* WT cell line) and HAP1 cells with Nutlin-3a, an MDM2 inhibitor. This enhanced p53 stability in A549 cells and ensuing induction of the p21 protein (Supplementary Fig. 5g). While we did observe low levels of p21 protein in HAP1 cells, this was not increased upon Nutlin-3a treatment, nor did Nutlin-3a increase p53 protein levels in such cells. Next, we tested whether Nutlin-3a treatment could sensitize HAP1 cells in both short-term and long-term dose-response assays (Supplementary Fig. 5h–j). We did not observe an increased sensitization to Nutlin-3a, which taken together with our other data, these findings indicate that p53 is only partially functional in HAP1 cells.

Loss of BLM reduces DNA damage and apoptosis of FA cells. To probe the molecular mechanism of the observed suppression, we measured generation and clearance of DNA damage using

Ser-139 phosphorylated histone H2AX (γH2AX) as a marker (Fig. 2d). This analysis indicated a reduction in DNA damage at later time points (48 and 72 h) in Δ*FANCC*Δ*BLM* cells compared to Δ*FANCC* cells which correlated with reduced levels of apoptosis (Fig. 2e and Supplementary Table 2). Next, we measured the impact of loss of BLM in Δ*FANCC* cells on chromosomal instability by assessing chromosomal aberrations (Fig. 2f). This indicated that shortly after ICL induction (24 h after MMC treatment), the number of chromosomal breaks and gaps in Δ*FANCC*Δ*BLM* cells were not significantly altered, compared to Δ*FANCC*.

Loss of BLM does not rescue general HR defects. DNA double-strand breaks are generated as an intermediate structure during ICL repair and are repaired through HR[26]. To test whether loss of BLM can rescue the DNA-damage hypersensitivity of cells defective in other HR proteins, we tested whether effects resulting from depletion of BRCA1 could be compensated for by loss of BLM. Hence, we depleted BRCA1 in WT and Δ*FANCC* cells, then exposed them to MMC (Supplementary Fig. 6a–c). These data indicated that loss of BLM did not alleviate the sensitivity of BRCA1 depleted cells to MMC, indicating that this genetic interaction with BLM is specific to the FA pathway.

MUS81 loss does not sensitize Δ*FANCC*Δ*BLM* cells to MMC. The BLM complex, also known as 'dissolvasome', can dissolve catenated DNA structures that arise during replication and HR repair[27]. The helicase activity of BLM in combination with the topoisomerase activity of TOP3A are required to dissolve the double Holliday junction that is formed during HR in a way that results in a non-crossover DNA product and prevents sister chromatid exchanges. Alternatively, the same structure can be resolved by structure-specific nucleases such as MUS81-EME1 or GEN1 that cut the DNA leading to crossover DNA products[28]. A possible hypothesis for the observed suppression of FA DNA-damage sensitivity by loss of BLM components is that in the absence of a functional FA pathway, inappropriate or incomplete processing of ICLs might result in a structure that cannot be efficiently dissolved by the helicase activity of BLM, resulting in a toxic intermediate. In the absence of the BLM complex, however, preferential resolution by structure-specific nucleases, such as MUS81-EME1, might be more efficient and promote survival. A recent study showed that BLM might contribute to the generation of chromosome breaks and radials in a FANCB deficient background, supporting this hypothesis[29]. A corollary of the above model is that loss of MUS81-EME1 function would re-sensitize Δ*FANCC*Δ*BLM* cells to DNA-damaging agents. However, when we tested this idea by depleting MUS81 using two independent shRNAs in Δ*FANCC*Δ*BLM* cells (Δ*FANCC*Δ*BLM shMUS81#1 and* Δ*FANCC*Δ*BLM shMUS81#2)* (Supplementary Fig. 6d), we found that Δ*FANCC*Δ*BLM* cells depleted for MUS81 were not re-sensitized to MMC (Supplementary Fig. 6e). Thus we conclude that MUS81 appears not to be used as an alternative nuclease to BLM in the context of our analyses.

PARP inhibition re-sensitizes Δ*FANCC*Δ*BLM* cells to MMC. Recently, a role for alternative end joining in the FA pathway has been reported[30,31]. As BLM may function in regulating the pathway choice for DNA double-strand break repair, by preventing alternative end-joining[32], we asked whether its absence could allow for the use of this pathway in the removal of ICLs in FA-deficient cells. As alternative end-joining is known to depend on PARP, we inhibited PARP with a small molecule inhibitor olaparib, and tested cellular survival to MMC. This led to a partial sensitization of Δ*FANCC*Δ*BLM* cells, thereby suggesting that alternative end-joining may enhance survival of FA cells in the absence of BLM function by repairing some DNA lesions (Fig. 2g and Supplementary Fig. 6f).

Discussion

Although the exact mechanisms by which the BLM complex impacts on the FA pathway still needs to be resolved, several levels of crosstalk have been described. Apart from its role in the resolution of HR intermediates, the BLM complex also plays an early role in replication fork protection and remodeling during ICL repair, since it is recruited to the site of the lesion upon recognition by FANCM[15,33]. BLM recruitment and helicase activity is important for proper downstream activation of the FA pathway[15], while FANCD2 is required for the maintenance of BLM protein stability, for mediating phosphorylation of the BLM complex members in response to DNA damage and to cooperate with BLM to promote restart of stalled replication forks while suppressing firing of new replication origins[34]. It is thus evident that coordinated action of BLM and FA proteins is necessary for efficient processing and repair of ICLs. Here we report that when members of both complexes are absent, ICL lesions can be channeled through alternative repair pathways, at the cost of genome integrity.

BLM has also been shown to prevent CtIP- and Mre11-mediated alternative non-homologous end-joining[32], a repair pathway that results in DNA sequence alterations and has also been shown to be involved in ICL repair[31]. Thus, loss of BLM might relieve suppression of alternative end-joining and promote repair of the lesions in an error-prone manner, a hypothesis supported by our data showing reduced γH2AX foci upon treatment with MMC, without decreasing chromosomal aberrations. This is supported by the partial sensitization of Δ*FANCC*Δ*BLM* cells to MMC upon inhibition of PARP.

In conclusion, through the use of parallel genome-wide screens, we have shown that synthetic viable (genetic suppression) interactions for Fanconi anemia can be systematically identified in human cells. We discovered that loss of the BLM complex rescues survival of Fanconi anemia deficient cells upon generation of DNA damage by reagents that generate ICLs.

Methods

Cell lines and culture conditions. HAP1 cells were grown in Iscove's Modified Dulbecco's Medium (IMDM) from GIBCO®, containing L-Glutamine and 25 mM HEPES and supplemented with 10% fetal bovine serum (FBS) and 1% Penicillin/Streptomycin (P/S). HEK293T cells for virus production were expanded in Dulbecco's Modified Eagle Medium (DMEM) from GIBCO, supplemented with 10% FBS. A549 cells were grown in DMEM supplemented with 10% FBS and 1% P/S. All cells were grown at 37 °C in a 3% oxygen and 5% CO_2 atmosphere. Diploid HAP1 clones used for all experiments (except the genome-wide screens) were obtained by serial dilution of mixed populations of cells (consisting of both haploid and diploid cells), followed by confirmation of the ploidy status by FACS. All cell lines used in this publication were tested negative for mycoplasma contamination using the MycoAlert™ Mycoplasma Detection Kit.

Gene editing. Guide RNA pair design and cloning: For the generation of *NQO1*-CRISPR knock-out cells, the Cas9 double-nickase system was used[14]. By combining the CRISPR Design Tool (http://crispr.mit.edu/) and the Desktop Genetics tool (https://www.deskgen.com/landing), we selected a pair of two guide RNA (gRNAs) sequences of 20 base pairs each, targeting exon 3 of the human *NQO1* gene (ENSG00000181019) with an offset distance of 9 base pairs. The gRNA sequences used were the following: *NQO1*-guideA (Sense): 5′-TAAGCCAGAACA-GACTCGGC-3′ and *NQO1*-guideB (Antisense): 5′-CCATCTGAGCCCAGA-TATTG-3′. The gRNA oligonucleotides were annealed and cloned into the pSpCas9n(BB)-2A-Puro (PX462) V2.0 vector (Addgene plasmid # 62987), following the recommended protocol[35].

Plasmid transfection: pSpCas9n(BB)-2A-Puro-NQO1-guideA and -guideB constructs were co-transfected into HAP1 cells using Xfect transfection reagent (Takara Bio USA, Inc.). After 2 days of selection with puromycin, loss of protein expression was tested by immunoblotting.

CRISPR-Cas9-mediated editing: Δ*LMNA* and HAP1 cells were purchased from Horizon Genomics. CRISPR-Cas9 knock-outs of FANCC, FANCI and BLM were

generated in collaboration with Horizon Genomics. CRISPR-Cas9 knock-outs of RMI1, FANCM, FANCC/BLM, FANCC/RMI1, FANCI/RMI1, and FANCD2/BLM were generated using the protocol of Horizon Genomics. Sequences for gRNAs were designed by Horizon Genomics or with the use of http://crispr.mit.edu/ and https://www.deskgen.com/landing/, respectively. Sequences of gRNAs used were:

FANCC: 5′-GCCAACAGTTGACCAATTGT-3′;
FANCI: 5′-GTATCCAGTTGGTGGAATCG-3′;
FANCM(1): 5′-AAAGACCTTTATTGCCGCCG-3′;
FANCM(2): 5′-GGTCTACACAAGCTTCCACC-3′;
BLM: 5′-AGATTTCTTGCAGACTCCGA-3′;
RMI1: 5′-ATGTTAAAGTACCTCCGATG-3′;
P53: 5′-TCCTCAGCATCTTATCCGAG-3′;

Sanger sequencing. Genomic DNA was extracted using the Viagen Biotech DirectPCR Lysis Reagent (Cell) according to the manufacture's protocol. Genomic regions around the gRNA-targeted sequences were amplified using the following primer pairs:

FANCC-For: 5′-CAAACCTACACACACATACATGGAC-3′;
FANCC-Rev: 5′-ACTAAACAAGAAGCATTCACGTTCC-3′;
FANCI-For: 5′-CTTTTTCAAAGCCCTTAACCATTGC-3′;
FANCI-Rev: 5′-CCCTCAACAAATTACAAACCCTCAA-3′;
FANCM(1)-For: 5′-CGGACGATGATGTGTTGCTT-3′;
FANCM(1)-Rev: 5′-CGATCTGCTGTGTCACCAAG-3′;
FANCM(2)-For: 5′-AGTCCTAGATAAGTGCCAGCT-3′;
FANCM(2)-Rev: 5′-TATTTCAGCAGCGGGACAAG-3′;
BLM-For: 5′-GAGCAGTGCTTACTCTTACAAAGTG-3′;
BLM-Rev: 5′-GTTACCGAAGACTTTTCCTTCAGTG-3′;
RMI1-For: 5′-AAAAATCTAAAGGGTGTGCCTGTC-3′;
RMI1-Rev: 5′-TGCCATCGGGTAAAAGAGGATG-3′;
P53-For: 5′-TTATAGGGAGGTCAAATAAGCAGCA-3′;
P53-Rev: 5′-ATCTACAAGCAGTCACAGCACAT-3′;

The following sequencing primers were used:
FANCC: 5′-ACTAAACAAGAAGCATTCACGTTCC-3′;
FANCI: 5′-CTTTTTCAAAGCCCTTAACCATTGC-3′;
FANCM(1): 5′-CGATCTGCTGTGTCACCAAG-3′;
FANCM(2): 5′-TATTTCAGCAGCGGGACAAG-3′;
BLM 5′-GTTACCGAAGACTTTTCCTTCAGTG-3′;
RMI1 5′-TGCCATCGGGTAAAAGAGGATG-3′;
P53: 5′-TTATAGGGAGGTCAAATAAGCAGCA-3′;
PCR amplification conditions: heat lid 110 °C; 94 °C 2 min; loop 35× (94 °C 30 s; 55 °C 30 s; 68 °C 1 min) 68 °C 7 min. Frameshift mutations were identified using Nucleotide BLAST against the reference genome GCF_000001405.33.

BRCA1 and MUS81 knock-down by shRNA. *BRCA1* knock-down: The shRNA constructs for *BRCA1* were kindly provided by Sebastian M. Nijman (Ludwig Institute for Cancer Research Ltd, UK). HAP1 cells were infected with the virus-containing supernatant in the presence of polybrene (final concentration 8 µg/ml), in IMDM (10% FBS, 1% P/S), with a viral supernatant to medium ratio of 1:3. Infected cells were selected using puromycin (2 µg/ml; Sigma-Aldrich) for 48 h. *MUS81* knock-down: Targeting sequences for MUS81 were selected using the Broad Institute Genetic Perturbation Platform. Sense targeting sequences: shMUS81#1: 5′-ACACTGCTGAGCACCATTAAG-3′; shMUS81#2: 5′-CACGCGCTTCGTATTTCAGAA-3′. Oligos were cloned into the "pLKO.2 stuffer" vector, provided by Sebastian M. Nijman. Virus was produced using the pCMV-VSV-G envelope plasmid (Addgene # 8454) and the psPAX2 packaging plasmid (Addene # 12260) in HEK293 cells. For infection, 150 ul viral supernatant was added to HAP1 cells 1 ml IMDM, following the Lipofectamine® 2000 Transfection protocol.

Quantitative reverse transcription PCR (RT-PCR). Cells were collected and RNA was isolated using Trizol extraction (following manufactures instructions). RNA was treated with 1 µl DNase (Sigma) and then reverse transcribed with the SuperScript III Reverse Transcriptase protocol (Invitrogen) to obtain cDNA. An amount of 1 µg of cDNA template was used for the qRT-PCR using SYBR Green qPCR Mastermix (Qiagen). Analysis was performed in biological triplicates using expression of GAPDH for normalization of data. The PCR was performed on a 7900HT Fast Real-Time PCR System (Applied Biosystems). The following primers were used:

BRCA1: 5′-TCAACTCCAGACAGATGGGAC-3′; 5′-GGCTGTGGGGTTTCTCAGAT-3′,
GAPDH: 5′-CGAGCCACATCGCTCAGACA-3′; 5′-GGCGCCCAATACGACCAAAT-3′.

Dose-response curves. Dose–response curves for MMC (Sigma-Aldrich), cisplatin (Sigma-Aldrich), Acetaldehyde (Sigma-Aldrich), Diepoxybutane (Sigma-Aldrich) and Nutlin-3a (Sigma-Aldrich) were performed as biolgical triplicates in 96-well plates by seeding 1000 cells per well, the day before treatment. The following day, drugs were added at 2-fold serial dilutions. Four days after the initiation of the treatment, cell viability was measured using CellTiter-Glo (Promega).

Colony formation assays. Cells were seeded in 6-well plates the day before the treatment (1000 cells per well). The next day MMC or Nutlin-3a were added at the indicated concentrations. Three days after the initiation of the treatment, drug-containing medium was changed with fresh drug-free medium. Cells were left in culture until visible colonies appeared (7–10 days). Colonies were then fixed in 3.7% formaldehyde in phosphate-buffered saline (PBS) for 1 h, washed in PBS and stained with 0.1% crystal violet solution in PBS supplemented with 10% ethanol for 1 h, followed by washing twice with H_2O. For quantification, crystal violet was extracted using 50% EtOH and absorbance was measured at 595 nm.

Remodelin incubation and microscopy. Cells were adhered onto coverslips and incubated with Remodelin at 1 µM for 2 days. To visualize nuclei, cells were subsequently fixed with 4% paraformaldehyde in PBS and stained with 4′,6-diamidino-2-phenylindole (DAPI). Images of cells were acquired using a Deconvolution microscope (Leica). CellProfiler software was used to quantify nuclear circularity and nuclear area from DAPI staining pictures, using the 'object size shape' measurement.

γH2AX staining and analysis. Cells were seeded in three 96-well plates (black with clear flat bottom tissue culture treated imaging microplates from Falcon) and left to adhere over-night. Cells were either treated with 60 nM MMC or left untreated. The experiments were done in triplicate wells. After 24, 48, and 72 h of treatment, cells were fixed with 100% methanol. Staining: Cells were blocked for 1 h with Blocking Buffer (10% FCS and 0.1% Triton X-100 in PBS), incubated for 1 h with the primary antibody (Anti-phospho-Histone H2A.X Ser139, clone JBW301 from Millipore/Upstate) at a dilution of 1:1000 in Blocking Buffer, washed three times with PBS, incubated for 1 h with secondary antibody (Alexa Fluor 488 goat anti-mouse IgG, H+L, from Invitrogen) diluted at 1:600 along with DAPI (0.2 mg/ml stock from Sigma-Aldrich), diluted at 1:1000 in Blocking Buffer, washed 3 times and left in PBS. Cells were imaged on the Operetta-High Content Imaging System (Perkin Elmer, ×20 objective). The image analysis software Cell Profiler was used to quantify the integrated intensity of nuclear γH2AX. Apoptotic cells were excluded from the analysis. For each condition at least 1000 cells were quantified, except for Δ*FANCC* time point 2 and 3 where 877 and 426 cells (respectively) were obtained. R was used for data processing and normalization. The threshold between γH2AX positive (integrated intensity > 10) and negative cells was determined by comparing treated and untreated cells.

Measurement of apoptosis. Cells were seeded as triplicates on day 1 in 10 cm dishes and treated with 46 nM MMC on day 2, day 3, and day 4. On day 5, cells were stained using the PE Annexin V Apoptosis Detection Kit I from BD Biosciences according to the provided protocol and analyzed by flow cytometry.

Metaphase spreads. Cells were seeded in 10 cm dishes and treated with MMC for the indicated times. Colcemid (KaryoMAX™, Gibco, Thermo Fisher Scientific) was added at a final concentration of 500 ng/ml 3 h before harvesting. Cells were trypsinized and incubated in KCl 0.075 M (KaryoMAX™, Gibco, Thermo Fisher Scientific) for 6 min. After centrifugation, cells were resuspended in fixation solution (methanol:acetic acid 3:1) and incubated for 15 min at room temperature. Centrifugation and re-suspension in fresh fixation solution was repeated two times. Metaphase spreads, slide preparation and measurement of chromosomal aberrations was performed at Karyologic Inc (North Carolina, USA).

Immunoblotting and antibodies. Cell extracts were prepared in RIPA lysis buffer (NEB) supplemented with protease inhibitors (Sigma) and phosphatase inhibitors (Sigma, NEB). Immunoblots were performed using standard procedures. Protein samples were separated by SDS–PAGE (4–12% gradient gels; Invitrogen) and subsequently transferred onto nitrocellulose membranes. All primary antibodies were used at 1:1000 dilution with the exception of BLM (1:500) and RMI1 (1:5000). Secondary antibodies were used at 1:5000. The following antibodies were used: FANCC clone 8F3 (Merck Millipore), FANCD2 EPR2302 (Abcam), FANCI A301-254 (Bethyl laboratories), NQO1 clone A180 (Cell Signaling), RMI1 (Proteintech), BLM clone C-18 (Santa Cruz), MUS81 clone MTA30 2G10/3 (Abcam), p21 clone F-5 (Santa Cruz), β-Actin clone 20–33 (Sigma), Tubulin clone DM1A (Cell Signaling), HRP-conjugated goat anti-mouse, rabbit or goat IgG (Jackson Immunochemicals). The p53 antibody (PAB 421) was from Cancer Research UK. Uncropped immunoblot images are shown in Supplementary Fig. 7.

Genome-wide CRISPR-Cas9 screen. GeCKO CRIPSR library virus was produced as reported[10] and described briefly following, using both CRISPR library A and library B in one production step: HEK-293T cells were seeded at 40% confluency in T-225 flasks and 24 h later were transfected with GeCKO CRISPR library A and B, pVSVg and psPAX2 plasmids using Lipofectamine® 2000 transfection reagent (Invitrogen, ThermoFisher Scientific) according to the manufacturer's protocol. After 6 h, the medium was changed with DMEM (10% FBS) and after 60 h, virus-

containing supernatant was centrifuged at 700 × g at 4°C for 10 min and then filtered through a 0.45 µM filter (Millipore Steriflip HV/PVDF). Cells were infected with a multiplicity of infection (MOI) between 0.3 and 0.5. For each screened cell line, 100 million HAP1 cells were spinfected by centrifugation. Day 1: 12 6-well plates were seeded with 1.5 million cells per well, supplemented with viral supernatant and IMDM (10% FBS, 1% P/S) to reach a volume of 1 ml per well. Polybrene was added at 8 µg/ml. Cells were spinfected for 3 h at 724×*g* at 37 °C, pooled and transferred into 15 cm dishes. Day 3: Cells were challenged with 2 µg/ml puromycin to deplete uninfected cells. Day 5: WT cells were challenged with 30 ml of 190 nM mitomycin C (MMC) in IMDM (10% FBS, 1% P/S) per 15 cm dish. Δ*FANCC* cells were challenged with 30 ml of 46 nM MMC in IMDM (10% FBS, 1% P/S) per 15 cm dish. Treated cells were incubated for 10 days following MMC challenge, WT untreated cells were split every 2–3 days for 10 days to avoid confluency, re-seeding > 100 million cells each time. Genomic DNA of at least 30 million cells per sample was extracted using the Qiagen Blood & Cell Culture DNA Maxi Kit according to the manufacture's protocol. PCR was performed in two steps, using PCR1- and barcoded PCR2 primers as reported[10], obtained from http://genome-engineering.org/gecko/wp-content/uploads/2013/12/GeCKO-plasmid-readout-primers-July2014.xlsx. PCR1 amplified the gRNA sequences of 130 µg genomic DNA in 13 × 100 µl reactions per sample using the Promega GoTaq® G2 DNA Polymerase. PCR1 reaction tubes were pooled for each sample. PCR2 added Illumina sequencing adapters by performing 16 × 100 µl PCR reactions per sample with 2 µl input DNA from PCR1 per reaction tube. PCR program for PCR1 and PCR2: Heat lid 110 °C; 94 °C 2 min; loop 18× (94 °C 30 s; 55 °C 30 s; 68 °C 1 min) 68 °C 7 min. PCR2 products were purified by running them on agarose gel and DNA was extracted using the Promega Wizard® SV Gel and PCR Clean-Up System. Barcoded samples were pooled and submitted to the Biomedical Sequencing Facility (BSF) for 61 base pair single-end sequencing. Barcoded samples from the CRIPSR library screen were de-multiplexed by the BSF. Enrichment analysis for gRNAs was performed using the MAGeCK-VISPR analysis and visualization software[36] by comparing the MMC treated Δ*FANCC* sample to WT untreated, or WT MMC treated to WT untreated respectively (positive selection).

Genome-wide insertional mutagenesis screen. For gene-trap insertional mutagenesis we followed the published protocol[5] as described briefly following: Gene-trap virus was produced in HEK293T, that were seeded in 15 cm dishes and transfected with the gene-trap plasmid and packaging plasmids VSVg, gag-pol and pAdVAntage™ Vector (Promega) using Lipofectamine® 2000 Transfection reagent (Invitrogen, ThermoFisher Scientific) according to manufacturer's protocol. The following day, medium was replaced with fresh DMEM (20% FBS, 1% Pen/strep). Retroviral supernatant was collected for three consecutive days, centrifuged at 700 × g for 10 min, filtered through a 0.45 µM filter (Millipore Steriflip HV/PVDF) and ultracentrifuged at 70,737 × g (average RCF) at 4 °C for 90 min with a SW 32Ti rotor (Beckman Coulter). Viral pellets were re-suspended in PBS, pooled and Δ*FANCC* HAP1 cells were transduced with concentrated retrovirus containing the gene-trap cassette[5]. After integration of the GFP-expressing gene-trap cassette, cells were analyzed by flow cytometry to measure efficiency of infection and populations with > 70% GFP-expressing cells were used for treatment with MMC. The control non-selected WT HAP1 data-set was taken from Blomen et al.[8]. 100 million cells from the mutagenized pools were seeded in 15 cm dishes at a density of 6 million cells per dish. The following day MMC was added at a concentration that selectively killed FANCC-deficient cells, leaving only around 5–10% of cells surviving (46 nM for FANCC). Cells were left to grow for 10 days. After the end of treatment cells were trypsinized and frozen at −80 °C. For preparation of the gene-trapped DNA libraries, genomic DNA was extracted from 30 million cells using QIAamp DNA mini kit (Qiagen), subjected to digestion with MseI (NEB) and NlaIII enzymes (NEB) and subsequently ligated by T4 DNA ligase (NEB). Digested and ligated fragments were used as template for inverse PCR with primers targeting the LTR regions of the gene-trap cassette. After amplification and purification of the fragments the DNA sample was submitted for next generation sequencing (Illumina HiSeq 2000, 50 base pair single-read) to the CeMM Biomedical Sequencing Facility (BSF). Bioinformatics analysis of the next generation sequencing data was done in R according to Carette et al.[5] as follows: Briefly, raw sequencing data was aligned to human reference genome hg19 (UCSC hg19 build) using bowtie2 (version 2.2.4) with default parameter. Reads were removed that did not meet the following criteria: (1) have a reported alignment-"mapped reads" (2) have a unique alignment (3) have a mapping quality (MAPQ) higher than 20. Duplicate reads were marked and discarded with Picard (version 1.111). Insertions in close proximity (1 or 2 base pairs distance from each other) were removed to avoid inclusion of insertions due to mapping errors. Insertions were annotated with gene build GRCh37.p13 (ENSEMBL 75-release February 2014) using bedtools (version 2.10.1) and custom scripts. The canonical transcripts (according to ENSEMBL) for each gene were used as a reference gene model to count insertions falling with exons, introns or intragenic. Insertions were considered mutagenic or disruptive to the gene if they occurred within exons irrespective of their orientation to the corresponding gene or if they were located within introns in sense orientation. Insertions in antisense direction in respect to the gene orientation were considered silent. All mutagenic insertions were summarized independently for each gene. For each gene a one-sided Fisher's exact-test was applied to estimate a significant enrichment of insertions over an unselected control data set.

Statistical analysis. For gene-trap and CRISPR library screens, hit selection was performed in two steps. First, each data set was partitioned into two groups, defining the hit-group as data points with $p < 0.001$ and fold-change $> 2^{1.5}$. In the second step, hit selection was optimized using linear discriminant function analysis. Dose-points of survival curves indicate the mean of biological triplicates, with S.E.M. shown as error bars. The *p*-values for the γH2AX staining were determined by two-way ANOVA. Means and S.E.M. of biological triplicates are plotted. The *p*-values for the chromosomal breaks and gaps/metaphase were determined by Mann–Whitney U test. Means and S.E.M. of biological triplicates are plotted.

Data Availability. All data generated or analyzed during this study is included in this published article and its Supplementary Information.

Received: 28 December 2016 Accepted: 15 September 2017
Published online: 01 November 2017

References

1. Jackson, S. P. & Bartek, J. The DNA-damage response in human biology and disease. *Nature* **461**, 1071–1078 (2009).
2. Hoeijmakers, J. H. Genome maintenance mechanisms for preventing cancer. *Nature* **411**, 366–374 (2001).
3. Crossan, G. P. & Patel, K. J. The Fanconi anaemia pathway orchestrates incisions at sites of crosslinked DNA. *J. Pathol.* **226**, 326–337 (2012).
4. Carette, J. E. et al. Haploid genetic screens in human cells identify host factors used by pathogens. *Science* **326**, 1231–1235 (2009).
5. Carette, J. E. et al. Global gene disruption in human cells to assign genes to phenotypes by deep sequencing. *Nat. Biotechnol.* **29**, 542–546 (2011).
6. Forment, J. V. et al. Genome-wide genetic screening with chemically mutagenized haploid embryonic stem cells. *Nat. Chem. Biol.* **13**, 12–14 (2017).
7. Wang, T. et al. Identification and characterization of essential genes in the human genome. *Science* **350**, 1096–1101 (2015).
8. Blomen, V. A. et al. Gene essentiality and synthetic lethality in haploid human cells. *Science* **350**, 1092–1096 (2015).
9. Larrieu, D., Britton, S., Demir, M., Rodriguez, R. & Jackson, S. P. Chemical inhibition of NAT10 corrects defects of laminopathic cells. *Science* **344**, 527–532 (2014).
10. Shalem, O. et al. Genome-scale CRISPR-Cas9 knockout screening in human cells. *Science* **343**, 84–87 (2014).
11. Carette, J. E. et al. Ebola virus entry requires the cholesterol transporter Niemann-Pick C1. *Nature* **477**, 340–343 (2011).
12. Siegel, D., Yan, C. & Ross, D. NAD(P)H:quinone oxidoreductase 1 (NQO1) in the sensitivity and resistance to antitumor quinones. *Biochem. Pharmacol.* **83**, 1033–1040 (2012).
13. Mikami, K. et al. DT-diaphorase as a critical determinant of sensitivity to mitomycin C in human colon and gastric carcinoma cell lines. *Cancer Res.* **56**, 2823–2826 (1996).
14. Ran, F. A. et al. Double nicking by RNA-guided CRISPR Cas9 for enhanced genome editing specificity. *Cell* **154**, 1380–1389 (2013).
15. Deans, A. J. & West, S. C. FANCM connects the genome instability disorders Bloom's Syndrome and Fanconi Anemia. *Mol. Cell* **36**, 943–953 (2009).
16. Wu, L. & Hickson, I. D. The Bloom's syndrome helicase suppresses crossing over during homologous recombination. *Nature* **426**, 870–874 (2003).
17. Mosedale, G. et al. The vertebrate Hef ortholog is a component of the Fanconi anemia tumor-suppressor pathway. *Nat. Struct. Mol. Biol.* **12**, 763–771 (2005).
18. Kim, T. M. et al. RECQL5 and BLM exhibit divergent functions in cells defective for the Fanconi anemia pathway. *Nucleic Acids Res.* **43**, 893–903 (2015).
19. Hirano, S. et al. Functional relationships of FANCC to homologous recombination, translesion synthesis, and BLM. *EMBO J.* **24**, 418–427 (2005).
20. Langevin, F., Crossan, G. P., Rosado, I. V., Arends, M. J. & Patel, K. J. Fancd2 counteracts the toxic effects of naturally produced aldehydes in mice. *Nature* **475**, 53–58 (2011).
21. Rosado, I. V., Langevin, F., Crossan, G. P., Takata, M. & Patel, K. J. Formaldehyde catabolism is essential in cells deficient for the Fanconi anemia DNA-repair pathway. *Nat. Struct. Mol. Biol.* **18**, 1432–1434 (2011).
22. Garaycoechea, J. I. et al. Genotoxic consequences of endogenous aldehydes on mouse haematopoietic stem cell function. *Nature* **489**, 571–575 (2012).
23. Ceccaldi, R. et al. Bone marrow failure in Fanconi anemia is triggered by an exacerbated p53/p21 DNA damage response that impairs hematopoietic stem and progenitor cells. *Cell. Stem. Cell.* **11**, 36–49 (2012).
24. Essletzbichler, P. et al. Megabase-scale deletion using CRISPR/Cas9 to generate a fully haploid human cell line. *Genome Res.* **24**, 2059–2065 (2014).
25. Burckstummer, T. et al. A reversible gene trap collection empowers haploid genetics in human cells. *Nat. Methods* **10**, 965–971 (2013).

26. Michl, J., Zimmer, J. & Tarsounas, M. Interplay between Fanconi anemia and homologous recombination pathways in genome integrity. *EMBO J.* **35**, 909–923 (2016).
27. Mankouri, H. W., Huttner, D. & Hickson, I. D. How unfinished business from S-phase affects mitosis and beyond. *EMBO J.* **32**, 2661–2671 (2013).
28. Sarbajna, S., Davies, D. & West, S. C. Roles of SLX1-SLX4, MUS81-EME1, and GEN1 in avoiding genome instability and mitotic catastrophe. *Genes Dev.* **28**, 1124–1136 (2014).
29. Kim, T. M., Ko, J. H., Choi, Y. J., Hu, L. & Hasty, P. The phenotype of FancB-mutant mouse embryonic stem cells. *Mutat. Res.* **712**, 20–27 (2011).
30. Murina, O. et al. FANCD2 and CtIP cooperate to repair DNA interstrand crosslinks. *Cell Rep.* **7**, 1030–1038 (2014).
31. Kais, Z. et al. FANCD2 maintains fork stability in BRCA1/2-deficient tumors and promotes alternative end-joining DNA repair. *Cell Rep.* **15**, 2488–2499 (2016).
32. Grabarz, A. et al. A role for BLM in double-strand break repair pathway choice: prevention of CtIP/Mre11-mediated alternative nonhomologous end-joining. *Cell Rep.* **5**, 21–28 (2013).
33. Meetei, A. R. et al. A multiprotein nuclear complex connects Fanconi anemia and Bloom syndrome. *Mol. Cell Biol.* **23**, 3417–3426 (2003).
34. Chaudhury, I., Sareen, A., Raghunandan, M. & Sobeck, A. FANCD2 regulates BLM complex functions independently of FANCI to promote replication fork recovery. *Nucleic Acids Res.* **41**, 6444–6459 (2013).
35. Ran, F. A. et al. Genome engineering using the CRISPR-Cas9 system. *Nat. Protoc.* **8**, 2281–2308 (2013).
36. Li, W. et al. Quality control, modeling, and visualization of CRISPR screens with MAGeCK-VISPR. *Genome Biol.* **16**, 281 (2015).

Acknowledgements

We thank the Biomedical Sequencing Facility (BSF) at CeMM for all next generation sequencing and related bioinformatics analyses. We thank Thijn Brummelkamp (NKI, The Netherlands) for providing protocols and the WT HAP1 insertional mutagenesis data. Δ*FANCD2* cells were kindly provided by Ketan J. Patel (LMB, Cambridge, UK). The FANCM antibody was generously provided by Weidong Wang (NIH, USA). The shRNA constructs for BRCA1 were kindly provided by Sebastian M. Nijman (Ludwig Institute for Cancer Research Ltd, UK). We thank Ian Hickson (University of Copenhagen, Denmark) for providing experimental advice and suggestions. We thank Óscar Fernández-Capetillo (Spanish National Cancer Research Center, Spain) for discussions and input. M.M. was partially funded by an FWF stand-alone grant to J.I.L. (FWF29763). G.V. was funded by an EMBO long-term fellowship (Grant number: ALTF 730 2014) and an FWF stand-alone grant to J.I.L. (FWF29555). L.G.R. was funded by a Boehringer Ingelheim Fonds PhD fellowship. A.M. was funded by a DOC fellowship (OAW24102). CeMM is funded by the Austrian Academy of Sciences. T.I. was supported by grant ES014811 from the US National Institutes of Health. J.M. was supported by a WWTF career grant (VRG15-005).

Author contributions

J.I.L. conceived the project; M.M. performed the genome-wide CRISPR screens and G.V. performed the genome-wide insertional mutagenesis screens, with input from M.O., A.M. and R.S.; M.M. and G.V. performed dose-responses and immunoblots and performed and analyzed the Annexin V FACS data with input from M.O.; M.W. generated CRISPR-Cas9 knock-out clones, as well as contributed to dose–response curves and immunoblots; M.M. generated the shMUS81 constructs and cells and performed the related dose-response assays on these cells; L.R.-G. generated the shBRCA1 cells and the RT-qPCR data and with G.V. generated the double nickase Cas9 NQO1 mutants and performed survival assays; M.O. contributed to dose-responses and performed the γH2AX staining and analysis, as well as the FACS for Annexin V.; F.S. analyzed the insertional mutagenesis data, along with M.S., who were supervised by R.K. and C.B., respectively; J.F.daS. assisted with data analysis, along with J.M.; T.I. gave experimental advice. S.P.J. provided Remodelin; J.I.L. wrote the manuscript, with input from all authors.

Additional information

Supplementary Information accompanies this paper at doi:10.1038/s41467-017-01439-x.

Competing interests: The authors declare no competing financial interests.

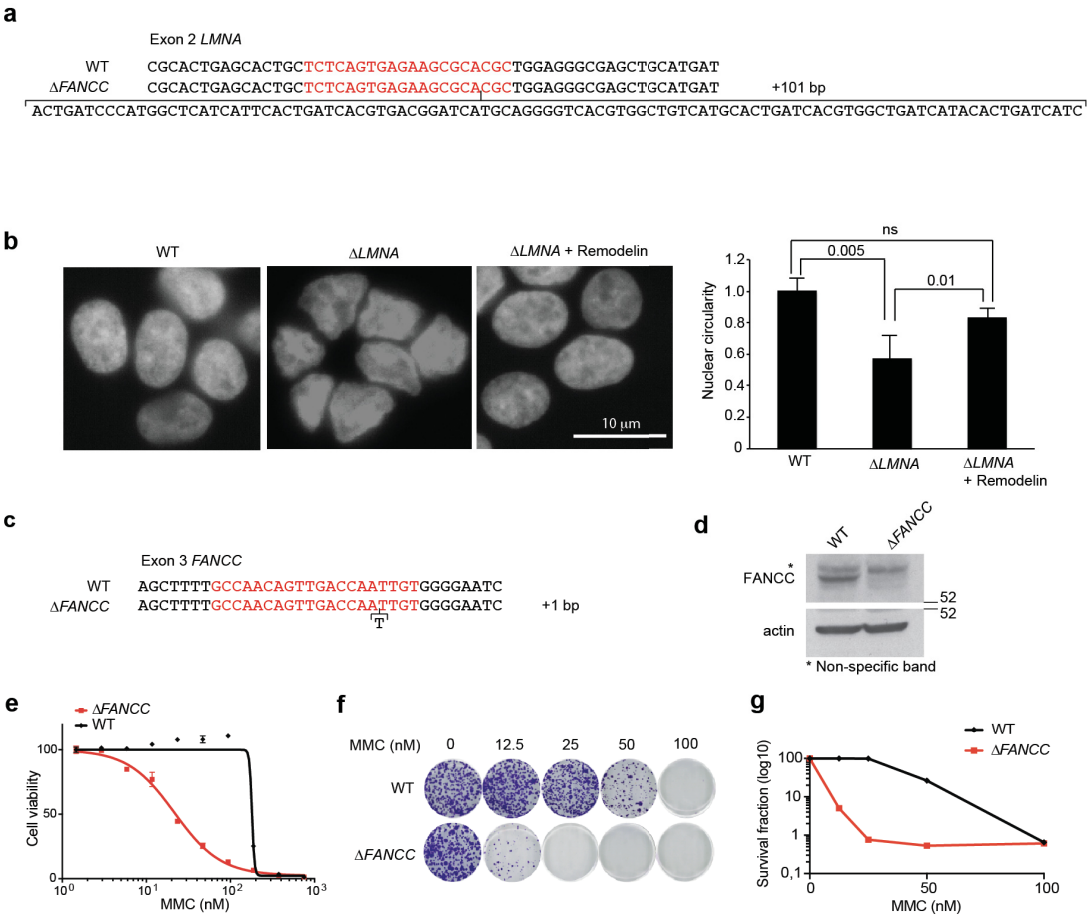

Supplementary Figure 1 Characterization of HAP1 cells for synthetic viable interactions and generation of Δ*FANCC* cells. (a) CRISPR-Cas9-mediated mutation of lamin A in human HAP1 cells (Δ*LMNA*). The red sequence in WT corresponds to the gRNA used. (b) DAPI staining of WT and Δ*LMNA* cells with or without incubation with the NAT10 inhibitor Remodelin, with quantification of nuclear circularity. (c) CRISPR-Cas9-mediated mutation of *FANCC* in human HAP1 cells (Δ*FANCC*). The red sequence in WT corresponds to the gRNA used. (d) Immunoblot of WT and Δ*FANCC* cell extracts for FANCC and actin. * denotes a non-specific band. (e) Survival of WT and Δ*FANCC* cells following MMC exposure for 4 days, assessed by CellTiter-Glo. Means and S.E.M. of triplicates are plotted. (f) Colony formation of WT and Δ*FANCC* cells following exposure to MMC for 10 days. (g) Quantification of colony formation shown in (f).

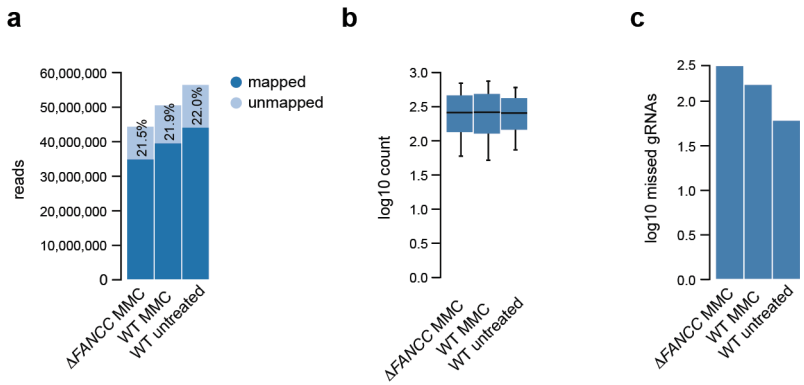

Supplementary Figure 2. Quality control of genome-wide CRISPR library and insertional mutagenesis. (a) 'Reads' depicts the total number of sequenced reads for each sequenced library. (b) 'Log10 count' indicates the average amount of sequenced reads for each gRNA. (c) 'Log 10 missed gRNAs' shows the average amount of gRNAs missing in the sequenced samples compared to the total list of gRNAs.

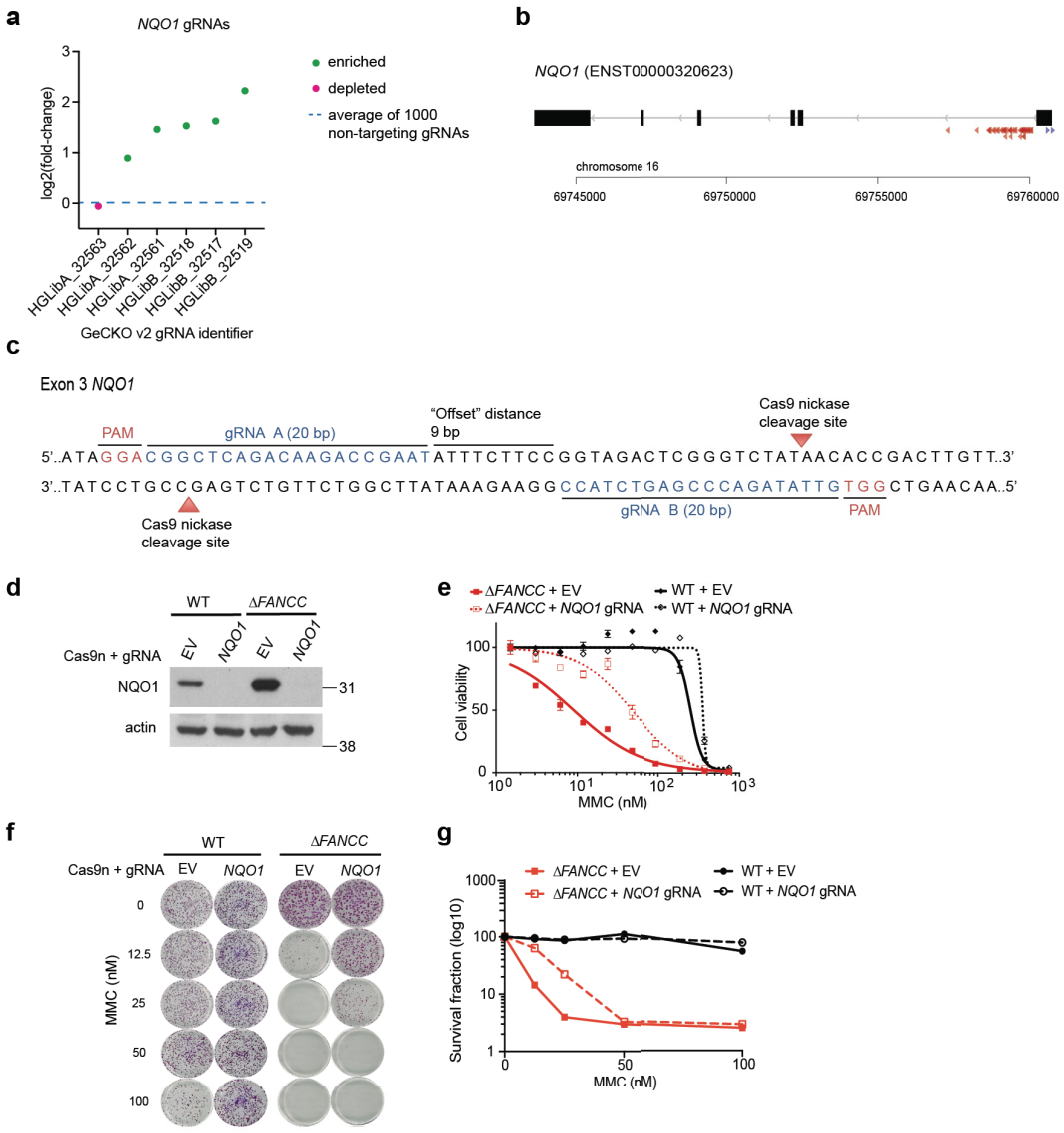

Supplementary Figure 3. Validation of NQO1 as a suppressor gene following exposure to MMC. (a) Enriched gRNAs (5 out of 6) for *NQO1* obtained in the CRISPR screen by treating Δ*FANCC* cells with MMC, compared to WT untreated cells. (b) Insertion sites (42) within *NQO1* obtained in Δ*FANCC* cells treated with MMC. Red arrows indicate insertions in the sense orientation (inactivating in both intronic and exonic regions, n=40) while blue arrows indicate insertions in the antisense orientation (inactivating only in exonic regions, n=2). (c) Sequences and position of the gRNA pair selected to target *NQO1* using Cas9 nickase. (d) Immunoblot for NQO1 expression in cell extracts obtained from WT or Δ*FANCC* cells either infected with an empty vector (EV) or with a vector expressing gRNAs and nickase Cas9 ('Cas9n + gRNA'). (e) Survival of WT and Δ*FANCC* cells transduced with an empty vector (EV) control plasmid ('WT + EV' and 'Δ*FANCC* + EV') or with a plasmid expressing gRNAs targeting *NQO1*, along with nickase Cas9 ('WT + *NQO1* gRNA' and 'Δ*FANCC* + *NQO1* gRNA'), following MMC exposure for 3 days, assessed by CellTiter-Glo. Means and S.E.M. of triplicates are plotted. (f) Colony formation assay of cells indicated in (e) following MMC exposure for 10 days. (g) Quantification of colony formation shown in (f).

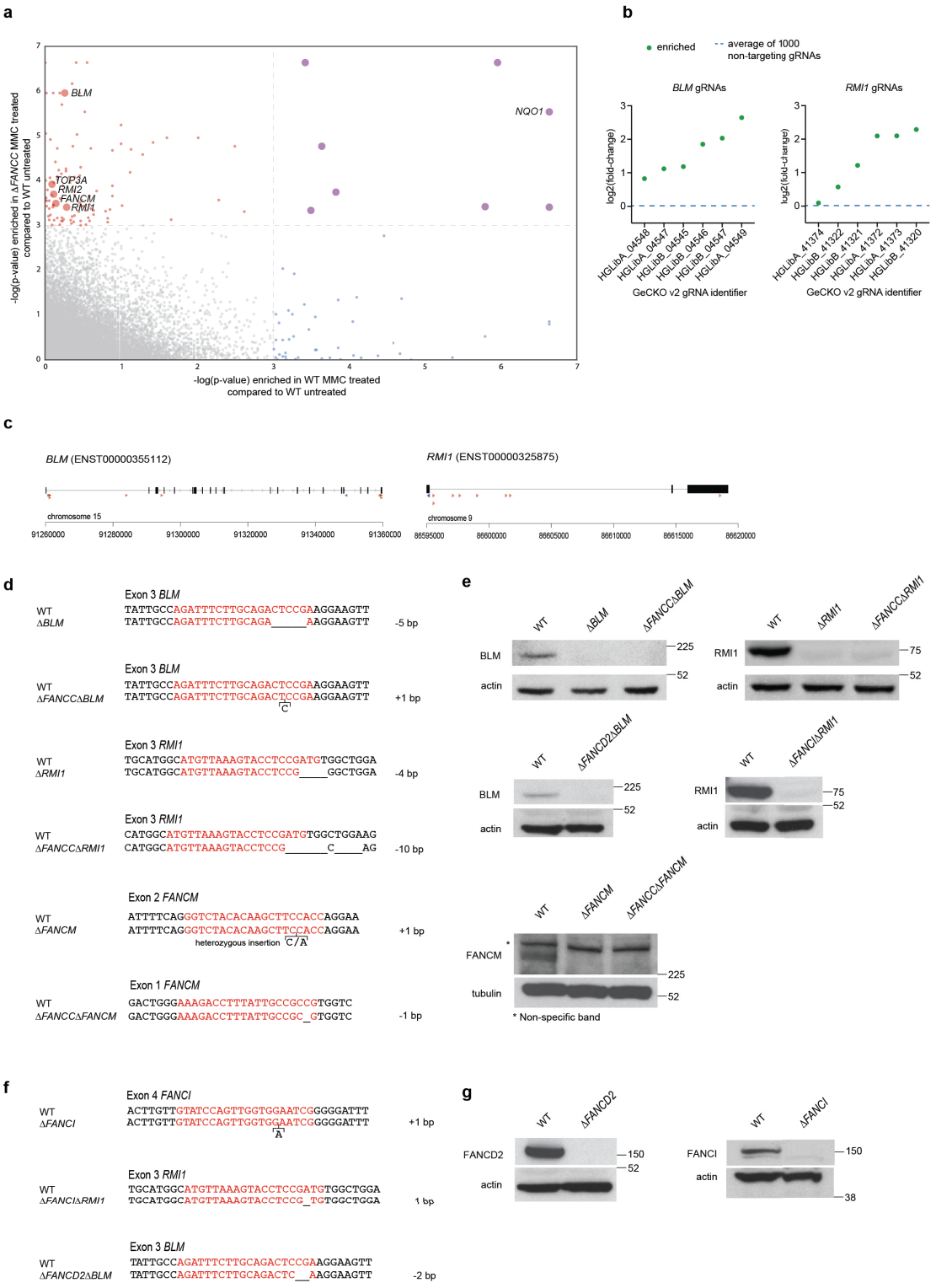

Supplementary Figure 4. Validation of the BLM complex as a suppressor for FA mutant cells following exposure to MMC. (a) Mutated genes enriched in MMC treated Δ*FANCC* cells, compared to untreated WT cells, plotted against mutated genes enriched in MMC treated WT cells, compared to untreated WT cells, according to p-values from the CRISPR screen. (b) Enriched gRNAs in the CRISPR screen for BLM and RMI1 in Δ*FANCC* cells treated with MMC compared to WT untreated cells.

(c) Gene-trap insertions within *BLM* and *RMI1* enriched in Δ*FANCC* cells treated with MMC. Red arrows indicate mutagenic insertions in the sense orientation (10 and 9 unique inactivating insertion sites for *BLM* and *RMI1* respectively) while blue arrows indicate insertions in the antisense orientation (inactivating only in exonic regions; 1 identified for both *BLM* and *RMI1*). (d) CRISPR-Cas9-mediated mutation of *BLM, RMI1* and *FANCM* in WT HAP1 cells or in Δ*FANCC* mutant cells. Red sequences in WT correspond to the gRNAs used. (e) Immunoblots of BLM, RMI1, FANCM and actin from cell extracts of indicated cells. (f) CRISPR-Cas9-mediated mutation of *FANCI* in WT cells, *RMI1* in Δ*FANCI* cells and *BLM* in Δ*FANCD2* cells. Red sequences in WT correspond to the gRNAs used. (g) Immunoblots of FANCD2, FANCI and actin from cell extracts of indicated cells.

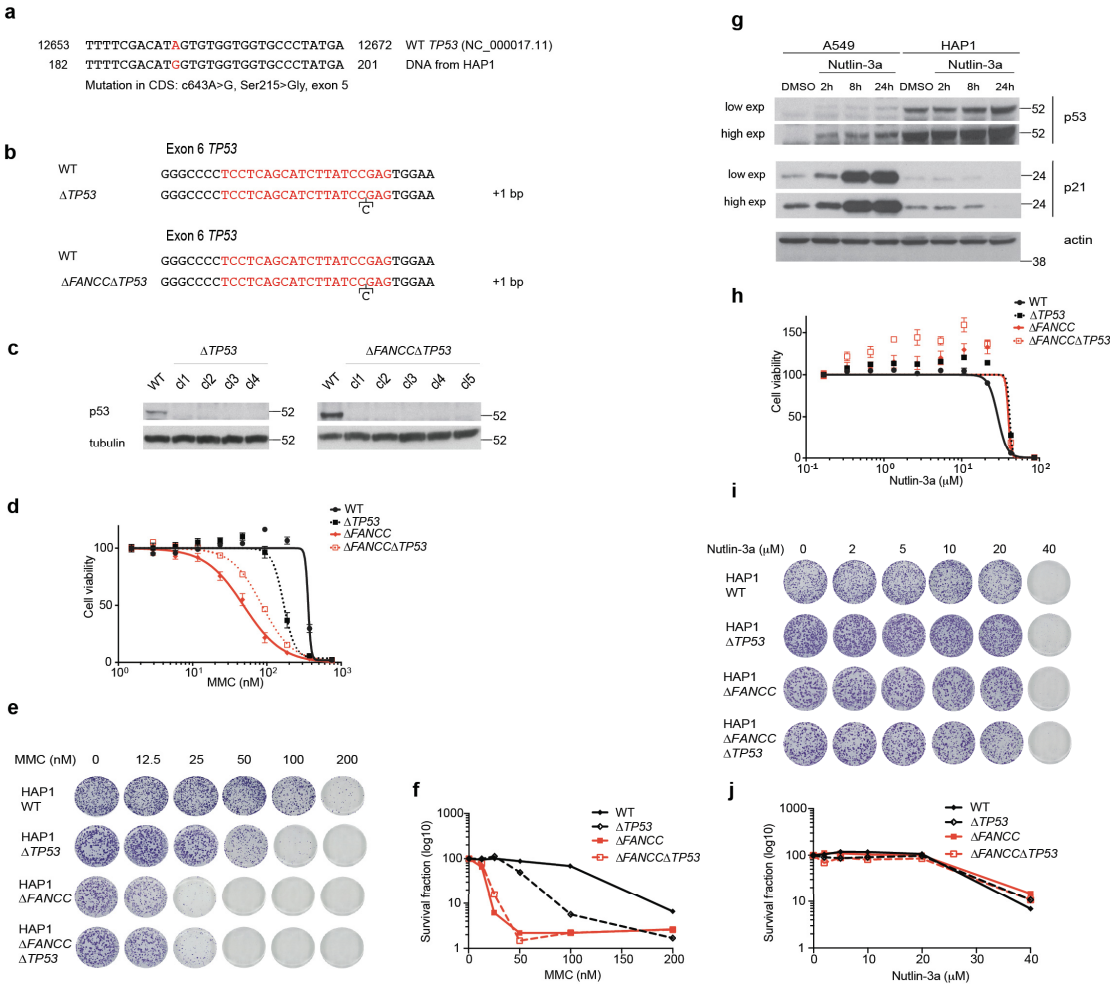

Supplementary Figure 5. Characterization of p53 in HAP1 cells. (a) Mutation of the *TP53* gene in HAP1. (b) Targeting of *TP53* by CRISPR-Cas9 in WT and Δ*FANCC* cells. Sequences of *TP53* in Δ*TP53* and Δ*FANCC*Δ*TP53* indicate mutations in clone 3 (cl3; see panel 'c') in both cell lines. (c) Immunoblot of p53 knock-out clones in WT and Δ*FANCC* deficient cells. Clone 3 (cl3) of cell lines was chosen for further experiments. (d) Survival of indicated cells after treatment with MMC. Means and S.E.M. of triplicates are plotted. (e) Colony formation assay of indicated cells exposed to MMC. (f) Quantification of (e). (g) Immunoblot of A549 and HAP1 cells exposed to Nutlin-3a at 10 μM for the indicated time points and probed for p53, p21 and actin. (h) Survival of indicated cells after Nutlin-3a treatment. Means and S.E.M. of triplicates are plotted. (i) Colony formation assay of indicated cells to Nutlin-3a. (j) Quantification of (i).

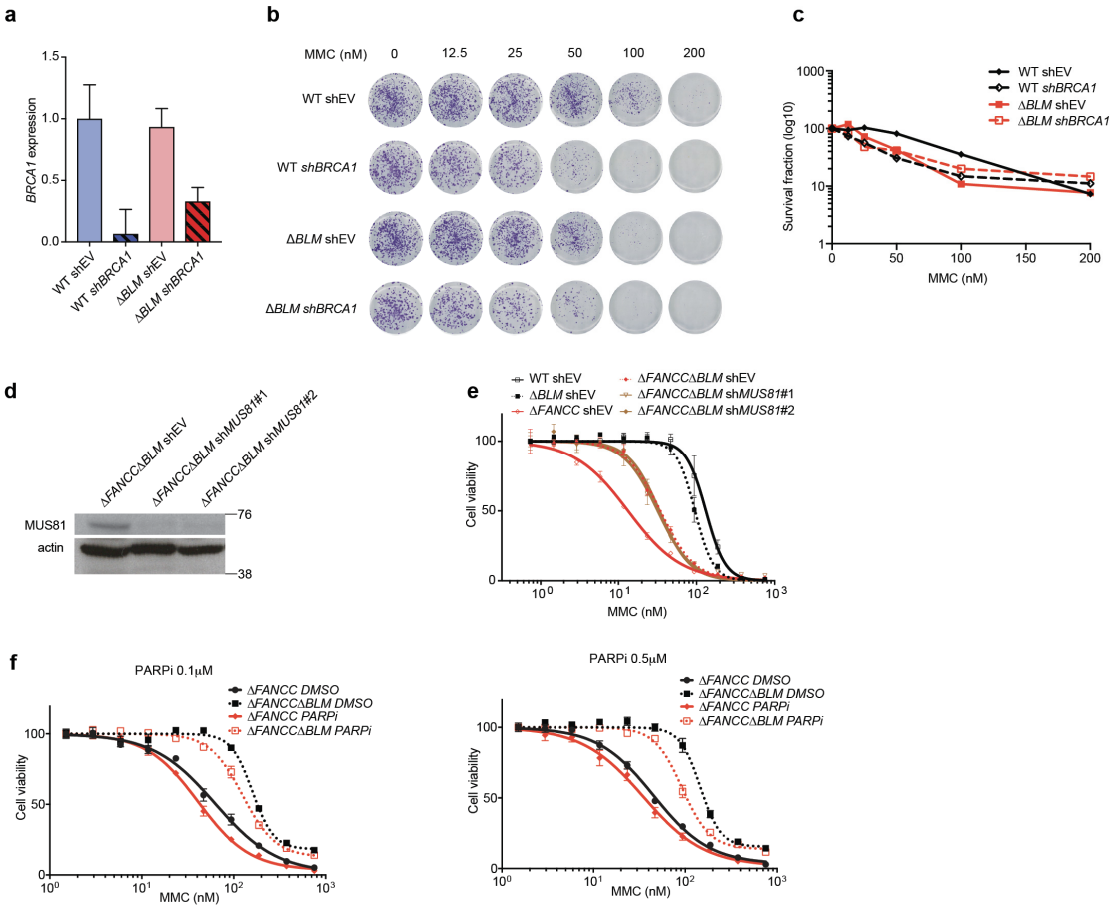

Supplementary Figure 6. Mechanisms of rescue in Δ*FANCC*Δ*BLM* cells. (a) Expression of *BRCA1* upon shRNA knock-down measured by quantitative reverse transcription PCR (q RT-PCR) in WT and Δ*BLM* cells compared to cells infected with empty vector (EV). (b) Colony formation assay of WT and Δ*BLM* cells infected with sh*BRCA1* or shEV treated with MMC. (c) Quantification of (b). (d) Immunoblot for MUS81 knock-down in Δ*FANCC*Δ*BLM* cells using two different shRNAs (sh*MUS81*#1, sh*MUS81*#2), compared to Δ*FANCC*Δ*BLM* cells infected with empty vector (shEV). (e) Survival of indicated cells infected with shEV, sh*MUS81*#1 or sh*MUS81*#2, treated with MMC, assessed after 4 days by CellTiter-Glo. (f) Survival of Δ*FANCC* or Δ*FANCC*Δ*BLM* cells treated with either the PARP inhibitor olaparib (PARPi) or DMSO for 4 hours, followed by MMC exposure for four days, assessed by CellTiter-Glo. Error bars of survival curves and expression data indicate S.E.M. of triplicates.

Supplementary Fig. 1

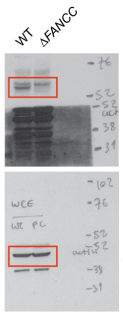

Supplementary Fig. 3

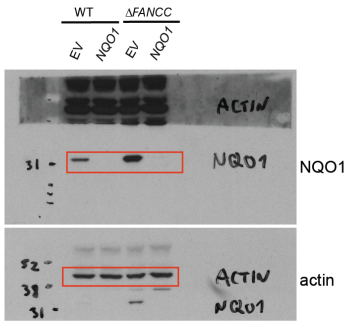

Supplementary Fig. 4

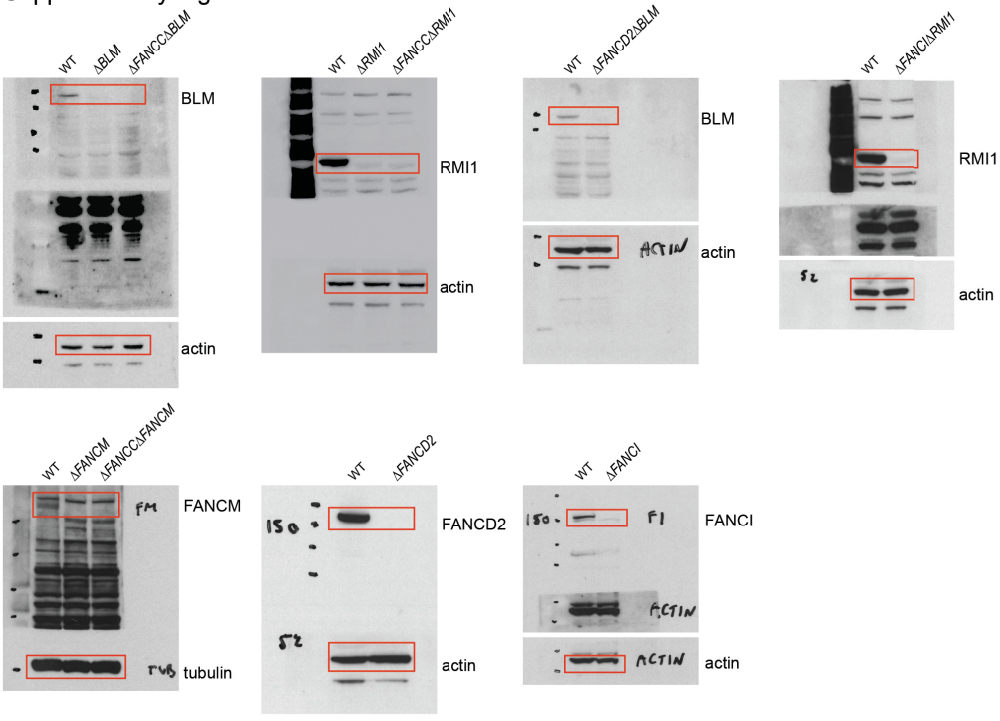

Supplementary Fig. 5

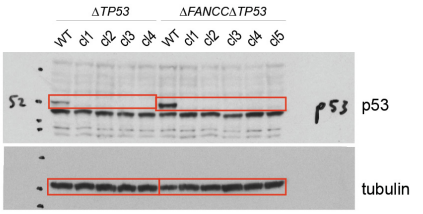

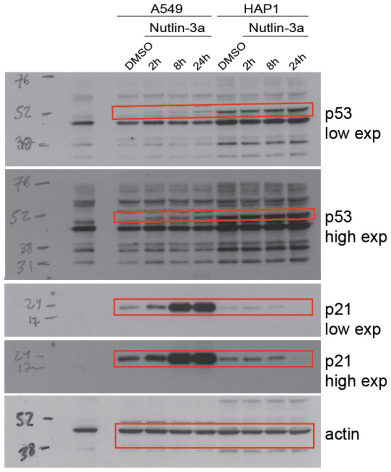

Supplementary Fig. 6

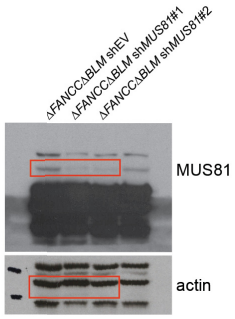

Supplementary Figure 7. Uncropped immunoblots.

Sample	Number of genes targeted*	Total number of insertions
HAP1 Δ*FANCC* + MMC	7,236	22,772
HAP1 WT untreated	17,907	2,274,503

***** protein-coding

Supplementary Table 1. Table depicting the number of genes targeted and the total number of unique insertions for each library sequenced using the insertional mutagenesis gene-trap approach.

		Viable		Late apoptosis		Early apoptosis	
	Time point	**Mean**	**S.E.M.**	**Mean**	**S.E.M.**	**Mean**	**S.E.M.**
Δ***WT***	**UT**	86.0	1.7	3.8	0.7	10.2	1.0
	24h	90.0	0.6	2.7	0.3	7.3	0.4
	48h	88.1	0.3	6.0	0.7	6.0	0.9
	72h	66.1	1.3	22.6	1.8	11.3	0.6
Δ***BLM***	**UT**	81.4	0.6	6.0	1.0	12.6	1.4
	24h	87.7	0.8	4.3	0.4	8.0	0.5
	48h	78.7	1.9	12.8	1.6	8.5	0.3
	72h	62.1	2.4	26.5	1.7	11.4	1.1
Δ***FANCC***	**UT**	71.3	1.7	3.5	0.1	25.3	1.8
	24h	68.9	0.5	4.6	0.7	26.5	0.6
	48h	37.4	1.3	33.1	0.6	29.5	1.9
	72h	15.4	1.1	63.6	1.7	21.1	0.7
Δ***FANCC*Δ*BLM***	**UT**	80.0	1.9	4.8	0.5	15.2	2.0
	24h	81.0	0.9	4.8	0.7	14.2	1.5
	48h	74.2	1.2	11.6	0.8	14.2	1.6
	72h	41.1	1.8	37.4	3.2	21.5	1.9

Supplementary Table 2. Table numerically showing the percentage of cells that are viable, in late or early apoptosis as graphically depicted in Fig. 2e.

CHAPTER THREE: DISCUSSION

3.1 General discussion

The DDR is a complex network of interacting and partially overlapping signaling pathways that enable cells to maintain genomic integrity despite constant challenges by mutagenic events. The interactive nature of those pathways enables targeted perturbations to affect the repair outcome in cells with defects in the DDR. This allows the utilization of synthetic viable interactions to promote a desired repair outcome, therefore ameliorating disease phenotypes associated with defective DDR. Recently, high-throughput genome-wide perturbation systems became applicable to human cells, enabling the systematic analysis of synthetic viable interactions in DDR defective cells. Using a CRISPR-based LOF screen parallel to a gene-trap insertional mutagenesis screen, we identified that loss of the BLM helicase complex rescues survival of FA defective cells upon induction of DNA ICLs. We found decreased levels of γH2AX upon loss of BLM and ICL induction in ∆*FANCC* cells and a partial dependence of this survival outcome on alt-NHEJ. The following subchapters will discuss possible biases of our screening approaches, a comparison between the gene-trap and CRISPR screen, a discussion of possible rescue mechanisms, the therapeutic potential and the possibility to derive further knowledge from our datasets.

3.2 Technical obstacles and possible biases

Every screening approach has its advantages and disadvantages. When performing LOF screens, the emergence of a KO phenotype depends on the turnover of the already transcribed mRNA and expressed protein. This turnover rate varies between genes and cell lines and can result in false-negative results in a positive selection screen. However, given the late time points of genomic harvest in our gene-trap and CRISPR screens and the comparatively rapid turnover rate of most human gene products, only a minute fraction of genes is expected to be susceptible to this bias. When using end point viability based readouts, depletion of a genotype over time does not necessarily reflect apoptosis, but can result from slightly reduced cell proliferation that will appear as dropout, when cultured for extended periods of time. However, since we use a positive selection screen and aim for restoring wild-type function, this is not relevant to our results. Potential false-positive results arising from overproliferation effects were excluded by comparing the CRISPR screen results from the ∆*FANCC* background to a similarly treated WT dataset. A relevant bias in

our study might arise at the stage of MMC selection in the CRISPR screen. Since Δ*FANCC* cells are more sensitive to ICLs than WT cells, the latter had to be treated with a higher dose of MMC to attain an equivalent amount of selection pressure. Δ*FANCC* cells were therefore treated with 46nM MMC, while WT cells were challenged with 190nM MMC to kill a similar percentage of cells in both genetic backgrounds. Both samples were compared to the appropriate untreated control data sets and enriched genes overlapping between WT and Δ*FANCC* were excluded as MMC signature. However, we cannot exclude that MMC might have different biological effects at different doses, therefore introducing a bias into this gene-exclusion approach. Nonetheless, the presence of overlapping MMC signature genes that are expected to increase cell abundance upon KO and selection pressure support the robustness of our approach in spite of this possible bias. Those include the gene encoding the metabolic enzyme NQO1, which is required for MMC to be metabolized into its active DNA crosslinking form (Siegel et al., 2012). Also we identified the pro-apoptotic gene *PMAIP1* as overlapping result, presumably due to aggravated apoptosis and increased survival in the presence of DNA damage. Additionally we recovered *FLCN* as an overlapping MMC signature gene, which upon LOF increases cell cycle progression in MEFs and human renal cell carcinoma, suggesting its role as a tumor suppressor gene (Laviolette et al., 2013). Nonetheless, we cannot exclude the possibility of biased MMC signature results due to the inability to compensate for the different doses of MMC applied to both genetic backgrounds. Alternatively, instead of comparing WT and Δ*FANCC* cells to the appropriate untreated data sets and excluding the overlapping genes between both genetic backgrounds, we could have directly analyzed differently enriched genes between the MMC treated WT dataset and the MMC treated Δ*FANCC* sample to reveal synthetic viable interactions specific to Δ*FANCC*. However, this would not have eliminated the mentioned bias nor compensated for possible unique characteristics of Δ*FANCC* cells. Additionally, a direct comparison between both MMC treated datasets would not have revealed whether the NQO1 KO clones became significantly enriched upon MMC selection to technically validate our screen.

3.3 Overlap between CRISPR and Gene-trap results

Both genome-wide screens were performed in near-haploid HAP1 cells, which are descendants of the KBM-7 cell line that was established from a chronic myeloid leukemia patient (Kotecki et al., 1999). HAP1 cells contain a single copy of each chromosome, except for a heterozygous 30-megabase fragment of Chromosome 15, encompassing 330 genes (Essletzbichler et al., 2014). In a gene-trap screen,

occasional insertional mutagenesis of these genes will not display a phenotype due to the presence of a second functional copy. CRISPR screens however are applicable to haploid- as well as diploid genetic backgrounds, enabling the identification of phenotypes associated with genes located on the heterozygous fragment. The probability of biallelic deleterious mutations using CRISPR is estimated to be 30-70% (Michlits et al., 2017). Although this needs to be considered when screening in HAP1, it can only account for a minute difference between the results of genome-wide CRISPR and gene-trap screens. When comparing the significantly enriched genes in our Δ*FANCC* CRISPR screen to the gene-trap screen however, we find little overlap of only 4 genes (*BLM, RMI1, NQO1, USP48*) between the two approaches (**Thesis Fig. 2**). BLM and RMI1 are components of the BLM helicase complex. Their enrichment in the gene-trap mutagenesis screen therefore confirms the recovery of BLM complex components in the CRISPR screen using an independent approach. Furthermore, the recovery of the NQO1 positive control in both genome-wide screens confirms the technical validity of both approaches. In the gene-trap screen, *NQO1* was the second most enriched gene, whereby the most enriched gene was *USP48*. USP48 functions as deubiquitinating enzyme and was recently shown to promote Mdm2 stability and enhance Mdm2-mediated p53 ubiquitination (Cetkovská et al., 2017). However, its role in the DDR is not well characterized, which is why USP48 constitutes an interesting candidate for further synthetic viability studies.

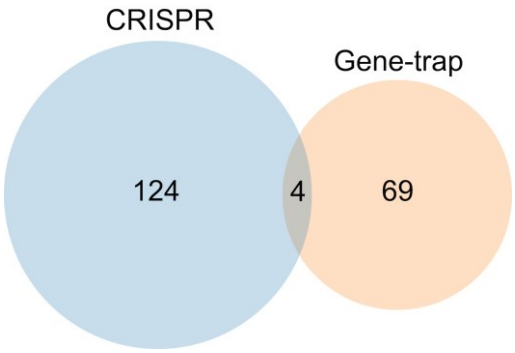

Thesis Figure 2: Significantly enriched genes in the Δ*FANCC* CRISPR- and gene-trap screen. The CRISPR screen revealed 124 significantly enriched genes when comparing Δ*FANCC* cells treated with MMC to an untreated control dataset. By comparison, 69 genes were enriched in an analogous gene-trap screen, whereby 4 genes (*BLM, RMI1, NQO1, USP48*) were overlapping between both approaches.

Several factors might contribute to the discrepancies between both screening results. Since the GeCKO library used in the CRISPR screen only targets protein-coding

genes, ncRNAs were removed from the gene-trap results for better comparability. An inherent bias of gene-trap screens is the increased probability of disrupting particularly transcriptionally active genes. We compensated for this bias by infecting a sufficient number of cells and choosing an adequate sequencing depth. The tendency of HAP1 cells to turn diploid over time, especially under stress conditions, could have contributed to the discovery of fewer enriched genes in the gene-trap screen, compared to the CRISPR screen. Although we analyzed the haplotype of ∆*FANCC* cells on a regular basis and started the screen with a predominantly haploid population, we cannot exclude that a fraction of cells might have turned diploid over the course of the gene-trap screen. Cells that turn diploid before infection with the insertional mutagenesis virus will not show a LOF phenotype due to the presence of a second copy and therefore cannot become enriched in the gene-trap screen. Haploinsufficient genes are an exception to that, however, they only constitute a small fraction of human genes. This haplotype obstacle cannot bias the CRISPR screen to the same extent, since gRNAs target both gene copies equally and allow diploid cells to display a LOF phenotype. The high frequency occurrence of biallelic mutations using CRISPR screens was recently demonstrated (Wang et al., 2015). Another difference between gene-trap and CRISPR screens is the readout used to determine the mutation occurrence. Gene-trap screens directly measure the disruption at the site of integration, therefore providing direct evidence of genetic perturbation. In contrast, CRISPR screens use the presence of the integrated gRNA sequence as indication for the presence of the gene editing machinery and the occurrence of a mutation at the target site has to be inferred. Inefficient gRNAs can fail to induce mutations at target sites or the occurrence of in-frame mutations can lead to genetic alterations that do not evoke a phenotype. However, since we performed a positive selection screen, cells without LOF phenotypes would not become enriched. We compensated for this bias by targeting each gene with 6 different gRNAs and using a sufficient number of cells to guarantee adequate representation and redundancy of each gRNA as confirmed by the quality control of our sequencing data (**Supplementary Fig. 2a-c**). Another peculiarity of CRISPR screens using a lentivirus is that besides the gene targeted by the gRNA, an additional gene-disruption can occur due to the random integration of the vector into the genomic DNA. However, these disruptions occur at different sites in each cell and sufficient infection redundancy of each gRNA prevents the integration events from biasing the outcome. In a previous study, gene-trap and CRISPR screens were performed in parallel to identify essential genes in KBM7 cells (Wang et al., 2015). Besides using a different scoring method, the study revealed a considerably higher

overlap between identified genes in both screens compared to our study. A possible explanation is that gene essentiality results in a stronger phenotype compared to synthetic viability, which can produce rescue effects of variable intensities. However, since we observed a considerable number of genes with few insertions in the gene-trap screen, we cannot exclude the possibility of false-negatives in that approach due to limited sequencing depth. We therefore consider the gene-trap screen primarily as a confirmation experiment for the CRISPR screen that reinforces the authenticity of the BLM complex as rescue interaction in ∆*FANCC* cells in an independent manner.

3.4 BLM dependent rescue mechanism

Although our study does not focus on exploring the exact rescue mechanism of the interaction between the BLM complex and the FA pathway, we propose mechanistic rescue hypotheses based on our data in the context of the respective literature. To measure the effect of BLM LOF in ∆*FANCC* cells, we used γH2AX staining as a marker of DNA damage. Histone H2A is one of the five main histones that direct chromatin structure in eukaryotic cells and encompasses multiple variants, including H2AX. This variant contains a C-terminal extension that is involved in DNA damage repair. Upon detection of DSBs, H2AX gets phosphorylated on serine 139 and is then referred to as γH2AX (Jakob et al., 2011). This can occur due to unrepaired ICLs that block replication and potentially lead to replication fork collapse when not repaired accordingly. In our study, we show that the percentage of γH2AX positive cells is significantly reduced at 48h and 72h after ICL induction in ∆*FANCC*∆*BLM* cells, compared to ∆*FANCC* cells (**Fig. 2d**). Unrepaired ICLs are highly deleterious lesions, since they tether complimentary strands that result in DSBs upon collision with a replication fork (Bessho, 2003). Previous studies have shown that BLM is recruited to sites of stalled replication forks and suggest a role of BLM in protecting against replicative stress by facilitating fork restart (Lönn et al., 1990; Sengupta et al., 2003). When treated with replication stress inducing drugs, BLM deficient PSNG13 cells showed reduced replication fork activity and defective replication-fork recovery compared to BLM proficient PSNF5 cells (Davies et al., 2007). The study also found BLM to be required for efficient replication-fork restart. Upon induction of replication stress, the ATR kinase phosphorylates BLM at threonine 99, which promotes the ability of cells to restart DNA synthesis at stalled replication forks (Davies et al., 2004). Likewise, loss of BLM reduces the ability of cells to suppress new origin firing during periods of replicative stress (Chaudhury et al., 2013; Davies et al., 2007).

We therefore propose our first hypothesis for the FA-BLM rescue interaction (**Thesis Fig. 3**): The absence of FANCC disables canonical ICL removal via FA signaling,

leading to an accumulation of ICLs that trigger stalled-fork induced replication stress during S phase. Presence of the BLM complex could restart stalled forks prematurely, leading to increased replication fork collapse followed by cell death. Likewise, the enhanced new origin firing in the presence of BLM could aggravate this effect. In this context, loss of BLM in ∆*FANCC* cells could allow alternative repair mechanisms to remove the ICLs early enough to escape cell death.

A more recent study examined the interplay between FANCB, which is a constituent of the FA core complex, and BLM in mouse embryonic stem cells (Kim et al., 2015). The study concludes that BLM is able to restart, but not protect stalled replication forks, strengthening our first hypothesis. The study also found that loss of BLM in a *FANCB* mutated background suppresses sensitivity to MMC. Similar to our results, loss of BLM by itself did not affect cellular survival upon ICL induction. The study shows that loss of BLM reduces nascent strand degradation in *FANCB* mutated cells, suggesting that presence of BLM enhances strand degradation in FA-defective cells. This is in line with our first hypothesis and could contribute to the reduced sensitivity to MMC upon loss of BLM in FA deficient backgrounds. Additionally, loss of BLM in a *FANCB* mutated background treated with MMC for 16h suppressed chromosomal abnormalities including chromatid breaks, isochromatid breaks and radials. This is additionally consistent with our first hypothesis, since a chromatid break is a single broken chromatid that often results from broken replication forks. Isochromatid breaks are breaks in two complementary sister chromatids at the same location, indicating failed SCE intermediates. Radials are the product of multiple chromosome attachments and result from broken chromatids. These results suggest that BLM promotes chromosomal defects in FA deficient cells exposed to MMC. However, our study did not reveal significantly different chromosomal aberrations in ∆*FANCC* cells compared to ∆*FANCC*∆*BLM* cells (**Fig. 2f**). This could point towards divergent functions of FANCC and FANCB within the FA core complex. Alternatively, the interplay between the BLM complex and the FA pathway could be different in mouse embryonic stem cells compared to human HAP1 cells. Although we do not observe a significantly different amount of chromosomal aberrations in ∆*FANCC* cells compared to ∆*FANCC*∆*BLM* 24h after MMC treatment (**Fig. 2f**), it needs to be considered that at this time point, we also do not observe significantly different amounts of γH2AX positive cells in both genetic backgrounds (**Fig. 2d**). However, the difference in γH2AX is significant at 48h and 72h, suggesting the possibility that at those later time points, divergent amounts of chromosomal aberrations could have been observable. The observation from FA-defective in mouse embryonic stem cells that the presence of BLM promotes MMC-induced chromosomal defects, including

failed SCE intermediates, highlights the possibility that in the absence of the FA pathway, inadequate BLM-mediated Holliday junction dissolution shifts repair from HR to a more mutagenic pathway, possibly NHEJ.

In combination with the finding that presence of FANCB promotes replication fork stability (Kim et al., 2015), we propose our second hypothesis for the FA-BLM synthetic viable interaction (**Thesis Fig. 3**): Presence of the FA core complex could promote replication fork stability in a manner that suppresses BLM-mediated chromosomal defects. However, in the absence of the FA core complex, presence of BLM might evoke toxic intermediate HR structures upon treatment with MMC that result in genotoxic lesions. A more direct relationship between BLM and HR was demonstrated by another study in mouse embryonic stem cells treated with MMC, whereby mutation of *Blm* rescued the survival of cells deficient for Rad54, a mayor component of HR (Chu et al., 2010). This was shown to result from a decreased conversion of ICLs to DSBs in the double deficient background, compared to solely Rad54 deficient cells. At least in part, conversion of MMC-induced ICLs into DSBs in mammalian cells requires the endonuclease Mus81 (Hanada et al., 2006). We examined the relevance of this for our result by knocking-down MUS81 with two different shRNAs and did not observe an effect on the survival of ∆*FANCC*∆*BLM* cells upon treatment with MMC (**Supplementary Fig. 6e**). Besides HR and canonical NHEJ, cells can repair DSBs using the highly mutagenic alt-NHEJ pathway that does not rely on canonical NHEJ factors, but requires the Poly (ADP-ribose) polymerase 1 (PARP1) (Ceccaldi et al., 2016; Deriano and Roth, 2013; Sfeir and Symington, 2015; Wang et al., 2006). Recent studies highlight the role of alt-NHEJ in the FA pathway (Kais et al., 2016; Murina et al., 2014). A study in human fibroblasts concludes that presence of BLM aggravates alt-NHEJ by counteracting CtIP/MRE11-dependent long-range deletions (Grabarz et al., 2013).

From that we derive our third hypothesis for the FA-BLM synthetic viable interaction (**Thesis Fig. 3**): Loss of BLM might enhance the survival of FA-deficient cells upon ICL induction, by facilitating alt-NHEJ. We tested this hypothesis by treating ∆*FANCC*∆*BLM* cells with the PARP inhibitor olaparip and observed a partial re-sensitization to MMC (**Fig. 2g and Supplementary Fig. 6f**). From this we conclude that to some extent, the increased survival of ∆*FANCC* cells upon loss of BLM is caused by the elevated capacity for alt-NHEJ. Since this is the most error-prone repair pathway, survival presumably comes at the cost of increased mutational burden. However, PARP inhibition did not completely re-sensitize ∆*FANCC*∆*BLM* cells to the level of DMSO-treated ∆*FANCC* cells, indicating that additional survival-

increasing mechanisms must contribute to the rescue effect and the overall repair outcome in ∆*FANCC*∆*BLM* cells could be more favorable than in ∆*FANCC* cells.

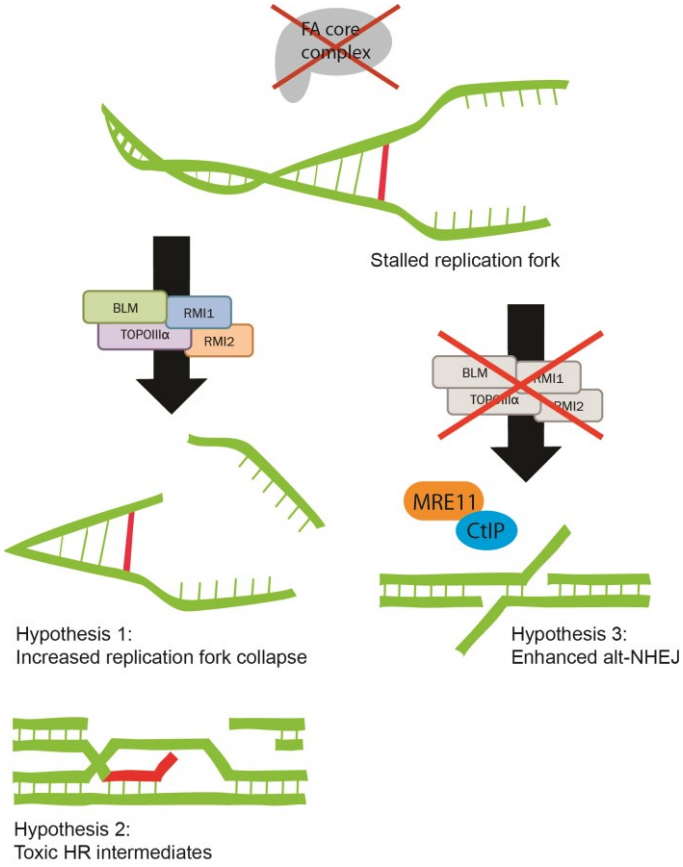

Thesis Figure 3: Preliminary models of the synthetic viable interaction between the BLM helicase complex and the Fanconi anemia pathway. Hypothesis 1: Perturbed FA-signaling in the presence of ICLs leads to the accumulation of stalled replication forks during cell division. The capacity of the BLM complex to prematurely restart replication forks and initiate new origin firing could contribute to the increased sensitivity to crosslinking agents. Hypothesis 2: In the absence of the FA pathway, the BLM complex could evoke toxic intermediate HR structures that result in chromosomal abnormalities and lethality. Hypothesis 3: Using the PARP inhibitor olaparib, we show that the reduced sensitivity of ∆*FANCC*∆*BLM* cells compared to ∆*FANCC* cells is in part dependent on alt-NHEJ.

3.5 Therapeutic potential

Defects in the DDR are commonly exploited for the treatment of cancer, by applying genotoxic drugs that exceed the repair capacity of malignant cells (Bouwman and Jonkers, 2012; Curtin, 2012; Helleday et al., 2008; Lord and Ashworth, 2012). The

initial rational for developing drugs targeting the DDR was to inhibit the repair of damage caused by radiotherapy or chemical genotoxins, thereby potentiating their efficacy (Curtin, 2012). Today, drugs directly targeting parts of the DNA repair machinery can be used as stand-alone therapy to induce synthetic lethality in cancer cells with already pre-existing DNA repair defects (Brough et al., 2011). The most prominent example for such an interaction is the treatment of BRCA1/2 deficient tumors with the PARP inhibitor olaparib. Since BRCA1/2 deficient tumor cells have increased reliance on PARP for DNA repair, inhibition of PARP1 via olaparib was demonstrated to be an effective treatment for appropriate forms of breast, ovarian, pancreatic and prostate cancers (Fong et al., 2009). Despite the recent success of small molecule inhibitors targeting DDR proteins in cancer therapy, to date, no approved therapy aims at inducing synthetic viability in diseases associated with defects in the DDR using small inhibitors. Such diseases are commonly associated with increased cancer susceptibility that is, where possible, accounted for by avoidance of patient-exposure to the relevant mutagens. However, to date no curative therapy for the alleviation of cancer susceptibility for such diseases is known. This is in part due to the inability of restoring the proper function of mutated genes, including those associated with the DDR. Future therapies could circumvent this shortcoming by compensating mutations in the DDR by exploiting synthetic viable interactions to restore a healthier phenotype despite the presence of a disease-inducting mutation. Analogous to cancer therapy, drugs could be used to inhibit DDR proteins that were demonstrated to partake in synthetic viable interactions with disease-causing mutations. Several factors contribute to the current unavailability of such therapies. First, the systematic search for synthetic viable interactions in the DDR is in its infancy since effective genome-wide high-throughput screening tools only became available in the recent past and focused mostly on the discovery of synthetic lethality. In our study, we therefore demonstrate the efficacy of identifying synthetic viable interactions in DDR defective cells, by applying two parallel screening approaches to FA-defective cells. Second, a limited number of drugs that directly target DDR pathways are under clinical evaluation, restraining the current applicability of drugs that exploit synthetic viable interactions to alleviate disease (Pearl et al., 2015). The number of proteins involved in the DDR in human cells is estimated to be around 450, including mostly enzymes, but also scaffold proteins, enzyme regulators, DNA-binding proteins, transcription regulators, transcription factors and others (Pearl et al., 2015). In 2015, only 26 of those DDR proteins could be targeted by compounds that were approved or under clinical evaluation in 2015 (Pearl et al., 2015). Although individual DDR pathways are mostly

depicted as linear signaling cascades, the majority of all DDR proteins are predicted to interact with proteins involved in other DDR pathways (Pearl et al., 2015). This complex interconnectedness challenges the development of targeted pharmacological interventions. Third, targeting DDR proteins to induce synthetic lethality in cancer cells is a time-restricted treatment for which severe side effects are acceptable due to the acute threat to the patient's life. In contrast, the treatment of DDR-associated diseases exploiting synthetic viable interactions would require long-term treatment and would therefore need a less severe spectrum of side effects. To date, no clinically approved BLM complex inhibitor is available. Recently however, a small molecule inhibitor for BLM called ML261 became available as a result of a high throughput screen of a chemical compound library (Nguyen et al., 2013). Upon application of ML261 on Δ*BLM* cells, we observed a reduction in cell viability at higher doses (**Thesis Fig. 4a**). This could result from off-target effects, since ML261 also targets the Werner syndrome ATP-dependent helicase (WRN) or from inhibiting BLM on DNA, thereby preventing the binding of other nucleases such as WRN that could compensate for the lack of BLM activity (Banerjee et al., 2013; Nguyen et al., 2013). Nevertheless, we tested whether ML261 is able to rescue Δ*FANCC* cells treated with MMC but observed an increased sensitivity that could be explained by the reasons mentioned above (**Thesis Fig. 4b**).

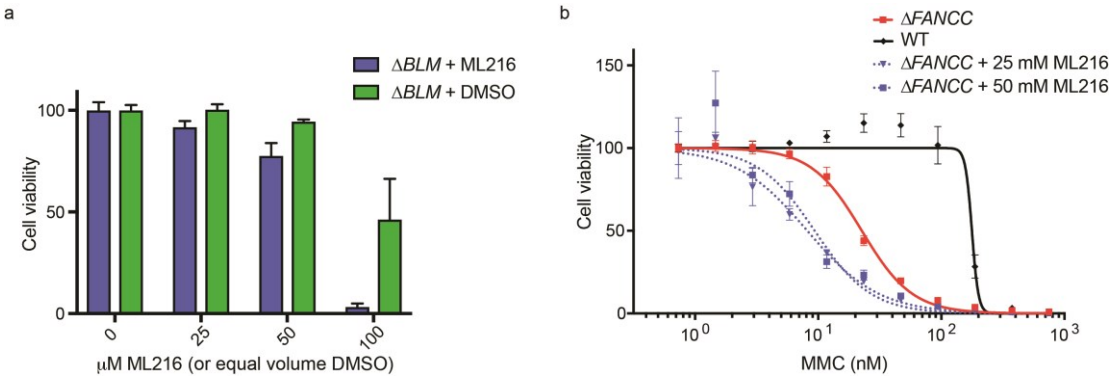

Thesis Figure 4: Effects of the BLM inhibitor ML261 on Δ*BLM* and Δ*FANCC* cells. (a) Δ*BLM* cells were incubated with the BLM inhibitor ML216 at the indicated concentrations (or equivalent volumes of DMSO) for 4 days followed by measurement of survival by CellTiter-Glo. (b) The indicated cell lines were incubated with the BLM inhibitor ML216 for 24 hours and then exposed to MMC for 4 days. Cell survival was measured by CellTiter-Glo. Error bars indicate means and S.E.M. of biological triplicates.

Whether inhibition of BLM harbors therapeutic value for FA patients is debatable, since loss of BLM itself is associated with a severe disorder called Bloom syndrome, characterized by short stature, cancer predisposition and genomic instability (Bischof et al., 2001). However, it cannot be excluded that the disease phenotype of combinatorial loss of BLM and FA-signaling could be less severe than of defective FA-signaling alone. To date, no patient carrying LOF mutations in a FA complementation group and a component of the BLM complex is described. However, both pathways physically interact with each other and bind to the DNA via FANCM (Deans and West, 2009). FANCM acts as a protein anchor that is required for recruiting key components of the FA core complex and the BLM complex to stalled replication forks via its protein-protein interaction motives MM1 and MM2. MM1 links FANCM to the FA core complex by binding FANCF, whereas MM2 interacts with RMI1 and TOP3A of the BLM complex (Deans and West, 2009). Both binding motives are independently required to activate the FA and BLM pathways. Loss of FANCM therefore approximates the inactivation of the FA pathway in combination with defective BLM signaling. Our CRISPR screen revealed *FANCM* mutations as enriched in ∆FANCC cells treated with MMC, probably due to the involvement of FANCM in BLM signaling. Because FANCM intersects with both pathways, patients carrying *FANCM* mutations can point towards potential consequences of BLM inhibition in FA patients. In 2005, the first patient (EUFA867) with biallelic *FANCM* mutations was described (Meetei et al., 2005). However, the phenotype of patient-derived cells could not be complemented by introducing wild-type *FANCM* complementary DNA (cDNA). This was explained by a paper published in 2009 that, in addition to mutated *FANCM*, identified biallelic *FANCA* mutations in the cells from the EUFA867 patient (Singh et al., 2009). Remarkably, a sibling of EUFA867 carried the same biallelic *FANCA* mutation, but only a heterozygous *FANCM* mutation, classifying the sibling as a FANCA patient. This sibling was diagnosed with FA before EUFA867, since she displayed typical FA features, whereas the ∆*FANCA*∆*FANCM* double deficient patient EUFA867 did not display obvious FA symptoms. EUFA867 was therefore diagnosed with FA later on the basis of a chromosomal breakage assay performed because of her brother's diagnosis. The unconventionally mild phenotype of EUFA867 suggested for the first time that FANCM deficient patients may display different symptoms than patients carrying mutations for other FA core complex members and that additional loss of FANCM may even alter the disease phenotype of otherwise FA-deficient patients. A similar interplay was observed in DT40 cells, in which disruption of the FANCM ortholog in a ∆*FANCC* background reduced sensitivity to the ICL-inducing agent cisplatin

compared to Δ*FANCC* single KO cells (Mosedale et al., 2005). Recently, three individuals with biallelic *FANCM* truncating mutations were reported (Bogliolo et al., 2017). Although these individuals displayed increased cellular sensitivity to ICL-inducing agents and early-onset cancer, they did not present congenital malformations or hematological disorders that typically accompany FA deficiencies. We hypothesize that this attenuation of symptoms may result from loss of BLM signaling in addition to perturbed FA-signaling in FANCM deficient cells. It is therefore not inconceivable, that FA patients could benefit from targeted inhibition of BLM signaling. Furthermore, since the Δ*FANCA*Δ*FANCM* patient EUFA867 displayed a milder FA phenotype compared to her FANCA deficient sibling and FANCM is predicted to be a druggable biological target, direct targeting of FANCM using small molecule inhibitors might provide therapeutic value (Pearl et al., 2015).

3.6 Further analysis of screening results

Our CRISPR screen revealed 124 genes that that upon disruption increased the survival of Δ*FANCC* cells treatment with MMC, compared to an untreated dataset. We followed up on the BLM complex due to the confirmation according to the gene-trap results and the promising relevance of identifying a complete complex. However, it is not to be excluded that further genes enriched in our dataset possess biological or clinical relevance. The choice of genes for further in-depth analysis is a crucial step for the successful discovery of relevant interactions. A possible choice-guiding principle is the discovery that synthetic viable interactions in the DDR frequently emerge due to the activation of alternative DNA repair pathways and tend to occur between functionally related genes that commonly act within the same pathway (van Leeuwen et al., 2016). A reasonable reference point for the choice of promising enriched genes therefore is their involvement in DNA repair. Of the 124 genes enriched in the CRISPR screen, 12 are annotated to be involved in the DDR (**Thesis Fig. 5**): *EYA3, BLM, RNF4, TOP3A, RMI2, FANCM, RAD23B, ALKBH5, H2AFX, RMI1, PALB2, FAAP10*. Their involvement in the DDR will be discussed in further detail below.

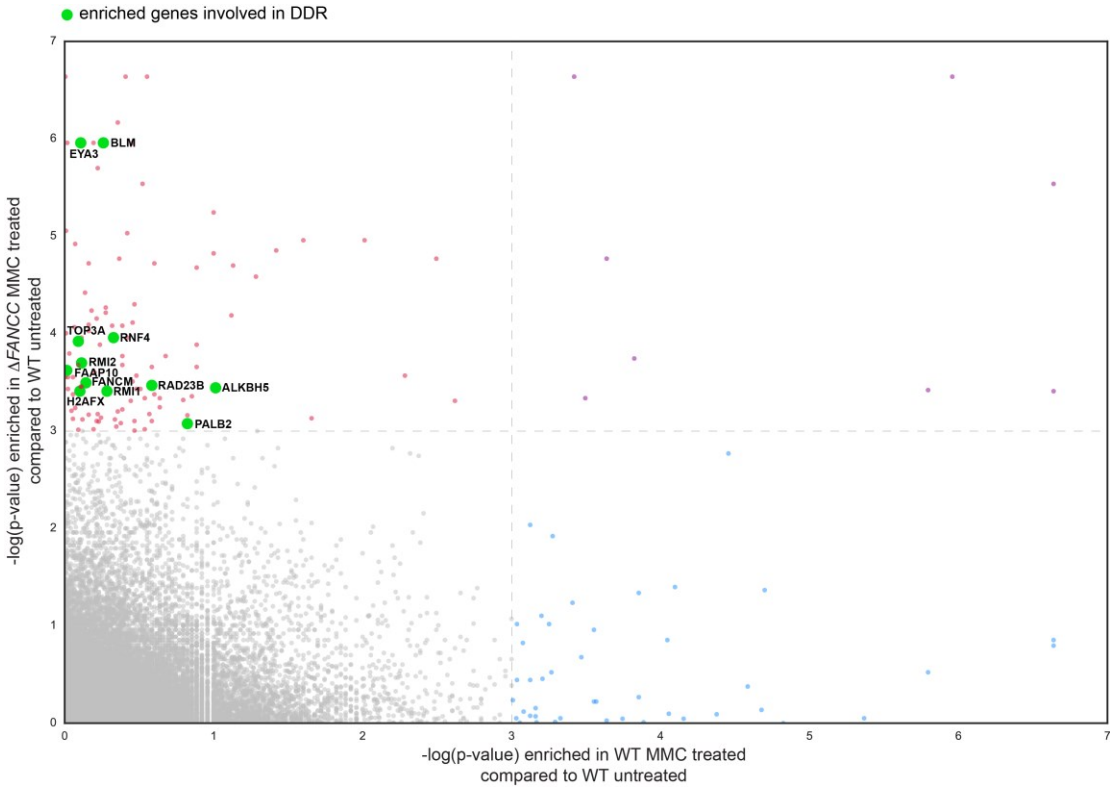

Thesis Figure 5: Genes involved in the DDR that were enriched in the CRISPR screen in Δ*FANCC* cells. Green dots represent DDR associated genes that were enriched upon MMC treatment in the CRISPR screen in Δ*FANCC*, but not WT cells.

Among them are the four genes encoding components of the BLM complex, *BLM*, *TOP3A*, *RMI1* and *RMI2*, but also related genes that produce proteins that directly interact with the BLM complex or act at a similar stage in DNA repair. FANCM physically connects the FA core complex to the BLM complex. Binding of FANCM to DNA requires the cofactor FAAP10 (also called CENPX or MHF2), which we also recovered in our CRISPR screen (Singh et al., 2010). FAAP10 stabilizes FANCM and is rapidly recruited to blocked replication forks where it promotes gene conversion (Singh et al., 2010; Yan et al., 2010). In addition, the CRISPR screen recovered PALB2 (also called FANCN) that binds to and colocalizes with BRCA2 during HR (Xia et al., 2006). PALB2 binds to ssDNA and interacts with RAD51 to stimulate strand invasion (Buisson et al., 2010). It therefore acts at a step in close proximity to BLM complex activity during HR. PALB2 is considered a druggable biological target (Pearl et al., 2015). Our screen also enriched for cells harboring mutations in the *H2AFX* gene that encodes histone H2AX that stabilizes DNA and partakes in multiple DNA repair processes (Fernandez-Capetillo et al., 2004). H2AX interacts with the tyrosine phosphatase EYA3 that dephosphorylates H2AX at tyrosine 142 and was also among the enriched DDR genes in our screen (Cook et

al., 2009; Krishnan et al., 2009). H2AX tyrosine 142 phosphorylation enables cells to distinguish between apoptotic and repair responses upon detection of genotoxic stress and determents the recruitment of either DNA repair- or pro-apoptotic factors, therefore influences the choice between DNA repair and cell death (Cook et al., 2009). *RNF4* encodes an ubiquitin E3 ligase that also interacts with H2AX and promotes DSB repair (Galanty et al., 2012). Depletion of RNF4 causes persistent H2AX phosphorylation associated with defective DSB repair, hypersensitivity towards DSB-inducing agents and ineffective replacement of RPA by BRCA2 and RAD51 on resected DNA during HR (Galanty et al., 2012). RAD23B acts together with XPC as an initial damage recognition factor in GG-NER (van der Spek et al., 1994). It was also shown to elevate the nucleotide excision activity of the 3-methyladenine-DNA glycosylase (MPG) that is involved in the initiation of BER (Miao et al., 2000). Finally, ALKBH5 is a mammalian m6A RNA demethylase that is associated with DNA damage reversal and DSB repair (Zheng et al., 2013). Among the 124 genes enriched in the CRISPR screen, disruption of those 12 DDR associated genes exhibits particular probability of changing the outcome of DNA damage repair in cells with DDR deficiencies and could be rewarding candidates for further studies. The basic premise that alterations to additional DNA repair pathways are most likely to improve repair outcome in DDR defective cells could be utilized in advance of the CRISPR screen to limit gRNA sequences to DDR associated genes. Using a commercially available human DNA damage response CRISPR library (Thermo Fisher: DNA Damage Response CRISPR Library) would allow deeper coverage of enriched genes and a reduced signal to noise ratio at similar sequencing depth. However, this would limit the possibility of discovering unexpected and more indirect mechanisms of synthetic viability. Nonetheless, this approach could be a valuable follow-up experiment to confirm the robustness of enriched DDR associated genes from an initial primary genome-wide screen therefore guiding the choice of genes for further analysis. A great opportunity presented by CRISPR screens is the potential to extend the approach beyond viability-based assays by using Fluorescence-activated cell sorting (FACS)-based readouts that reveal more mechanistic insights. FACS-based methods are well suited for pooled screenings and allow the separation of cell populations using reporter gene essays based on the expression of fluorescent proteins or by staining of endogenous markers. A FACS-based method called ‘traffic light’ reporter system allows flow-cytometric analysis of repair pathway choice between HR and NHEJ in human cells (Certo et al., 2011; Kuhar et al., 2014). This could provide a valuable addition to our CRISPR screen by systematically identifying genes that upon disruption increase desired HR in FA-deficient cells. Additional

readouts could provide further specificity to the FA-pathway. A recently developed psoralen probe generates ICLs upon UV-activation that are susceptible to post-labeling with a fluorescent reporter (Evison et al., 2016). This method offers a more direct monitoring of ICLs removal in FA-defective cells, compared to survival-based readouts.

Besides pointing towards potential treatments for FA patients, the synthetic viable interactions revealed in our screens have additional clinical implications. The described interaction between the FA pathway and the BLM complex also points towards a potential chemotherapy escape-strategy. Loss of BLM in FA-deficient cancer cells could result in reduced respondence of FA-deficient tumors to ICL-inducing chemotherapeutic drugs (Kim et al., 2015). In addition, MMC-resistant cancers were found to carry *NQO1* LOF mutations (Mikami et al., 1996). Expression-level analysis of chemotherapy resistant tumors analyzing genes enriched in our screens in could provide valuable clues for studying chemotherapy escape-mechanisms. Along the same lines, our datasets could be utilized to identify synthetic lethal interactions specific to FA-deficient tumors. This could be achieved by dropout analysis of the WT untreated dataset compared to the ∆*FANCC* untreated dataset from the CRISPR screen. Genes depleted in ∆*FANCC* compared to WT could indicate specific gene-dependencies of FA-deficient tumors and aid the development of targeted tumor therapies.

3.7 Conclusion & further prospects

In this project we performed two parallel genome-wide screens to identify genetic synthetic viable interactions specific to human ∆*FANCC* cells. We found that loss of the BLM complex alleviates cellular sensitivity to ICLs and confirmed this interaction using different ICL-inducing agents and various FA complementation group deficiencies. Our study demonstrates a robust method for the identification of synthetic viable interactions in cells carrying defects in DDR associated genes. This approach can be applied to cells carrying disease-associated mutations in DNA repair pathways other than FA. By using the latest generation of optimized CRISPR libraries and additional readouts that allow direct surveillance of pathway choice, further studies can extend our approach and promote the development of novel therapeutic interventions for DDR-associated diseases by exploiting synthetic viable interactions.

REFERENCES

Adamo, A., Collis, S.J., Adelman, C.A., Silva, N., Horejsi, Z., Ward, J.D., Martinez-Perez, E., Boulton, S.J., and La Volpe, A. (2010). Preventing nonhomologous end joining suppresses DNA repair defects of Fanconi anemia. Mol. Cell *39*, 25–35.

Almeida, K.H., and Sobol, R.W. (2007). A unified view of base excision repair: lesion-dependent protein complexes regulated by post-translational modification. DNA Repair *6*, 695–711.

Alpi, A.F., Pace, P.E., Babu, M.M., and Patel, K.J. (2008). Mechanistic insight into site-restricted monoubiquitination of FANCD2 by Ube2t, FANCL, and FANCI. Mol. Cell *32*, 767–777.

Amangyeld, T., Shin, Y.-K., Lee, M., Kwon, B., and Seo, Y.-S. (2014). Human MUS81-EME2 can cleave a variety of DNA structures including intact Holliday junction and nicked duplex. Nucleic Acids Res. *42*, 5846–5862.

Andersen, S.L., Bergstralh, D.T., Kohl, K.P., LaRocque, J.R., Moore, C.B., and Sekelsky, J. (2009). Drosophila MUS312 and the vertebrate ortholog BTBD12 interact with DNA structure-specific endonucleases in DNA repair and recombination. Mol. Cell *35*, 128–135.

Anderson, E.M., Birmingham, A., Baskerville, S., Reynolds, A., Maksimova, E., Leake, D., Fedorov, Y., Karpilow, J., and Khvorova, A. (2008). Experimental validation of the importance of seed complement frequency to siRNA specificity. RNA *14*, 853–861.

Andres, S.N., Vergnes, A., Ristic, D., Wyman, C., Modesti, M., and Junop, M. (2012). A human XRCC4-XLF complex bridges DNA. Nucleic Acids Res. *40*, 1868–1878.

Auerbach, A.D. (2009). Fanconi anemia and its diagnosis. Mutat. Res. *668*, 4–10.

Bae, S., Kweon, J., Kim, H.S., and Kim, J.-S. (2014a). Microhomology-based choice of Cas9 nuclease target sites. Nat. Methods *11*, 705–706.

Bae, S., Park, J., and Kim, J.-S. (2014b). Cas-OFFinder: a fast and versatile algorithm that searches for potential off-target sites of Cas9 RNA-guided endonucleases. Bioinforma. Oxf. Engl. *30*, 1473–1475.

Banerjee, T., Aggarwal, M., and Brosh, Jr., R.M. (2013). A new development in DNA repair modulation. Cell Cycle *12*, 713–714.

Barretina, J., Caponigro, G., Stransky, N., Venkatesan, K., Margolin, A.A., Kim, S., Wilson, C.J., Lehár, J., Kryukov, G.V., Sonkin, D., et al. (2012). The Cancer Cell Line Encyclopedia enables predictive modelling of anticancer drug sensitivity. Nature *483*, 603–607.

Bassik, M.C., Kampmann, M., Lebbink, R.J., Wang, S., Hein, M.Y., Poser, I., Weibezahn, J., Horlbeck, M.A., Chen, S., Mann, M., et al. (2013). A systematic

mammalian genetic interaction map reveals pathways underlying ricin susceptibility. Cell *152*, 909–922.

Bauer, M., Goldstein, M., Christmann, M., Becker, H., Heylmann, D., and Kaina, B. (2011). Human monocytes are severely impaired in base and DNA double-strand break repair that renders them vulnerable to oxidative stress. Proc. Natl. Acad. Sci. U. S. A. *108*, 21105–21110.

Beerens, N., Hoeijmakers, J.H.J., Kanaar, R., Vermeulen, W., and Wyman, C. (2005). The CSB protein actively wraps DNA. J. Biol. Chem. *280*, 4722–4729.

Berns, K., Hijmans, E.M., Mullenders, J., Brummelkamp, T.R., Velds, A., Heimerikx, M., Kerkhoven, R.M., Madiredjo, M., Nijkamp, W., Weigelt, B., et al. (2004). A large-scale RNAi screen in human cells identifies new components of the p53 pathway. Nature *428*, 431–437.

Bessho, T. (2003). Induction of DNA Replication-mediated Double Strand Breaks by Psoralen DNA Interstrand Cross-links. J. Biol. Chem. *278*, 5250–5254.

Bhagwat, N., Olsen, A.L., Wang, A.T., Hanada, K., Stuckert, P., Kanaar, R., D'Andrea, A., Niedernhofer, L.J., and McHugh, P.J. (2009). XPF-ERCC1 Participates in the Fanconi Anemia Pathway of Cross-Link Repair. Mol. Cell. Biol. *29*, 6427–6437.

Bischof, O., Kim, S.-H., Irving, J., Beresten, S., Ellis, N.A., and Campisi, J. (2001). Regulation and Localization of the Bloom Syndrome Protein in Response to DNA Damage. J. Cell Biol. *153*, 367–380.

Blier, P.R., Griffith, A.J., Craft, J., and Hardin, J.A. (1993). Binding of Ku protein to DNA. Measurement of affinity for ends and demonstration of binding to nicks. J. Biol. Chem. *268*, 7594–7601.

Blomen, V.A., Májek, P., Jae, L.T., Bigenzahn, J.W., Nieuwenhuis, J., Staring, J., Sacco, R., van Diemen, F.R., Olk, N., Stukalov, A., et al. (2015). Gene essentiality and synthetic lethality in haploid human cells. Science *350*, 1092–1096.

Bogliolo, M., Bluteau, D., Lespinasse, J., Pujol, R., Vasquez, N., d'Enghien, C.D., Stoppa-Lyonnet, D., Leblanc, T., Soulier, J., and Surrallés, J. (2017). Biallelic truncating FANCM mutations cause early-onset cancer but not Fanconi anemia. Genet. Med. Off. J. Am. Coll. Med. Genet.

Boulin, T., and Bessereau, J.-L. (2007). Mos1-mediated insertional mutagenesis in Caenorhabditis elegans. Nat. Protoc. *2*, 1276–1287.

Boutros, M., and Ahringer, J. (2008). The art and design of genetic screens: RNA interference. Nat. Rev. Genet. *9*, 554–566.

Boutros, M., Kiger, A.A., Armknecht, S., Kerr, K., Hild, M., Koch, B., Haas, S.A., Paro, R., Perrimon, N., and Heidelberg Fly Array Consortium (2004). Genome-wide RNAi analysis of growth and viability in Drosophila cells. Science *303*, 832–835.

Bouwman, P., and Jonkers, J. (2012). The effects of deregulated DNA damage signalling on cancer chemotherapy response and resistance. Nat. Rev. Cancer *12*, 587–598.

Brass, A.L., Dykxhoorn, D.M., Benita, Y., Yan, N., Engelman, A., Xavier, R.J., Lieberman, J., and Elledge, S.J. (2008). Identification of host proteins required for HIV infection through a functional genomic screen. Science *319*, 921–926.

Bridges, C.B. (1922). The Origin of Variations in Sexual and Sex-Limited Characters (The American Naturalist).

Brough, R., Frankum, J.R., Costa-Cabral, S., Lord, C.J., and Ashworth, A. (2011). Searching for synthetic lethality in cancer. Curr. Opin. Genet. Dev. *21*, 34–41.

Bryant, H.E., Schultz, N., Thomas, H.D., Parker, K.M., Flower, D., Lopez, E., Kyle, S., Meuth, M., Curtin, N.J., and Helleday, T. (2005). Specific killing of BRCA2-deficient tumours with inhibitors of poly(ADP-ribose) polymerase. Nature *434*, 913–917.

Buehler, E., Khan, A.A., Marine, S., Rajaram, M., Bahl, A., Burchard, J., and Ferrer, M. (2012). siRNA off-target effects in genome-wide screens identify signaling pathway members. Sci. Rep. *2*, 428.

Buisson, R., Dion-Côté, A.-M., Coulombe, Y., Launay, H., Cai, H., Stasiak, A.Z., Stasiak, A., Xia, B., and Masson, J.-Y. (2010). Cooperation of breast cancer proteins PALB2 and piccolo BRCA2 in stimulating homologous recombination. Nat. Struct. Mol. Biol. *17*, 1247–1254.

Burma, S., Chen, B.P.C., and Chen, D.J. (2006). Role of non-homologous end joining (NHEJ) in maintaining genomic integrity. DNA Repair *5*, 1042–1048.

Camenisch, U., Dip, R., Schumacher, S.B., Schuler, B., and Naegeli, H. (2006). Recognition of helical kinks by xeroderma pigmentosum group A protein triggers DNA excision repair. Nat. Struct. Mol. Biol. *13*, 278–284.

Carette, J.E., Guimaraes, C.P., Varadarajan, M., Park, A.S., Wuethrich, I., Godarova, A., Kotecki, M., Cochran, B.H., Spooner, E., Ploegh, H.L., et al. (2009). Haploid genetic screens in human cells identify host factors used by pathogens. Science *326*, 1231–1235.

Carette, J.E., Guimaraes, C.P., Wuethrich, I., Blomen, V.A., Varadarajan, M., Sun, C., Bell, G., Yuan, B., Muellner, M.K., Nijman, S.M., et al. (2011). Global gene disruption in human cells to assign genes to phenotypes by deep sequencing. Nat. Biotechnol. *29*, 542–546.

Cary, R.B., Peterson, S.R., Wang, J., Bear, D.G., Bradbury, E.M., and Chen, D.J. (1997). DNA looping by Ku and the DNA-dependent protein kinase. Proc. Natl. Acad. Sci. U. S. A. *94*, 4267–4272.

Ceccaldi, R., Rondinelli, B., and D'Andrea, A.D. (2016). Repair Pathway Choices and Consequences at the Double-Strand Break. Trends Cell Biol. *26*, 52–64.

Cejka, P., Plank, J.L., Bachrati, C.Z., Hickson, I.D., and Kowalczykowski, S.C. (2010). Rmi1 stimulates decatenation of double Holliday junctions during dissolution by Sgs1–Top3. Nat. Struct. Mol. Biol. *17*, 1377–1382.

Certo, M.T., Ryu, B.Y., Annis, J.E., Garibov, M., Jarjour, J., Rawlings, D.J., and Scharenberg, A.M. (2011). Tracking genome engineering outcome at individual DNA breakpoints. Nat. Methods *8*, 671–676.

Cetkovská, K., Šustová, H., and Uldrijan, S. (2017). Ubiquitin-specific peptidase 48 regulates Mdm2 protein levels independent of its deubiquitinase activity. Sci. Rep. *7*, 43180.

Chan, K.L., Palmai-Pallag, T., Ying, S., and Hickson, I.D. (2009). Replication stress induces sister-chromatid bridging at fragile site loci in mitosis. Nat. Cell Biol. *11*, 753–760.

Chaudhury, I., Sareen, A., Raghunandan, M., and Sobeck, A. (2013). FANCD2 regulates BLM complex functions independently of FANCI to promote replication fork recovery. Nucleic Acids Res. *41*, 6444–6459.

Chavez, A., Scheiman, J., Vora, S., Pruitt, B.W., Tuttle, M., P R Iyer, E., Lin, S., Kiani, S., Guzman, C.D., Wiegand, D.J., et al. (2015). Highly efficient Cas9-mediated transcriptional programming. Nat. Methods *12*, 326–328.

Chavez, A., Tuttle, M., Pruitt, B.W., Ewen-Campen, B., Chari, R., Ter-Ovanesyan, D., Haque, S.J., Cecchi, R.J., Kowal, E.J.K., Buchthal, J., et al. (2016). Comparison of Cas9 activators in multiple species. Nat. Methods *13*, 563–567.

Chen, R., Shi, L., Hakenberg, J., Naughton, B., Sklar, P., Zhang, J., Zhou, H., Tian, L., Prakash, O., Lemire, M., et al. (2016). Analysis of 589,306 genomes identifies individuals resilient to severe Mendelian childhood diseases. Nat. Biotechnol. *34*, 531.

Cheung, H.W., Cowley, G.S., Weir, B.A., Boehm, J.S., Rusin, S., Scott, J.A., East, A., Ali, L.D., Lizotte, P.H., Wong, T.C., et al. (2011). Systematic investigation of genetic vulnerabilities across cancer cell lines reveals lineage-specific dependencies in ovarian cancer. Proc. Natl. Acad. Sci. U. S. A. *108*, 12372–12377.

Cho, S.W., Kim, S., Kim, J.M., and Kim, J.-S. (2013). Targeted genome engineering in human cells with the Cas9 RNA-guided endonuclease. Nat. Biotechnol. *31*, 230–232.

Chu, W.K., Hanada, K., Kanaar, R., and Hickson, I.D. (2010). BLM has early and late functions in homologous recombination repair in mouse embryonic stem cells. Oncogene *29*, 4705–4714.

Citterio, E., Van Den Boom, V., Schnitzler, G., Kanaar, R., Bonte, E., Kingston, R.E., Hoeijmakers, J.H., and Vermeulen, W. (2000). ATP-dependent chromatin remodeling by the Cockayne syndrome B DNA repair-transcription-coupling factor. Mol. Cell. Biol. *20*, 7643–7653.

Clauson, C., Schärer, O.D., and Niedernhofer, L. (2013). Advances in understanding the complex mechanisms of DNA interstrand cross-link repair. Cold Spring Harb. Perspect. Biol. *5*, a012732.

Cohen, J., Pertsemlidis, A., Kotowski, I.K., Graham, R., Garcia, C.K., and Hobbs, H.H. (2005). Low LDL cholesterol in individuals of African descent resulting from frequent nonsense mutations in PCSK9. Nat. Genet. *37*, 161–165.

Compe, E., and Egly, J.-M. (2012). TFIIH: when transcription met DNA repair. Nat. Rev. Mol. Cell Biol. *13*, 343–354.

Cong, L., Ran, F.A., Cox, D., Lin, S., Barretto, R., Habib, N., Hsu, P.D., Wu, X., Jiang, W., Marraffini, L.A., et al. (2013). Multiplex Genome Engineering Using CRISPR/Cas Systems. Science *339*, 819–823.

Cook, P.J., Ju, B.G., Telese, F., Wang, X., Glass, C.K., and Rosenfeld, M.G. (2009). Tyrosine dephosphorylation of H2AX modulates apoptosis and survival decisions. Nature *458*, 591–596.

Cooper, M.P., Machwe, A., Orren, D.K., Brosh, R.M., Ramsden, D., and Bohr, V.A. (2000). Ku complex interacts with and stimulates the Werner protein. Genes Dev. *14*, 907–912.

Costantini, S., Woodbine, L., Andreoli, L., Jeggo, P.A., and Vindigni, A. (2007). Interaction of the Ku heterodimer with the DNA ligase IV/Xrcc4 complex and its regulation by DNA-PK. DNA Repair *6*, 712–722.

Costanzo, M., Baryshnikova, A., Bellay, J., Kim, Y., Spear, E.D., Sevier, C.S., Ding, H., Koh, J.L.Y., Toufighi, K., Mostafavi, S., et al. (2010). The genetic landscape of a cell. Science *327*, 425–431.

Cowley, G.S., Weir, B.A., Vazquez, F., Tamayo, P., Scott, J.A., Rusin, S., East-Seletsky, A., Ali, L.D., Gerath, W.F., Pantel, S.E., et al. (2014). Parallel genome-scale loss of function screens in 216 cancer cell lines for the identification of context-specific genetic dependencies. Sci. Data *1*, 140035.

Curtin, N.J. (2012). DNA repair dysregulation from cancer driver to therapeutic target. Nat. Rev. Cancer *12*, 801–817.

Daley, J.M., Chiba, T., Xue, X., Niu, H., and Sung, P. (2014). Multifaceted role of the Topo IIIα–RMI1-RMI2 complex and DNA2 in the BLM-dependent pathway of DNA break end resection. Nucleic Acids Res. *42*, 11083–11091.

Davies, S.L., North, P.S., Dart, A., Lakin, N.D., and Hickson, I.D. (2004). Phosphorylation of the Bloom's syndrome helicase and its role in recovery from S-phase arrest. Mol. Cell. Biol. *24*, 1279–1291.

Davies, S.L., North, P.S., and Hickson, I.D. (2007). Role for BLM in replication-fork restart and suppression of origin firing after replicative stress. Nat. Struct. Mol. Biol. *14*, 677–679.

Davis, A.J., and Chen, D.J. (2013). DNA double strand break repair via non-homologous end-joining. Transl. Cancer Res. *2*, 130–143.

De Vos, M., Schreiber, V., and Dantzer, F. (2012). The diverse roles and clinical relevance of PARPs in DNA damage repair: Current state of the art. Biochem. Pharmacol. *84*, 137–146.

Deans, A.J., and West, S.C. (2009). FANCM connects the genome instability disorders Bloom's Syndrome and Fanconi Anemia. Mol. Cell *36*, 943–953.

Deans, A.J., and West, S.C. (2011). DNA interstrand crosslink repair and cancer. Nat. Rev. Cancer *11*, 467–480.

Deriano, L., and Roth, D.B. (2013). Modernizing the nonhomologous end-joining repertoire: alternative and classical NHEJ share the stage. Annu. Rev. Genet. *47*, 433–455.

Dietz, H.C. (2010). New Therapeutic Approaches to Mendelian Disorders. N. Engl. J. Med. *363*, 852–863.

Dobzhansky, T. (1946). Genetics of natural populations; recombination and variability in populations of Drosophila pseudoobscura. Genetics *31*, 269–290.

Doench, J.G., Hartenian, E., Graham, D.B., Tothova, Z., Hegde, M., Smith, I., Sullender, M., Ebert, B.L., Xavier, R.J., and Root, D.E. (2014). Rational design of highly active sgRNAs for CRISPR-Cas9-mediated gene inactivation. Nat. Biotechnol. *32*, 1262–1267.

Doench, J.G., Fusi, N., Sullender, M., Hegde, M., Vaimberg, E.W., Donovan, K.F., Smith, I., Tothova, Z., Wilen, C., Orchard, R., et al. (2016). Optimized sgRNA design to maximize activity and minimize off-target effects of CRISPR-Cas9. Nat. Biotechnol. *34*, 184–191.

Dolan, D.W.P., Zupanic, A., Nelson, G., Hall, P., Miwa, S., Kirkwood, T.B.L., and Shanley, D.P. (2015). Integrated Stochastic Model of DNA Damage Repair by Non-homologous End Joining and p53/p21-Mediated Early Senescence Signalling. PLoS Comput. Biol. *11*, e1004246.

Dominguez, A.A., Lim, W.A., and Qi, L.S. (2016). Beyond editing: repurposing CRISPR-Cas9 for precision genome regulation and interrogation. Nat. Rev. Mol. Cell Biol. *17*, 5–15.

Doudna, J.A., and Charpentier, E. (2014). Genome editing. The new frontier of genome engineering with CRISPR-Cas9. Science *346*, 1258096.

Downs, J.A., and Jackson, S.P. (2004). A means to a DNA end: the many roles of Ku. Nat. Rev. Mol. Cell Biol. *5*, 367–378.

Drabløs, F., Feyzi, E., Aas, P.A., Vaagbø, C.B., Kavli, B., Bratlie, M.S., Peña-Diaz, J., Otterlei, M., Slupphaug, G., and Krokan, H.E. (2004). Alkylation damage in DNA

and RNA--repair mechanisms and medical significance. DNA Repair *3*, 1389–1407.

Dray, E., Etchin, J., Wiese, C., Saro, D., Williams, G.J., Hammel, M., Yu, X., Galkin, V.E., Liu, D., Tsai, M.-S., et al. (2010). Enhancement of RAD51 recombinase activity by the tumor suppressor PALB2. Nat. Struct. Mol. Biol. *17*, 1255–1259.

Dronamraju, K. (2017). Decoding the Language of Genetics by David Botstein. Q. Rev. Biol. *92*, 107–107.

Drummond, J.T., Li, G.M., Longley, M.J., and Modrich, P. (1995). Isolation of an hMSH2-p160 heterodimer that restores DNA mismatch repair to tumor cells. Science *268*, 1909–1912.

Eker, A.P.M., Quayle, C., Chaves, I., and van der Horst, G.T.J. (2009). DNA repair in mammalian cells: Direct DNA damage reversal: elegant solutions for nasty problems. Cell. Mol. Life Sci. CMLS *66*, 968–980.

Elling, U., Taubenschmid, J., Wirnsberger, G., O'Malley, R., Demers, S.-P., Vanhaelen, Q., Shukalyuk, A.I., Schmauss, G., Schramek, D., Schnuetgen, F., et al. (2011). Forward and reverse genetics through derivation of haploid mouse embryonic stem cells. Cell Stem Cell *9*, 563–574.

Ellis, N.A., and Offit, K. (2012). Heterozygous mutations in DNA repair genes and hereditary breast cancer: a question of power. PLoS Genet. *8*, e1003008.

Ellis, N.A., Groden, J., Ye, T.Z., Straughen, J., Lennon, D.J., Ciocci, S., Proytcheva, M., and German, J. (1995). The Bloom's syndrome gene product is homologous to RecQ helicases. Cell *83*, 655–666.

Essletzbichler, P., Konopka, T., Santoro, F., Chen, D., Gapp, B.V., Kralovics, R., Brummelkamp, T.R., Nijman, S.M.B., and Bürckstümmer, T. (2014). Megabase-scale deletion using CRISPR/Cas9 to generate a fully haploid human cell line. Genome Res. *24*, 2059–2065.

Evison, B.J., Actis, M.L., and Fujii, N. (2016). A clickable psoralen to directly quantify DNA interstrand crosslinking and repair. Bioorg. Med. Chem. *24*, 1071–1078.

Fagbemi, A.F., Orelli, B., and Schärer, O.D. (2011). Regulation of endonuclease activity in human nucleotide excision repair. DNA Repair *10*, 722–729.

Falck, J., Coates, J., and Jackson, S.P. (2005). Conserved modes of recruitment of ATM, ATR and DNA-PKcs to sites of DNA damage. Nature *434*, 605–611.

Falnes, P.Ø., Klungland, A., and Alseth, I. (2007). Repair of methyl lesions in DNA and RNA by oxidative demethylation. Neuroscience *145*, 1222–1232.

Fan, L., Fuss, J.O., Cheng, Q.J., Arvai, A.S., Hammel, M., Roberts, V.A., Cooper, P.K., and Tainer, J.A. (2008). XPD Helicase Structures and Activities: Insights into the Cancer and Aging Phenotypes from XPD Mutations. Cell *133*, 789–800.

Fanconi anemia complementation groups | HUGO Gene Nomenclature Committee Fanconi anemia complementation groups (FANC) Gene Family | HUGO Gene Nomenclature Committee.

FANTOM Consortium and the RIKEN PMI and CLST (DGT), Forrest, A.R.R., Kawaji, H., Rehli, M., Baillie, J.K., de Hoon, M.J.L., Haberle, V., Lassmann, T., Kulakovskiy, I.V., Lizio, M., et al. (2014). A promoter-level mammalian expression atlas. Nature *507*, 462–470.

Farmer, H., McCabe, N., Lord, C.J., Tutt, A.N.J., Johnson, D.A., Richardson, T.B., Santarosa, M., Dillon, K.J., Hickson, I., Knights, C., et al. (2005). Targeting the DNA repair defect in BRCA mutant cells as a therapeutic strategy. Nature *434*, 917–921.

Fekairi, S., Scaglione, S., Chahwan, C., Taylor, E.R., Tissier, A., Coulon, S., Dong, M.-Q., Ruse, C., Yates, J.R., Russell, P., et al. (2009). Human SLX4 is a Holliday junction resolvase subunit that binds multiple DNA repair/recombination endonucleases. Cell *138*, 78–89.

Fernandez-Capetillo, O., Lee, A., Nussenzweig, M., and Nussenzweig, A. (2004). H2AX: the histone guardian of the genome. DNA Repair *3*, 959–967.

Fire, A., Xu, S., Montgomery, M.K., Kostas, S.A., Driver, S.E., and Mello, C.C. (1998). Potent and specific genetic interference by double-stranded RNA in Caenorhabditis elegans. Nature *391*, 806–811.

Flannick, J., Thorleifsson, G., Beer, N.L., Jacobs, S.B.R., Grarup, N., Burtt, N.P., Mahajan, A., Fuchsberger, C., Atzmon, G., Benediktsson, R., et al. (2014). Loss-of-function mutations in SLC30A8 protect against type 2 diabetes. Nat. Genet. *46*, 357–363.

Fong, P.C., Boss, D.S., Yap, T.A., Tutt, A., Wu, P., Mergui-Roelvink, M., Mortimer, P., Swaisland, H., Lau, A., O'Connor, M.J., et al. (2009). Inhibition of poly(ADP-ribose) polymerase in tumors from BRCA mutation carriers. N. Engl. J. Med. *361*, 123–134.

Forment, J.V., Herzog, M., Coates, J., Konopka, T., Gapp, B.V., Nijman, S.M., Adams, D.J., Keane, T.M., and Jackson, S.P. (2017). Genome-wide genetic screening with chemically mutagenized haploid embryonic stem cells. Nat. Chem. Biol. *13*, 12–14.

Fortini, P., and Dogliotti, E. (2007). Base damage and single-strand break repair: mechanisms and functional significance of short- and long-patch repair subpathways. DNA Repair *6*, 398–409.

Fortini, P., Parlanti, E., Sidorkina, O.M., Laval, J., and Dogliotti, E. (1999). The type of DNA glycosylase determines the base excision repair pathway in mammalian cells. J. Biol. Chem. *274*, 15230–15236.

Fousteri, M., Vermeulen, W., van Zeeland, A.A., and Mullenders, L.H.F. (2006). Cockayne syndrome A and B proteins differentially regulate recruitment of

chromatin remodeling and repair factors to stalled RNA polymerase II in vivo. Mol. Cell *23*, 471–482.

Friedrich, G., and Soriano, P. (1991). Promoter traps in embryonic stem cells: a genetic screen to identify and mutate developmental genes in mice. Genes Dev. *5*, 1513–1523.

Frock, R.L., Hu, J., Meyers, R.M., Ho, Y.-J., Kii, E., and Alt, F.W. (2015). Genome-wide detection of DNA double-stranded breaks induced by engineered nucleases. Nat. Biotechnol. *33*, 179–186.

Fromme, J.C., Banerjee, A., and Verdine, G.L. (2004). DNA glycosylase recognition and catalysis. Curr. Opin. Struct. Biol. *14*, 43–49.

Fu, D., Calvo, J.A., and Samson, L.D. (2012). Balancing repair and tolerance of DNA damage caused by alkylating agents. Nat. Rev. Cancer *12*, 104–120.

Galanty, Y., Belotserkovskaya, R., Coates, J., and Jackson, S.P. (2012). RNF4, a SUMO-targeted ubiquitin E3 ligase, promotes DNA double-strand break repair. Genes Dev. *26*, 1179–1195.

Galarneau, G., Palmer, C.D., Sankaran, V.G., Orkin, S.H., Hirschhorn, J.N., and Lettre, G. (2010). Fine-mapping at three loci known to affect fetal hemoglobin levels explains additional genetic variation. Nat. Genet. *42*, 1049–1051.

Gari, K., Décaillet, C., Stasiak, A.Z., Stasiak, A., and Constantinou, A. (2008). The Fanconi anemia protein FANCM can promote branch migration of Holliday junctions and replication forks. Mol. Cell *29*, 141–148.

Gasiunas, G., Barrangou, R., Horvath, P., and Siksnys, V. (2012). Cas9-crRNA ribonucleoprotein complex mediates specific DNA cleavage for adaptive immunity in bacteria. Proc. Natl. Acad. Sci. U. S. A. *109*, E2579-2586.

Gell, D., and Jackson, S.P. (1999). Mapping of protein-protein interactions within the DNA-dependent protein kinase complex. Nucleic Acids Res. *27*, 3494–3502.

Gilbert, L.A., Larson, M.H., Morsut, L., Liu, Z., Brar, G.A., Torres, S.E., Stern-Ginossar, N., Brandman, O., Whitehead, E.H., Doudna, J.A., et al. (2013). CRISPR-mediated modular RNA-guided regulation of transcription in eukaryotes. Cell *154*, 442–451.

Gilbert, L.A., Horlbeck, M.A., Adamson, B., Villalta, J.E., Chen, Y., Whitehead, E.H., Guimaraes, C., Panning, B., Ploegh, H.L., Bassik, M.C., et al. (2014). Genome-Scale CRISPR-Mediated Control of Gene Repression and Activation. Cell *159*, 647–661.

Goff, S.P. (2008). Knockdown screens to knockout HIV-1. Cell *135*, 417–420.

González, F., Zhu, Z., Shi, Z.-D., Lelli, K., Verma, N., Li, Q.V., and Huangfu, D. (2014). An iCRISPR platform for rapid, multiplexable, and inducible genome editing in human pluripotent stem cells. Cell Stem Cell *15*, 215–226.

Grabarz, A., Guirouilh-Barbat, J., Barascu, A., Pennarun, G., Genet, D., Rass, E., Germann, S.M., Bertrand, P., Hickson, I.D., and Lopez, B.S. (2013). A role for BLM in double-strand break repair pathway choice: prevention of CtIP/Mre11-mediated alternative nonhomologous end-joining. Cell Rep. *5*, 21–28.

Graham, D.B., and Root, D.E. (2015). Resources for the design of CRISPR gene editing experiments. Genome Biol. *16*, 260.

Grawunder, U., Wilm, M., Wu, X., Kulesza, P., Wilson, T.E., Mann, M., and Lieber, M.R. (1997). Activity of DNA ligase IV stimulated by complex formation with XRCC4 protein in mammalian cells. Nature *388*, 492–495.

Grundy, G.J., Rulten, S.L., Zeng, Z., Arribas-Bosacoma, R., Iles, N., Manley, K., Oliver, A., and Caldecott, K.W. (2013). APLF promotes the assembly and activity of non-homologous end joining protein complexes. EMBO J. *32*, 112–125.

Gu, J., Lu, H., Tippin, B., Shimazaki, N., Goodman, M.F., and Lieber, M.R. (2007). XRCC4:DNA ligase IV can ligate incompatible DNA ends and can ligate across gaps. EMBO J. *26*, 1010–1023.

Haeussler, M., Schönig, K., Eckert, H., Eschstruth, A., Mianné, J., Renaud, J.-B., Schneider-Maunoury, S., Shkumatava, A., Teboul, L., Kent, J., et al. (2016). Evaluation of off-target and on-target scoring algorithms and integration into the guide RNA selection tool CRISPOR. Genome Biol. *17*, 148.

Hammel, M., Yu, Y., Fang, S., Lees-Miller, S.P., and Tainer, J.A. (2010). XLF regulates filament architecture of the XRCC4·ligase IV complex. Struct. Lond. Engl. 1993 *18*, 1431–1442.

Hammel, M., Rey, M., Yu, Y., Mani, R.S., Classen, S., Liu, M., Pique, M.E., Fang, S., Mahaney, B.L., Weinfeld, M., et al. (2011). XRCC4 protein interactions with XRCC4-like factor (XLF) create an extended grooved scaffold for DNA ligation and double strand break repair. J. Biol. Chem. *286*, 32638–32650.

Hanada, K., Budzowska, M., Modesti, M., Maas, A., Wyman, C., Essers, J., and Kanaar, R. (2006). The structure-specific endonuclease Mus81-Eme1 promotes conversion of interstrand DNA crosslinks into double-strands breaks. EMBO J. *25*, 4921–4932.

Hart, T., Chandrashekhar, M., Aregger, M., Steinhart, Z., Brown, K.R., MacLeod, G., Mis, M., Zimmermann, M., Fradet-Turcotte, A., Sun, S., et al. (2015). High-Resolution CRISPR Screens Reveal Fitness Genes and Genotype-Specific Cancer Liabilities. Cell *163*, 1515–1526.

Hassa, P.O., Haenni, S.S., Elser, M., and Hottiger, M.O. (2006). Nuclear ADP-ribosylation reactions in mammalian cells: where are we today and where are we going? Microbiol. Mol. Biol. Rev. MMBR *70*, 789–829.

Heigwer, F., Kerr, G., and Boutros, M. (2014). E-CRISP: fast CRISPR target site identification. Nat. Methods *11*, 122–123.

Helleday, T., Petermann, E., Lundin, C., Hodgson, B., and Sharma, R.A. (2008). DNA repair pathways as targets for cancer therapy. Nat. Rev. Cancer *8*, 193–204.

High Throughput Screening Methods (2016). High Throughput Screening Methods.

Hoffman, G.R., Rahal, R., Buxton, F., Xiang, K., McAllister, G., Frias, E., Bagdasarian, L., Huber, J., Lindeman, A., Chen, D., et al. (2014). Functional epigenetics approach identifies BRM/SMARCA2 as a critical synthetic lethal target in BRG1-deficient cancers. Proc. Natl. Acad. Sci. U. S. A. *111*, 3128–3133.

Holliday, R. (2007). A mechanism for gene conversion in fungi. Genet. Res. *89*, 285–307.

Hombauer, H., Campbell, C.S., Smith, C.E., Desai, A., and Kolodner, R.D. (2011). Visualization of eukaryotic DNA mismatch repair reveals distinct recognition and repair intermediates. Cell *147*, 1040–1053.

Horlbeck, M.A., Gilbert, L.A., Villalta, J.E., Adamson, B., Pak, R.A., Chen, Y., Fields, A.P., Park, C.Y., Corn, J.E., Kampmann, M., et al. (2016). Compact and highly active next-generation libraries for CRISPR-mediated gene repression and activation. ELife *5*.

Hou, P., Chen, S., Wang, S., Yu, X., Chen, Y., Jiang, M., Zhuang, K., Ho, W., Hou, W., Huang, J., et al. (2015). Genome editing of CXCR4 by CRISPR/cas9 confers cells resistant to HIV-1 infection. Sci. Rep. *5*, 15577.

Howlett, N.G., Taniguchi, T., Olson, S., Cox, B., Waisfisz, Q., De Die-Smulders, C., Persky, N., Grompe, M., Joenje, H., Pals, G., et al. (2002). Biallelic inactivation of BRCA2 in Fanconi anemia. Science *297*, 606–609.

Howlett, N.G., Taniguchi, T., Durkin, S.G., D'Andrea, A.D., and Glover, T.W. (2005). The Fanconi anemia pathway is required for the DNA replication stress response and for the regulation of common fragile site stability. Hum. Mol. Genet. *14*, 693–701.

Huffman, J.L., Sundheim, O., and Tainer, J.A. (2005). DNA base damage recognition and removal: new twists and grooves. Mutat. Res. *577*, 55–76.

Huttlin, E.L., Ting, L., Bruckner, R.J., Gebreab, F., Gygi, M.P., Szpyt, J., Tam, S., Zarraga, G., Colby, G., Baltier, K., et al. (2015). The BioPlex Network: A Systematic Exploration of the Human Interactome. Cell *162*, 425–440.

Ivics, Z., Hackett, P.B., Plasterk, R.H., and Izsvák, Z. (1997). Molecular reconstruction of Sleeping Beauty, a Tc1-like transposon from fish, and its transposition in human cells. Cell *91*, 501–510.

Jakob, B., Splinter, J., Conrad, S., Voss, K.-O., Zink, D., Durante, M., Löbrich, M., and Taucher-Scholz, G. (2011). DNA double-strand breaks in heterochromatin elicit fast repair protein recruitment, histone H2AX phosphorylation and relocation to euchromatin. Nucleic Acids Res. *39*, 6489–6499.

Jensen, R.B., Carreira, A., and Kowalczykowski, S.C. (2010). Purified human BRCA2 stimulates RAD51-mediated recombination. Nature *467*, 678–683.

Jeppesen, D.K., Bohr, V.A., and Stevnsner, T. (2011). DNA repair deficiency in neurodegeneration. Prog. Neurobiol. *94*, 166–200.

Jinek, M., Chylinski, K., Fonfara, I., Hauer, M., Doudna, J.A., and Charpentier, E. (2012). A programmable dual-RNA-guided DNA endonuclease in adaptive bacterial immunity. Science *337*, 816–821.

Jinek, M., East, A., Cheng, A., Lin, S., Ma, E., and Doudna, J. (2013). RNA-programmed genome editing in human cells. ELife *2*, e00471.

Joenje, H., Levitus, M., Waisfisz, Q., D'Andrea, A., Garcia-Higuera, I., Pearson, T., van Berkel, C.G., Rooimans, M.A., Morgan, N., Mathew, C.G., et al. (2000). Complementation analysis in Fanconi anemia: assignment of the reference FA-H patient to group A. Am. J. Hum. Genet. *67*, 759–762.

Junne, T., Wong, J., Studer, C., Aust, T., Bauer, B.W., Beibel, M., Bhullar, B., Bruccoleri, R., Eichenberger, J., Estoppey, D., et al. (2015). Decatransin, a new natural product inhibiting protein translocation at the Sec61/SecYEG translocon. J Cell Sci *128*, 1217–1229.

Kais, Z., Rondinelli, B., Holmes, A., O'Leary, C., Kozono, D., D'Andrea, A.D., and Ceccaldi, R. (2016). FANCD2 maintains fork stability in BRCA1/2-deficient tumors and promotes alternative end-joining DNA repair. Cell Rep. *15*, 2488–2499.

Kampmann, M., Bassik, M.C., and Weissman, J.S. (2013). Integrated platform for genome-wide screening and construction of high-density genetic interaction maps in mammalian cells. Proc. Natl. Acad. Sci. U. S. A. *110*, E2317-2326.

Kampmann, M., Bassik, M.C., and Weissman, J.S. (2014). Functional genomics platform for pooled screening and generation of mammalian genetic interaction maps. Nat. Protoc. *9*, 1825–1847.

Kampmann, M., Horlbeck, M.A., Chen, Y., Tsai, J.C., Bassik, M.C., Gilbert, L.A., Villalta, J.E., Kwon, S.C., Chang, H., Kim, V.N., et al. (2015). Next-generation libraries for robust RNA interference-based genome-wide screens. Proc. Natl. Acad. Sci. U. S. A. *112*, E3384–E3391.

Kanno, S., Kuzuoka, H., Sasao, S., Hong, Z., Lan, L., Nakajima, S., and Yasui, A. (2007). A novel human AP endonuclease with conserved zinc-finger-like motifs involved in DNA strand break responses. EMBO J. *26*, 2094–2103.

Karmakar, P., Snowden, C.M., Ramsden, D.A., and Bohr, V.A. (2002). Ku heterodimer binds to both ends of the Werner protein and functional interaction occurs at the Werner N-terminus. Nucleic Acids Res. *30*, 3583–3591.

Karow, J.K., Constantinou, A., Li, J.L., West, S.C., and Hickson, I.D. (2000). The Bloom's syndrome gene product promotes branch migration of holliday junctions. Proc. Natl. Acad. Sci. U. S. A. *97*, 6504–6508.

Kim, T.M., Son, M.Y., Dodds, S., Hu, L., Luo, G., and Hasty, P. (2015). RECQL5 and BLM exhibit divergent functions in cells defective for the Fanconi anemia pathway. Nucleic Acids Res. *43*, 893–903.

Kim, Y., Spitz, G.S., Veturi, U., Lach, F.P., Auerbach, A.D., and Smogorzewska, A. (2013). Regulation of multiple DNA repair pathways by the Fanconi anemia protein SLX4. Blood *121*, 54–63.

Kleinstiver, B.P., Pattanayak, V., Prew, M.S., Tsai, S.Q., Nguyen, N.T., Zheng, Z., and Joung, J.K. (2016). High-fidelity CRISPR-Cas9 nucleases with no detectable genome-wide off-target effects. Nature *529*, 490–495.

Koike-Yusa, H., Li, Y., Tan, E.-P., Velasco-Herrera, M.D.C., and Yusa, K. (2014). Genome-wide recessive genetic screening in mammalian cells with a lentiviral CRISPR-guide RNA library. Nat. Biotechnol. *32*, 267–273.

Koivisto, P., Robins, P., Lindahl, T., and Sedgwick, B. (2004). Demethylation of 3-methylthymine in DNA by bacterial and human DNA dioxygenases. J. Biol. Chem. *279*, 40470–40474.

Konermann, S., Brigham, M.D., Trevino, A.E., Joung, J., Abudayyeh, O.O., Barcena, C., Hsu, P.D., Habib, N., Gootenberg, J.S., Nishimasu, H., et al. (2015). Genome-scale transcriptional activation by an engineered CRISPR-Cas9 complex. Nature *517*, 583–588.

König, R., Zhou, Y., Elleder, D., Diamond, T.L., Bonamy, G.M.C., Irelan, J.T., Chiang, C.-Y., Tu, B.P., De Jesus, P.D., Lilley, C.E., et al. (2008). Global analysis of host-pathogen interactions that regulate early-stage HIV-1 replication. Cell *135*, 49–60.

Kotecki, M., Reddy, P.S., and Cochran, B.H. (1999). Isolation and characterization of a near-haploid human cell line. Exp. Cell Res. *252*, 273–280.

Kottemann, M.C., and Smogorzewska, A. (2013). Fanconi anemia and the repair of Watson and Crick crosslinks. Nature *493*, 356–363.

Kowalczykowski, S.C. (2015). An Overview of the Molecular Mechanisms of Recombinational DNA Repair. Cold Spring Harb. Perspect. Biol. *7*.

Krishnan, N., Jeong, D.G., Jung, S.-K., Ryu, S.E., Xiao, A., Allis, C.D., Kim, S.J., and Tonks, N.K. (2009). Dephosphorylation of the C-terminal tyrosyl residue of the DNA damage-related histone H2A.X is mediated by the protein phosphatase eyes absent. J. Biol. Chem. *284*, 16066–16070.

Krokan, H.E., and Bjørås, M. (2013). Base excision repair. Cold Spring Harb. Perspect. Biol. *5*, a012583.

Kryukov, G.V., Wilson, F.H., Ruth, J.R., Paulk, J., Tsherniak, A., Marlow, S.E., Vazquez, F., Weir, B.A., Fitzgerald, M.E., Tanaka, M., et al. (2016). MTAP deletion confers enhanced dependency on the PRMT5 arginine methyltransferase in cancer cells. Science *351*, 1214–1218.

Kuhar, R., Gwiazda, K.S., Humbert, O., Mandt, T., Pangallo, J., Brault, M., Khan, I., Maizels, N., Rawlings, D.J., Scharenberg, A.M., et al. (2014). Novel fluorescent genome editing reporters for monitoring DNA repair pathway utilization at endonuclease-induced breaks. Nucleic Acids Res. *42*, e4.

Kunkel, T.A., and Erie, D.A. (2015). Eukaryotic Mismatch Repair in Relation to DNA Replication. Annu. Rev. Genet. *49*, 291–313.

Kusumoto, R., Dawut, L., Marchetti, C., Wan Lee, J., Vindigni, A., Ramsden, D., and Bohr, V.A. (2008). Werner protein cooperates with the XRCC4-DNA ligase IV complex in end-processing. Biochemistry (Mosc.) *47*, 7548–7556.

Lamarche, B.J., Orazio, N.I., and Weitzman, M.D. (2010). The MRN complex in Double-Strand Break Repair and Telomere Maintenance. FEBS Lett. *584*, 3682–3695.

Larson, M.H., Gilbert, L.A., Wang, X., Lim, W.A., Weissman, J.S., and Qi, L.S. (2013). CRISPR interference (CRISPRi) for sequence-specific control of gene expression. Nat. Protoc. *8*, 2180–2196.

Laviolette, L.A., Wilson, J., Koller, J., Neil, C., Hulick, P., Rejtar, T., Karger, B., Teh, B.T., and Iliopoulos, O. (2013). Human folliculin delays cell cycle progression through late S and G2/M-phases: effect of phosphorylation and tumor associated mutations. PloS One *8*, e66775.

Leeb, M., and Wutz, A. (2011). Derivation of haploid embryonic stem cells from mouse embryos. Nature *479*, 131–134.

van Leeuwen, J., Pons, C., Mellor, J.C., Yamaguchi, T.N., Friesen, H., Koschwanez, J., Ušaj, M.M., Pechlaner, M., Takar, M., Ušaj, M., et al. (2016). Exploring genetic suppression interactions on a global scale. Science *354*.

Li, Y., Qian, H., Wang, Y., and Cucinotta, F.A. (2012). A stochastic model of DNA fragments rejoining. PloS One *7*, e44293.

Liang, X., Potter, J., Kumar, S., Zou, Y., Quintanilla, R., Sridharan, M., Carte, J., Chen, W., Roark, N., Ranganathan, S., et al. (2015). Rapid and highly efficient mammalian cell engineering via Cas9 protein transfection. J. Biotechnol. *208*, 44–53.

Lieber, M.R. (2010). The Mechanism of Double-Strand DNA Break Repair by the Nonhomologous DNA End Joining Pathway. Annu. Rev. Biochem. *79*, 181–211.

Lindahl, T. (1993). Instability and decay of the primary structure of DNA. Nature *362*, 709.

Lindahl, T. (2001). Keynote: past, present, and future aspects of base excision repair. Prog. Nucleic Acid Res. Mol. Biol. *68*, xvii–xxx.

Lindahl, T., and Barnes, D.E. (2000). Repair of endogenous DNA damage. Cold Spring Harb. Symp. Quant. Biol. *65*, 127–133.

Lipinski, M.M., Hoffman, G., Ng, A., Zhou, W., Py, B.F., Hsu, E., Liu, X., Eisenberg, J., Liu, J., Blenis, J., et al. (2010). A genome-wide siRNA screen reveals multiple mTORC1 independent signaling pathways regulating autophagy under normal nutritional conditions. Dev. Cell *18*, 1041–1052.

Liu, H., Rudolf, J., Johnson, K.A., McMahon, S.A., Oke, M., Carter, L., McRobbie, A.-M., Brown, S.E., Naismith, J.H., and White, M.F. (2008). Structure of the DNA repair helicase XPD. Cell *133*, 801–812.

Liu, J., Doty, T., Gibson, B., and Heyer, W.-D. (2010a). Human BRCA2 protein promotes RAD51 filament formation on RPA-covered single-stranded DNA. Nat. Struct. Mol. Biol. *17*, 1260–1262.

Liu, Y., Prasad, R., and Wilson, S.H. (2010b). HMGB1: Roles in Base Excision Repair and Related Function. Biochim. Biophys. Acta *1799*, 119.

Lönn, U., Lönn, S., Nylen, U., Winblad, G., and German, J. (1990). An abnormal profile of DNA replication intermediates in Bloom's syndrome. Cancer Res. *50*, 3141–3145.

Lord, C.J., and Ashworth, A. (2012). The DNA damage response and cancer therapy. Nature *481*, 287–294.

Machida, Y.J., Machida, Y., Chen, Y., Gurtan, A.M., Kupfer, G.M., D'Andrea, A.D., and Dutta, A. (2006). UBE2T is the E2 in the Fanconi anemia pathway and undergoes negative autoregulation. Mol. Cell *23*, 589–596.

MacKeigan, J.P., Murphy, L.O., and Blenis, J. (2005). Sensitized RNAi screen of human kinases and phosphatases identifies new regulators of apoptosis and chemoresistance. Nat. Cell Biol. *7*, 591–600.

Macrae, C.J., McCulloch, R.D., Ylanko, J., Durocher, D., and Koch, C.A. (2008). APLF (C2orf13) facilitates nonhomologous end-joining and undergoes ATM-dependent hyperphosphorylation following ionizing radiation. DNA Repair *7*, 292–302.

Maeder, M.L., and Gersbach, C.A. (2016). Genome-editing Technologies for Gene and Cell Therapy. Mol. Ther. J. Am. Soc. Gene Ther. *24*, 430–446.

Maeder, M.L., Linder, S.J., Cascio, V.M., Fu, Y., Ho, Q.H., and Joung, J.K. (2013). CRISPR RNA-guided activation of endogenous human genes. Nat. Methods *10*, 977–979.

Magtanong, L., Ho, C.H., Barker, S.L., Jiao, W., Baryshnikova, A., Bahr, S., Smith, A.M., Heisler, L.E., Choy, J.S., Kuzmin, E., et al. (2011). Dosage suppression genetic

interaction networks enhance functional wiring diagrams of the cell. Nat. Biotechnol. *29*, 505–511.

Mali, P., Esvelt, K.M., and Church, G.M. (2013a). Cas9 as a versatile tool for engineering biology. Nat. Methods *10*, 957–963.

Mali, P., Yang, L., Esvelt, K.M., Aach, J., Guell, M., DiCarlo, J.E., Norville, J.E., and Church, G.M. (2013b). RNA-guided human genome engineering via Cas9. Science *339*, 823–826.

Malivert, L., Ropars, V., Nunez, M., Drevet, P., Miron, S., Faure, G., Guerois, R., Mornon, J.-P., Revy, P., Charbonnier, J.-B., et al. (2010). Delineation of the Xrcc4-interacting region in the globular head domain of cernunnos/XLF. J. Biol. Chem. *285*, 26475–26483.

Malu, S., Malshetty, V., Francis, D., and Cortes, P. (2012). Role of non-homologous end joining in V(D)J recombination. Immunol. Res. *54*, 233–246.

Mandal, P.K., Ferreira, L.M.R., Collins, R., Meissner, T.B., Boutwell, C.L., Friesen, M., Vrbanac, V., Garrison, B.S., Stortchevoi, A., Bryder, D., et al. (2014). Efficient ablation of genes in human hematopoietic stem and effector cells using CRISPR/Cas9. Cell Stem Cell *15*, 643–652.

Marcotte, R., Brown, K.R., Suarez, F., Sayad, A., Karamboulas, K., Krzyzanowski, P.M., Sircoulomb, F., Medrano, M., Fedyshyn, Y., Koh, J.L.Y., et al. (2012). Essential gene profiles in breast, pancreatic, and ovarian cancer cells. Cancer Discov. *2*, 172–189.

Mari, P.-O., Florea, B.I., Persengiev, S.P., Verkaik, N.S., Brüggenwirth, H.T., Modesti, M., Giglia-Mari, G., Bezstarosti, K., Demmers, J.A.A., Luider, T.M., et al. (2006). Dynamic assembly of end-joining complexes requires interaction between Ku70/80 and XRCC4. Proc. Natl. Acad. Sci. U. S. A. *103*, 18597–18602.

Marteijn, J.A., Lans, H., Vermeulen, W., and Hoeijmakers, J.H.J. (2014). Understanding nucleotide excision repair and its roles in cancer and ageing. Nat. Rev. Mol. Cell Biol. *15*, 465–481.

Masutani, C., Kusumoto, R., Yamada, A., Dohmae, N., Yokoi, M., Yuasa, M., Araki, M., Iwai, S., Takio, K., and Hanaoka, F. (1999). The XPV (xeroderma pigmentosum variant) gene encodes human DNA polymerase eta. Nature *399*, 700–704.

Mathieu, N., Kaczmarek, N., Rüthemann, P., Luch, A., and Naegeli, H. (2013). DNA quality control by a lesion sensor pocket of the xeroderma pigmentosum group D helicase subunit of TFIIH. Curr. Biol. CB *23*, 204–212.

Matos, J., and West, S.C. (2014). Holliday junction resolution: Regulation in space and time. DNA Repair *19*, 176–181.

McDonald, E.R., de Weck, A., Schlabach, M.R., Billy, E., Mavrakis, K.J., Hoffman, G.R., Belur, D., Castelletti, D., Frias, E., Gampa, K., et al. (2017). Project DRIVE: A

Compendium of Cancer Dependencies and Synthetic Lethal Relationships Uncovered by Large-Scale, Deep RNAi Screening. Cell *170*, 577–592.e10.

McKusick, V.A. (2007). Mendelian Inheritance in Man and its online version, OMIM. Am. J. Hum. Genet. *80*, 588–604.

Meetei, A.R., de Winter, J.P., Medhurst, A.L., Wallisch, M., Waisfisz, Q., van de Vrugt, H.J., Oostra, A.B., Yan, Z., Ling, C., Bishop, C.E., et al. (2003). A novel ubiquitin ligase is deficient in Fanconi anemia. Nat. Genet. *35*, 165–170.

Meetei, A.R., Medhurst, A.L., Ling, C., Xue, Y., Singh, T.R., Bier, P., Steltenpool, J., Stone, S., Dokal, I., Mathew, C.G., et al. (2005). A human ortholog of archaeal DNA repair protein Hef is defective in Fanconi anemia complementation group M. Nat. Genet. *37*, 958–963.

Meier, J.A., Zhang, F., and Sanjana, N.E. (2017). GUIDES: sgRNA design for loss-of-function screens. Nat. Methods *14*, 831–832.

Meindl, A., Hellebrand, H., Wiek, C., Erven, V., Wappenschmidt, B., Niederacher, D., Freund, M., Lichtner, P., Hartmann, L., Schaal, H., et al. (2010). Germline mutations in breast and ovarian cancer pedigrees establish *RAD51C* as a human cancer susceptibility gene. Nat. Genet. *42*, 410.

Miao, F., Bouziane, M., Dammann, R., Masutani, C., Hanaoka, F., Pfeifer, G., and O'Connor, T.R. (2000). 3-Methyladenine-DNA glycosylase (MPG protein) interacts with human RAD23 proteins. J. Biol. Chem. *275*, 28433–28438.

Michlits, G., Hubmann, M., Wu, S.-H., Vainorius, G., Budusan, E., Zhuk, S., Burkard, T.R., Novatchkova, M., Aichinger, M., Lu, Y., et al. (2017). CRISPR-UMI: single-cell lineage tracing of pooled CRISPR-Cas9 screens. Nat. Methods *14*, 1191–1197.

Mikami, K., Naito, M., Tomida, A., Yamada, M., Sirakusa, T., and Tsuruo, T. (1996). DT-diaphorase as a critical determinant of sensitivity to mitomycin C in human colon and gastric carcinoma cell lines. Cancer Res. *56*, 2823–2826.

Mimitou, E.P., and Symington, L.S. (2008). Sae2, Exo1 and Sgs1 collaborate in DNA double-strand break processing. Nature *455*, 770–774.

Mimori, T., Hardin, J.A., and Steitz, J.A. (1986). Characterization of the DNA-binding protein antigen Ku recognized by autoantibodies from patients with rheumatic disorders. J. Biol. Chem. *261*, 2274–2278.

Moffat, J., Grueneberg, D.A., Yang, X., Kim, S.Y., Kloepfer, A.M., Hinkle, G., Piqani, B., Eisenhaure, T.M., Luo, B., Grenier, J.K., et al. (2006). A lentiviral RNAi library for human and mouse genes applied to an arrayed viral high-content screen. Cell *124*, 1283–1298.

Mojica, F.J.M., Díez-Villaseñor, C., García-Martínez, J., and Almendros, C. (2009). Short motif sequences determine the targets of the prokaryotic CRISPR defence system. Microbiol. Read. Engl. *155*, 733–740.

Moon, A.F., Garcia-Diaz, M., Batra, V.K., Beard, W.A., Bebenek, K., Kunkel, T.A., Wilson, S.H., and Pedersen, L.C. (2007). The X family portrait: structural insights into biological functions of X family polymerases. DNA Repair *6*, 1709–1725.

Mosedale, G., Niedzwiedz, W., Alpi, A., Perrina, F., Pereira-Leal, J.B., Johnson, M., Langevin, F., Pace, P., and Patel, K.J. (2005). The vertebrate Hef ortholog is a component of the Fanconi anemia tumor-suppressor pathway. Nat. Struct. Mol. Biol. *12*, 763–771.

Moser, J., Kool, H., Giakzidis, I., Caldecott, K., Mullenders, L.H.F., and Fousteri, M.I. (2007). Sealing of chromosomal DNA nicks during nucleotide excision repair requires XRCC1 and DNA ligase III alpha in a cell-cycle-specific manner. Mol. Cell *27*, 311–323.

Munoz, D.M., Cassiani, P.J., Li, L., Billy, E., Korn, J.M., Jones, M.D., Golji, J., Ruddy, D.A., Yu, K., McAllister, G., et al. (2016). CRISPR Screens Provide a Comprehensive Assessment of Cancer Vulnerabilities but Generate False-Positive Hits for Highly Amplified Genomic Regions. Cancer Discov. *6*, 900–913.

Muñoz, I.M., Hain, K., Déclais, A.-C., Gardiner, M., Toh, G.W., Sanchez-Pulido, L., Heuckmann, J.M., Toth, R., Macartney, T., Eppink, B., et al. (2009). Coordination of structure-specific nucleases by human SLX4/BTBD12 is required for DNA repair. Mol. Cell *35*, 116–127.

Murina, O., von Aesch, C., Karakus, U., Ferretti, L.P., Bolck, H.A., Hänggi, K., and Sartori, A.A. (2014). FANCD2 and CtIP cooperate to repair DNA interstrand crosslinks. Cell Rep. *7*, 1030–1038.

Narciso, L., Fortini, P., Pajalunga, D., Franchitto, A., Liu, P., Degan, P., Frechet, M., Demple, B., Crescenzi, M., and Dogliotti, E. (2007). Terminally differentiated muscle cells are defective in base excision DNA repair and hypersensitive to oxygen injury. Proc. Natl. Acad. Sci. U. S. A. *104*, 17010–17015.

Nelson, J.R., Lawrence, C.W., and Hinkle, D.C. (1996). Deoxycytidyl transferase activity of yeast REV1 protein. Nature *382*, 729–731.

Nguyen, G.H., Dexheimer, T.S., Rosenthal, A.S., Chu, W.K., Singh, D.K., Mosedale, G., Bachrati, C.Z., Schultz, L., Sakurai, M., Savitsky, P., et al. (2013). A small molecule inhibitor of the BLM helicase modulates chromosome stability in human cells. Chem. Biol. *20*, 55–62.

Nick McElhinny, S.A., Snowden, C.M., McCarville, J., and Ramsden, D.A. (2000). Ku recruits the XRCC4-ligase IV complex to DNA ends. Mol. Cell. Biol. *20*, 2996–3003.

Nick McElhinny, S.A., Havener, J.M., Garcia-Diaz, M., Juárez, R., Bebenek, K., Kee, B.L., Blanco, L., Kunkel, T.A., and Ramsden, D.A. (2005). A gradient of template dependence defines distinct biological roles for family X polymerases in nonhomologous end joining. Mol. Cell *19*, 357–366.

Nijman, S.M.B. (2011). Synthetic lethality: General principles, utility and detection using genetic screens in human cells. Febs Lett. *585*, 1–6.

Nimonkar, A.V., Ozsoy, A.Z., Genschel, J., Modrich, P., and Kowalczykowski, S.C. (2008). Human exonuclease 1 and BLM helicase interact to resect DNA and initiate DNA repair. Proc. Natl. Acad. Sci. U. S. A. *105*, 16906–16911.

Ogi, T., Limsirichaikul, S., Overmeer, R.M., Volker, M., Takenaka, K., Cloney, R., Nakazawa, Y., Niimi, A., Miki, Y., Jaspers, N.G., et al. (2010). Three DNA polymerases, recruited by different mechanisms, carry out NER repair synthesis in human cells. Mol. Cell *37*, 714–727.

Ohmori, H., Friedberg, E.C., Fuchs, R.P., Goodman, M.F., Hanaoka, F., Hinkle, D., Kunkel, T.A., Lawrence, C.W., Livneh, Z., Nohmi, T., et al. (2001). The Y-family of DNA polymerases. Mol. Cell *8*, 7–8.

Pace, P., Mosedale, G., Hodskinson, M.R., Rosado, I.V., Sivasubramaniam, M., and Patel, K.J. (2010). Ku70 corrupts DNA repair in the absence of the Fanconi anemia pathway. Science *329*, 219–223.

Paddison, P.J., Silva, J.M., Conklin, D.S., Schlabach, M., Li, M., Aruleba, S., Balija, V., O'Shaughnessy, A., Gnoj, L., Scobie, K., et al. (2004). A resource for large-scale RNA-interference-based screens in mammals. Nature *428*, 427–431.

Pang, D., Yoo, S., Dynan, W.S., Jung, M., and Dritschilo, A. (1997). Ku proteins join DNA fragments as shown by atomic force microscopy. Cancer Res. *57*, 1412–1415.

Paull, T.T., and Gellert, M. (1999). Nbs1 potentiates ATP-driven DNA unwinding and endonuclease cleavage by the Mre11/Rad50 complex. Genes Dev. *13*, 1276–1288.

Pearl, L.H., Schierz, A.C., Ward, S.E., Al-Lazikani, B., and Pearl, F.M.G. (2015). Therapeutic opportunities within the DNA damage response. Nat. Rev. Cancer *15*, 166–180.

Pepe, A., and West, S.C. (2014). Substrate specificity of the MUS81-EME2 structure selective endonuclease. Nucleic Acids Res. *42*, 3833–3845.

Perez-Pinera, P., Kocak, D.D., Vockley, C.M., Adler, A.F., Kabadi, A.M., Polstein, L.R., Thakore, P.I., Glass, K.A., Ousterout, D.G., Leong, K.W., et al. (2013). RNA-guided gene activation by CRISPR-Cas9-based transcription factors. Nat. Methods *10*, 973–976.

Philpott, S., Burger, H., Charbonneau, T., Grimson, R., Vermund, S.H., Visosky, A., Nachman, S., Kovacs, A., Tropper, P., Frey, H., et al. (1999). CCR5 genotype and resistance to vertical transmission of HIV-1. J. Acquir. Immune Defic. Syndr. 1999 *21*, 189–193.

Prakash, S., Johnson, R.E., and Prakash, L. (2005). Eukaryotic translesion synthesis DNA polymerases: specificity of structure and function. Annu. Rev. Biochem. *74*, 317–353.

Prasad, R., Liu, Y., Deterding, L.J., Poltoratsky, V.P., Kedar, P.S., Horton, J.K., Kanno, S.-I., Asagoshi, K., Hou, E.W., Khodyreva, S.N., et al. (2007). HMGB1 is a cofactor in mammalian base excision repair. Mol. Cell *27*, 829–841.

Pugh, R.A., Wu, C.G., and Spies, M. (2012). Regulation of translocation polarity by helicase domain 1 in SF2B helicases. EMBO J. *31*, 503–514.

Qi, L.S., Larson, M.H., Gilbert, L.A., Doudna, J.A., Weissman, J.S., Arkin, A.P., and Lim, W.A. (2013). Repurposing CRISPR as an RNA-guided platform for sequence-specific control of gene expression. Cell *152*, 1173–1183.

Rafnar, T., Gudbjartsson, D.F., Sulem, P., Jonasdottir, A., Sigurdsson, A., Jonasdottir, A., Besenbacher, S., Lundin, P., Stacey, S.N., Gudmundsson, J., et al. (2011). Mutations in BRIP1 confer high risk of ovarian cancer. Nat. Genet. *43*, 1104–1107.

Rahman, N., Seal, S., Thompson, D., Kelly, P., Renwick, A., Elliott, A., Reid, S., Spanova, K., Barfoot, R., Chagtai, T., et al. (2007). PALB2, which encodes a BRCA2-interacting protein, is a breast cancer susceptibility gene. Nat. Genet. *39*, 165–167.

Ramadan, K., Shevelev, I.V., Maga, G., and Hübscher, U. (2004). De novo DNA synthesis by human DNA polymerase lambda, DNA polymerase mu and terminal deoxyribonucleotidyl transferase. J. Mol. Biol. *339*, 395–404.

Ray, J.H., and German, J. (1984). Bloom's syndrome and EM9 cells in BrdU-containing medium exhibit similarly elevated frequencies of sister chromatid exchange but dissimilar amounts of cellular proliferation and chromosome disruption. Chromosoma *90*, 383–388.

Read, A., Gao, S., Batchelor, E., and Luo, J. (2017). Flexible CRISPR library construction using parallel oligonucleotide retrieval. Nucleic Acids Res. *45*, e101.

Riedl, T., Hanaoka, F., and Egly, J.-M. (2003). The comings and goings of nucleotide excision repair factors on damaged DNA. EMBO J. *22*, 5293–5303.

Robertson, A.B., Klungland, A., Rognes, T., and Leiros, I. (2009). DNA repair in mammalian cells: Base excision repair: the long and short of it. Cell. Mol. Life Sci. CMLS *66*, 981–993.

Rosenberg, P.S., Tamary, H., and Alter, B.P. (2011). How high are carrier frequencies of rare recessive syndromes? Contemporary estimates for Fanconi Anemia in the United States and Israel. Am. J. Med. Genet. A. *155A*, 1877–1883.

Rulten, S.L., Fisher, A.E.O., Robert, I., Zuma, M.C., Rouleau, M., Ju, L., Poirier, G., Reina-San-Martin, B., and Caldecott, K.W. (2011). PARP-3 and APLF function together to accelerate nonhomologous end-joining. Mol. Cell *41*, 33–45.

Sale, J.E., Lehmann, A.R., and Woodgate, R. (2012). Y-family DNA polymerases and their role in tolerance of cellular DNA damage. Nat. Rev. Mol. Cell Biol. *13*, 141–152.

Sander, J.D., and Joung, J.K. (2014). CRISPR-Cas systems for editing, regulating and targeting genomes. Nat. Biotechnol. *32*, 347–355.

Sanjana, N.E., Shalem, O., and Zhang, F. (2014). Improved vectors and genome-wide libraries for CRISPR screening. Nat. Methods *11*, 783–784.

Sato, K., Toda, K., Ishiai, M., Takata, M., and Kurumizaka, H. (2012). DNA robustly stimulates FANCD2 monoubiquitylation in the complex with FANCI. Nucleic Acids Res. *40*, 4553–4561.

Schmidt, T., Schmid-Burgk, J.L., and Hornung, V. (2015). Synthesis of an arrayed sgRNA library targeting the human genome. Sci. Rep. *5*.

Schwertman, P., Lagarou, A., Dekkers, D.H.W., Raams, A., van der Hoek, A.C., Laffeber, C., Hoeijmakers, J.H.J., Demmers, J.A.A., Fousteri, M., Vermeulen, W., et al. (2012). UV-sensitive syndrome protein UVSSA recruits USP7 to regulate transcription-coupled repair. Nat. Genet. *44*, 598–602.

Scrima, A., Koníčková, R., Czyzewski, B.K., Kawasaki, Y., Jeffrey, P.D., Groisman, R., Nakatani, Y., Iwai, S., Pavletich, N.P., and Thomä, N.H. (2008). Structural basis of UV DNA damage recognition by the DDB1-DDB2 complex. Cell *135*, 1213–1223.

Seal, S., Thompson, D., Renwick, A., Elliott, A., Kelly, P., Barfoot, R., Chagtai, T., Jayatilake, H., Ahmed, M., Spanova, K., et al. (2006). Truncating mutations in the Fanconi anemia J gene BRIP1 are low-penetrance breast cancer susceptibility alleles. Nat. Genet. *38*, 1239–1241.

Sengupta, S., Linke, S.P., Pedeux, R., Yang, Q., Farnsworth, J., Garfield, S.H., Valerie, K., Shay, J.W., Ellis, N.A., Wasylyk, B., et al. (2003). BLM helicase-dependent transport of p53 to sites of stalled DNA replication forks modulates homologous recombination. EMBO J. *22*, 1210–1222.

Sfeir, A., and Symington, L.S. (2015). Microhomology-Mediated End Joining: A Back-up Survival Mechanism or Dedicated Pathway? Trends Biochem. Sci. *40*, 701–714.

Shalem, O., Sanjana, N.E., Hartenian, E., Shi, X., Scott, D.A., Mikkelson, T., Heckl, D., Ebert, B.L., Root, D.E., Doench, J.G., et al. (2014). Genome-scale CRISPR-Cas9 knockout screening in human cells. Science *343*, 84–87.

Shalem, O., Sanjana, N.E., and Zhang, F. (2015). High-throughput functional genomics using CRISPR-Cas9. Nat. Rev. Genet. *16*, 299–311.

Shen, X., Do, H., Li, Y., Chung, W.-H., Tomasz, M., de Winter, J.P., Xia, B., Elledge, S.J., Wang, W., and Li, L. (2009). Recruitment of Fanconi Anemia and Breast Cancer Proteins to DNA Damage Sites is differentially Governed by Replication. Mol. Cell *35*, 716–723.

Shi, J., Wang, E., Milazzo, J.P., Wang, Z., Kinney, J.B., and Vakoc, C.R. (2015). Discovery of cancer drug targets by CRISPR-Cas9 screening of protein domains. Nat. Biotechnol. *33*, 661–667.

Shrivastav, N., Li, D., and Essigmann, J.M. (2010). Chemical biology of mutagenesis and DNA repair: cellular responses to DNA alkylation. Carcinogenesis *31*, 59–70.

Siegel, D., Yan, C., and Ross, D. (2012). NAD(P)H:Quinone Oxidoreductase 1 (NQO1) in the Sensitivity and Resistance to Antitumor Quinones. Biochem. Pharmacol. *83*, 1033–1040.

Sigoillot, F.D., and King, R.W. (2011). Vigilance and validation: Keys to success in RNAi screening. ACS Chem. Biol. *6*, 47–60.

Sigoillot, F.D., Lyman, S., Huckins, J.F., Adamson, B., Chung, E., Quattrochi, B., and King, R.W. (2012). A bioinformatics method identifies prominent off-targeted transcripts in RNAi screens. Nat. Methods *9*, 363–366.

Silva, J.M., Li, M.Z., Chang, K., Ge, W., Golding, M.C., Rickles, R.J., Siolas, D., Hu, G., Paddison, P.J., Schlabach, M.R., et al. (2005). Second-generation shRNA libraries covering the mouse and human genomes. Nat. Genet. *37*, 1281–1288.

Silva, J.M., Marran, K., Parker, J.S., Silva, J., Golding, M., Schlabach, M.R., Elledge, S.J., Hannon, G.J., and Chang, K. (2008). Profiling essential genes in human mammary cells by multiplex RNAi screening. Science *319*, 617–620.

Singh, T.R., Bakker, S.T., Agarwal, S., Jansen, M., Grassman, E., Godthelp, B.C., Ali, A.M., Du, C., Rooimans, M.A., Fan, Q., et al. (2009). Impaired FANCD2 monoubiquitination and hypersensitivity to camptothecin uniquely characterize Fanconi anemia complementation group M. Blood *114*, 174–180.

Singh, T.R., Saro, D., Ali, A.M., Zheng, X.-F., Du, C., Killen, M.W., Sachpatzidis, A., Wahengbam, K., Pierce, A.J., Xiong, Y., et al. (2010). MHF1-MHF2, a histone-fold-containing protein complex, participates in the Fanconi anemia pathway via FANCM. Mol. Cell *37*, 879–886.

Singleton, B.K., Torres-Arzayus, M.I., Rottinghaus, S.T., Taccioli, G.E., and Jeggo, P.A. (1999). The C terminus of Ku80 activates the DNA-dependent protein kinase catalytic subunit. Mol. Cell. Biol. *19*, 3267–3277.

Skipper, K.A., Andersen, P.R., Sharma, N., and Mikkelsen, J.G. (2013). DNA transposon-based gene vehicles - scenes from an evolutionary drive. J. Biomed. Sci. *20*, 92.

Smith, C., Gore, A., Yan, W., Abalde-Atristain, L., Li, Z., He, C., Wang, Y., Brodsky, R.A., Zhang, K., Cheng, L., et al. (2014). Whole-genome sequencing analysis reveals high specificity of CRISPR/Cas9 and TALEN-based genome editing in human iPSCs. Cell Stem Cell *15*, 12–13.

Smogorzewska, A., Matsuoka, S., Vinciguerra, P., McDonald, E.R., Hurov, K.E., Luo, J., Ballif, B.A., Gygi, S.P., Hofmann, K., D'Andrea, A.D., et al. (2007). Identification of the FANCI protein, a monoubiquitinated FANCD2 paralog required for DNA repair. Cell *129*, 289–301.

Soutoglou, E., Dorn, J.F., Sengupta, K., Jasin, M., Nussenzweig, A., Ried, T., Danuser, G., and Misteli, T. (2007). Positional stability of single double-strand breaks in mammalian cells. Nat. Cell Biol. *9*, 675–682.

van der Spek, P.J., Smit, E.M., Beverloo, H.B., Sugasawa, K., Masutani, C., Hanaoka, F., Hoeijmakers, J.H., and Hagemeijer, A. (1994). Chromosomal localization of three repair genes: the xeroderma pigmentosum group C gene and two human homologs of yeast RAD23. Genomics *23*, 651–658.

Staresincic, L., Fagbemi, A.F., Enzlin, J.H., Gourdin, A.M., Wijgers, N., Dunand-Sauthier, I., Giglia-Mari, G., Clarkson, S.G., Vermeulen, W., and Schärer, O.D. (2009). Coordination of dual incision and repair synthesis in human nucleotide excision repair. EMBO J. *28*, 1111–1120.

Sternberg, S.H., and Doudna, J.A. (2015). Expanding the Biologist's Toolkit with CRISPR-Cas9. Mol. Cell *58*, 568–574.

Straughen, J.E., Johnson, J., McLaren, D., Proytcheva, M., Ellis, N., German, J., and Groden, J. (1998). A rapid method for detecting the predominant Ashkenazi Jewish mutation in the Bloom's syndrome gene. Hum. Mutat. *11*, 175–178.

Sturzenegger, A., Burdova, K., Kanagaraj, R., Levikova, M., Pinto, C., Cejka, P., and Janscak, P. (2014). DNA2 cooperates with the WRN and BLM RecQ helicases to mediate long-range DNA end resection in human cells. J. Biol. Chem. *289*, 27314–27326.

Sugasawa, K., Ng, J.M., Masutani, C., Iwai, S., van der Spek, P.J., Eker, A.P., Hanaoka, F., Bootsma, D., and Hoeijmakers, J.H. (1998). Xeroderma pigmentosum group C protein complex is the initiator of global genome nucleotide excision repair. Mol. Cell *2*, 223–232.

Sugasawa, K., Akagi, J., Nishi, R., Iwai, S., and Hanaoka, F. (2009). Two-step recognition of DNA damage for mammalian nucleotide excision repair: Directional binding of the XPC complex and DNA strand scanning. Mol. Cell *36*, 642–653.

Suhasini, A.N., Rawtani, N.A., Wu, Y., Sommers, J.A., Sharma, S., Mosedale, G., North, P.S., Cantor, S.B., Hickson, I.D., and Brosh, R.M. (2011). Interaction between the helicases genetically linked to Fanconi anemia group J and Bloom's syndrome. EMBO J. *30*, 692–705.

Svendsen, J.M., Smogorzewska, A., Sowa, M.E., O'Connell, B.C., Gygi, S.P., Elledge, S.J., and Harper, J.W. (2009). Mammalian BTBD12/SLX4 assembles a Holliday junction resolvase and is required for DNA repair. Cell *138*, 63–77.

Svilar, D., Goellner, E.M., Almeida, K.H., and Sobol, R.W. (2011). Base excision repair and lesion-dependent subpathways for repair of oxidative DNA damage. Antioxid. Redox Signal. *14*, 2491–2507.

Symington, L.S. (2014). End resection at double-strand breaks: mechanism and regulation. Cold Spring Harb. Perspect. Biol. *6*.

Tan, J., and Martin, S.E. (2016). Validation of Synthetic CRISPR Reagents as a Tool for Arrayed Functional Genomic Screening. PLOS ONE *11*, e0168968.

Tanenbaum, M.E., Gilbert, L.A., Qi, L.S., Weissman, J.S., and Vale, R.D. (2014). A protein-tagging system for signal amplification in gene expression and fluorescence imaging. Cell *159*, 635–646.

Taniguchi, T., Garcia-Higuera, I., Andreassen, P.R., Gregory, R.C., Grompe, M., and D'Andrea, A.D. (2002). S-phase-specific interaction of the Fanconi anemia protein, FANCD2, with BRCA1 and RAD51. Blood *100*, 2414–2420.

Tapias, A., Auriol, J., Forget, D., Enzlin, J.H., Schärer, O.D., Coin, F., Coulombe, B., and Egly, J.-M. (2004). Ordered Conformational Changes in Damaged DNA Induced by Nucleotide Excision Repair Factors. J. Biol. Chem. *279*, 19074–19083.

Thermo Fisher: DNA Damage Response CRISPR Library LentiArray Human DNA Damage Response CRISPR Library, Glycerol - Thermo Fisher Scientific.

Tichy, E.D., Liang, L., Deng, L., Tischfield, J., Schwemberger, S., Babcock, G., and Stambrook, P.J. (2011). Mismatch and base excision repair proficiency in murine embryonic stem cells. DNA Repair *10*, 445–451.

Tischkowitz, M., Xia, B., Sabbaghian, N., Reis-Filho, J.S., Hamel, N., Li, G., van Beers, E.H., Li, L., Khalil, T., Quenneville, L.A., et al. (2007). Analysis of PALB2/FANCN-associated breast cancer families. Proc. Natl. Acad. Sci. U. S. A. *104*, 6788–6793.

Tomimatsu, N., Mukherjee, B., Deland, K., Kurimasa, A., Bolderson, E., Khanna, K.K., and Burma, S. (2012). Exo1 plays a major role in DNA end resection in humans and influences double-strand break repair and damage signaling decisions. DNA Repair *11*, 441–448.

Tornaletti, S., Reines, D., and Hanawalt, P.C. (1999). Structural Characterization of RNA Polymerase II Complexes Arrested by a Cyclobutane Pyrimidine Dimer in the Transcribed Strand of Template DNA. J. Biol. Chem. *274*, 24124–24130.

Tsai, S.Q., Zheng, Z., Nguyen, N.T., Liebers, M., Topkar, V.V., Thapar, V., Wyvekens, N., Khayter, C., Iafrate, A.J., Le, L.P., et al. (2015). GUIDE-seq enables genome-wide profiling of off-target cleavage by CRISPR-Cas nucleases. Nat. Biotechnol. *33*, 187–197.

Tsherniak, A., Vazquez, F., Montgomery, P.G., Weir, B.A., Kryukov, G., Cowley, G.S., Gill, S., Harrington, W.F., Pantel, S., Krill-Burger, J.M., et al. (2017). Defining a Cancer Dependency Map. Cell *170*, 564–576.e16.

Tzelepis, K., Koike-Yusa, H., De Braekeleer, E., Li, Y., Metzakopian, E., Dovey, O.M., Mupo, A., Grinkevich, V., Li, M., Mazan, M., et al. (2016). A CRISPR Dropout Screen Identifies Genetic Vulnerabilities and Therapeutic Targets in Acute Myeloid Leukemia. Cell Rep. *17*, 1193–1205.

Uematsu, N., Weterings, E., Yano, K., Morotomi-Yano, K., Jakob, B., Taucher-Scholz, G., Mari, P.-O., van Gent, D.C., Chen, B.P.C., and Chen, D.J. (2007).

Autophosphorylation of DNA-PKCS regulates its dynamics at DNA double-strand breaks. J. Cell Biol. *177*, 219–229.

Uren, A.G., Kool, J., Berns, A., and van Lohuizen, M. (2005). Retroviral insertional mutagenesis: past, present and future. Oncogene *24*, 7656–7672.

Veres, A., Gosis, B.S., Ding, Q., Collins, R., Ragavendran, A., Brand, H., Erdin, S., Cowan, C.A., Talkowski, M.E., and Musunuru, K. (2014). Low incidence of off-target mutations in individual CRISPR-Cas9 and TALEN targeted human stem cell clones detected by whole-genome sequencing. Cell Stem Cell *15*, 27–30.

Vermeulen, W., and Fousteri, M. (2013). Mammalian transcription-coupled excision repair. Cold Spring Harb. Perspect. Biol. *5*, a012625.

Vieira, N.M., Elvers, I., Alexander, M.S., Moreira, Y.B., Eran, A., Gomes, J.P., Marshall, J.L., Karlsson, E.K., Verjovski-Almeida, S., Lindblad-Toh, K., et al. (2015). Jagged 1 Rescues the Duchenne Muscular Dystrophy Phenotype. Cell *163*, 1204–1213.

Volker, M., Moné, M.J., Karmakar, P., van Hoffen, A., Schul, W., Vermeulen, W., Hoeijmakers, J.H., van Driel, R., van Zeeland, A.A., and Mullenders, L.H. (2001). Sequential assembly of the nucleotide excision repair factors in vivo. Mol. Cell *8*, 213–224.

Wacker, S.A., Houghtaling, B.R., Elemento, O., and Kapoor, T.M. (2012). Using transcriptome sequencing to identify mechanisms of drug action and resistance. Nat. Chem. Biol. *8*, 235–237.

Wakasugi, M., Kawashima, A., Morioka, H., Linn, S., Sancar, A., Mori, T., Nikaido, O., and Matsunaga, T. (2002). DDB accumulates at DNA damage sites immediately after UV irradiation and directly stimulates nucleotide excision repair. J. Biol. Chem. *277*, 1637–1640.

Walker, J.R., Corpina, R.A., and Goldberg, J. (2001). Structure of the Ku heterodimer bound to DNA and its implications for double-strand break repair. Nature *412*, 607–614.

Wallace, S.S., Murphy, D.L., and Sweasy, J.B. (2012). Base excision repair and cancer. Cancer Lett. *327*, 73–89.

Walsh, T., Casadei, S., Lee, M.K., Pennil, C.C., Nord, A.S., Thornton, A.M., Roeb, W., Agnew, K.J., Stray, S.M., Wickramanayake, A., et al. (2011). Mutations in 12 genes for inherited ovarian, fallopian tube, and peritoneal carcinoma identified by massively parallel sequencing. Proc. Natl. Acad. Sci. U. S. A. *108*, 18032–18037.

Wang, A.T., and Smogorzewska, A. (2015). SnapShot: Fanconi anemia and associated proteins. Cell *160*, 354–354.e1.

Wang, H., and Xu, X. (2017). Microhomology-mediated end joining: new players join the team. Cell Biosci. *7*, 6.

Wang, A.T., Sengerová, B., Cattell, E., Inagawa, T., Hartley, J.M., Kiakos, K., Burgess-Brown, N.A., Swift, L.P., Enzlin, J.H., Schofield, C.J., et al. (2011). Human SNM1A and XPF–ERCC1 collaborate to initiate DNA interstrand cross-link repair. Genes Dev. *25*, 1859–1870.

Wang, M., Wu, W., Wu, W., Rosidi, B., Zhang, L., Wang, H., and Iliakis, G. (2006). PARP-1 and Ku compete for repair of DNA double strand breaks by distinct NHEJ pathways. Nucleic Acids Res. *34*, 6170–6182.

Wang, T., Wei, J.J., Sabatini, D.M., and Lander, E.S. (2014). Genetic screens in human cells using the CRISPR-Cas9 system. Science *343*, 80–84.

Wang, T., Birsoy, K., Hughes, N.W., Krupczak, K.M., Post, Y., Wei, J.J., Lander, E.S., and Sabatini, D.M. (2015). Identification and characterization of essential genes in the human genome. Science *350*, 1096–1101.

Wang, T., Yu, H., Hughes, N.W., Liu, B., Kendirli, A., Klein, K., Chen, W.W., Lander, E.S., and Sabatini, D.M. (2017). Gene Essentiality Profiling Reveals Gene Networks and Synthetic Lethal Interactions with Oncogenic Ras. Cell *168*, 890–903.e15.

Wechsler, T., Newman, S., and West, S.C. (2011). Aberrant chromosome morphology in human cells defective for Holliday junction resolution. Nature *471*, 642–646.

Weterings, E., and van Gent, D.C. (2004). The mechanism of non-homologous end-joining: a synopsis of synapsis. DNA Repair *3*, 1425–1435.

Wilson, R.C., and Doudna, J.A. (2013). Molecular mechanisms of RNA interference. Annu. Rev. Biophys. *42*, 217–239.

Winzeler, E.A., Shoemaker, D.D., Astromoff, A., Liang, H., Anderson, K., Andre, B., Bangham, R., Benito, R., Boeke, J.D., Bussey, H., et al. (1999). Functional characterization of the S. cerevisiae genome by gene deletion and parallel analysis. Science *285*, 901–906.

Wolski, S.C., Kuper, J., Hänzelmann, P., Truglio, J.J., Croteau, D.L., Houten, B.V., and Kisker, C. (2008). Crystal Structure of the FeS Cluster–Containing Nucleotide Excision Repair Helicase XPD. PLOS Biol. *6*, e149.

Wright, A.V., Nuñez, J.K., and Doudna, J.A. (2016). Biology and Applications of CRISPR Systems: Harnessing Nature's Toolbox for Genome Engineering. Cell *164*, 29–44.

Wu, L., and Hickson, I.D. (2003). The Bloom's syndrome helicase suppresses crossing over during homologous recombination. Nature *426*, 870.

Wyatt, H.D.M., Sarbajna, S., Matos, J., and West, S.C. (2013). Coordinated actions of SLX1-SLX4 and MUS81-EME1 for Holliday junction resolution in human cells. Mol. Cell *52*, 234–247.

Xia, B., Sheng, Q., Nakanishi, K., Ohashi, A., Wu, J., Christ, N., Liu, X., Jasin, M., Couch, F.J., and Livingston, D.M. (2006). Control of BRCA2 cellular and clinical functions by a nuclear partner, PALB2. Mol. Cell *22*, 719–729.

Xue, H.-Y., Ji, L.-J., Gao, A.-M., Liu, P., He, J.-D., and Lu, X.-J. (2016). CRISPR-Cas9 for medical genetic screens: applications and future perspectives. J. Med. Genet. *53*, 91–97.

Yan, Z., Delannoy, M., Ling, C., Daee, D., Osman, F., Muniandy, P.A., Shen, X., Oostra, A.B., Du, H., Steltenpool, J., et al. (2010). A histone-fold complex and FANCM form a conserved DNA-remodeling complex to maintain genome stability. Mol. Cell *37*, 865–878.

Yano, K., Morotomi-Yano, K., Wang, S.-Y., Uematsu, N., Lee, K.-J., Asaithamby, A., Weterings, E., and Chen, D.J. (2008). Ku recruits XLF to DNA double-strand breaks. EMBO Rep. *9*, 91–96.

Yeung, M.L., Houzet, L., Yedavalli, V.S.R.K., and Jeang, K.-T. (2009). A genome-wide short hairpin RNA screening of jurkat T-cells for human proteins contributing to productive HIV-1 replication. J. Biol. Chem. *284*, 19463–19473.

Yi, C., Yang, C.-G., and He, C. (2009). A non-heme iron-mediated chemical demethylation in DNA and RNA. Acc. Chem. Res. *42*, 519–529.

Yin, Z., Sadok, A., Sailem, H., McCarthy, A., Xia, X., Li, F., Garcia, M.A., Evans, L., Barr, A.R., Perrimon, N., et al. (2013). A screen for morphological complexity identifies regulators of switch-like transitions between discrete cell shapes. Nat. Cell Biol. *15*, 860–871.

Zheng, G., Dahl, J.A., Niu, Y., Fedorcsak, P., Huang, C.-M., Li, C.J., Vågbø, C.B., Shi, Y., Wang, W.-L., Song, S.-H., et al. (2013). ALKBH5 Is a Mammalian RNA Demethylase that Impacts RNA Metabolism and Mouse Fertility. Mol. Cell *49*, 18–29.

Zhou, H., Xu, M., Huang, Q., Gates, A.T., Zhang, X.D., Castle, J.C., Stec, E., Ferrer, M., Strulovici, B., Hazuda, D.J., et al. (2008). Genome-scale RNAi screen for host factors required for HIV replication. Cell Host Microbe *4*, 495–504.

Zhu, J., Davoli, T., Perriera, J.M., Chin, C.R., Gaiha, G.D., John, S.P., Sigiollot, F.D., Gao, G., Xu, Q., Qu, H., et al. (2014). Comprehensive identification of host modulators of HIV-1 replication using multiple orthologous RNAi reagents. Cell Rep. *9*, 752–766.

Zhu, Z., Chung, W.-H., Shim, E.Y., Lee, S.E., and Ira, G. (2008). Sgs1 helicase and two nucleases Dna2 and Exo1 resect DNA double-strand break ends. Cell *134*, 981–994.

CURRICULUM VITAE

Name: Martin Moder, MSc

Nationality: Austria

Date of Birth: January 10th 1988

Position: PhD student

Email: martin-moder@gmx.at

Mobile: 0043677 61213705

Current address: Schönbrunner Straße 152 / 2 / 5
1120 Wien
Österreich

Education

2014 – present: PhD student at the Research Center for Molecular Medicine of the Austrian Academy of Sciences (CeMM)
Thematic program: Malignant Diseases
Supervisor: Dr. Joanna Loizou

2012 – 2014: Master student at the University of Vienna
Specialization: Molecular Biology
Master thesis at the Institute of Molecular Biotechnology (IMBA)
Supervisor: Dr. Jürgen Knoblich

2007 – 2011: Bachelor student at the University of Vienna
Specialization: Microbiology and Genetics
Bachelor thesis at the General Hospital Vienna (AKH)
Supervisor: Rodrig Marculescu

Attended conferences

Oral presentation at the EMBO conference 'The DNA damage response in cell physiology and disease', October 2nd – 6th 2017, Athens, Greece

Internships

2012: Institute of Molecular Pathology (IMP), Vienna
Group: Carrie Cowan, PhD
Topic: Molecular mechanisms of asymmetric mitochondria segregation in *C. elegans* development

2009: University of Vienna - department of population ecology, Vienna
Group: Univ. Prof. Dr. Konrad Fiedler
Topic: Genetic analysis of the phylogenetics of tropical butterflies

Publications

Moder M, Velimezi G, Owusu M, Mazouzi A, Wiedner M, Ferreira da Silva J, Robinson-Garcia L, Schischlik F, Slavkovsky R, Kralovics R, Schuster M, Bock C, Ideker T, Jackson SP, Menche J, Loizou JI. Parallel genome-wide screens identify synthetic viable interactions between the BLM helicase complex and Fanconi anemia. Nat Commun. 2017 Nov 1;8(1):1238.

Prochazkova J, Sakaguchi S, Owusu M, Mazouzi A, Wiedner M, Velimezi G, **Moder M**, Turchinovich G, Hladik A, Gurnhofer E, Hayday A, Behrens A, Knapp S, Kenner L, Ellmeier W, Loizou JI. DNA Repair Cofactors ATMIN and NBS1 Are Required to Suppress T Cell Activation. PLoS Genet. 2015 Nov 6;11(11):e1005645.